# MISSION ORIENTED ADVANCED NUCLEAR SYSTEM PARAMETERS STUDY

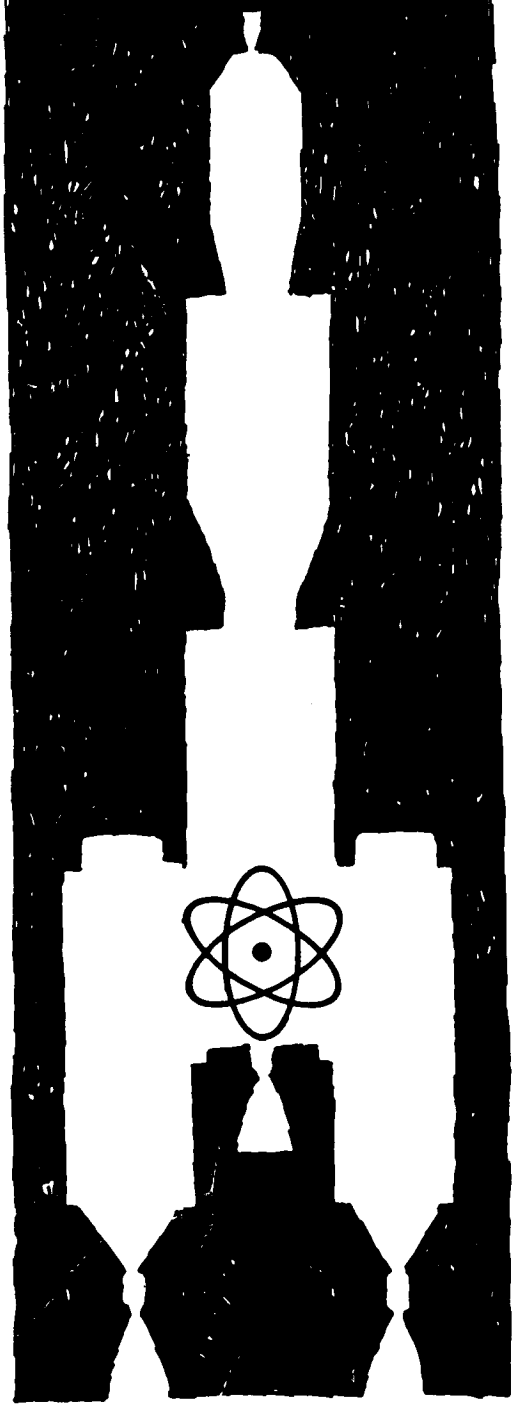

MARCH 1965

FINAL REPORT



GPO PRICE $ _____

CFSTI PRICE(S) $ _____

Hard copy (HC) 6.00

Microfiche (MF) 1.25

ff 653 July 65

VOLUME II

8423-6006-RU000

## DETAILED TECHNICAL REPORT MISSION AND VEHICLE ANALYSIS

FOR

GEORGE C. MARSHALL SPACE FLIGHT CENTER

BY


**TRW SPACE TECHNOLOGY LABORATORIES**

THOMPSON RAMO WOOLDRIDGE INC.

8423-6006-RU000

# MISSION ORIENTED ADVANCED NUCLEAR SYSTEM PARAMETERS STUDY

Final Report
Volume II

Detailed Technical Report
Mission and Vehicle Analysis

for

George C. Marshall Space Flight Center
National Aeronautics and Space Administration

by

TRW Space Technology Laboratories
Redondo Beach, California

Volume II Detailed Technical Report
Mission and Vehicle Analysis

Prepared By: A. R Chovit, Systems Research and Engineering Laboratory
Dr. C. D. Kylstra, Nuclear Technology Department

Approved:
A. R. Chovit, Project Director
Mission Oriented Advanced Nuclear
System Parameter Study

Dr. P. Dergarabedian, Director
Systems Research and Engineering Laboratory

# FOREWORD

This volume, which is one of a set of nine volumes, describes in part the studies, analyses, and results that were accomplished under contract NAS8-5371, Mission Oriented Advanced Nuclear Systems Parameters Study, for George C. Marshall Space Flight Center, Huntsville, Alabama. This work was performed during the period from April 1963 to March 1965 and covers Phases I, II, and III of the subject contract.

This final report has been organized into nine separate volumes on the basis of contractual requirements and to provide a useful and manageable set of documents. The volumes in this set are:

| | |
|---|---|
| Volume I | Summary Technical Report |
| Volume II | Detailed Technical Report; Mission and Vehicle Analysis |
| Volume III | Parametric Mission Performance Data |
| Volume IV | Detailed Technical Report; Nuclear Rocket Engine Analysis |
| Volume V | Nuclear Rocket Engine Analysis Results |
| Volume VI | Research and Technology Implications Report |
| Volume VII | Computer Program Documentation; Mission Optimization Program; Planetary Stopover and Swingby Missions |
| Volume VIII | Computer Program Documentation; Mission Optimization Program; Planetary Flyby Mission |
| Volume IX | Computer Program Documentation; Nuclear Rocket Engine Optimization Program |

Volumes I, II, and IV include the details of the study approach and basic guidelines, the analytic techniques developed, the analyses performed, the results obtained and an evaluation of these results together with specific conclusions and recommendations. Volumes III and V contain parametric mission, vehicle, and engine data and results primarily in graphical form. These data present the interrelationships existing among the parameters that define the mission, vehicle, and engine. Volume VI delineates those areas of research and technology wherein further efforts would be desirable based on the results of the study. Volumes VII through IX describe the computer programs developed and utilized during the study and present instructions and test cases to enable operation of the programs.

The principal contributors to this study were:

| | | |
|---|---|---|
| E. W. Allen | R. D. Fiscus | V. J. Smith |
| P. D. Burgess | C. D. Kylstra | J. R. Taylor |
| R. W. Bussard | J. R. McDougall | T. H. Vickers |
| A. R. Chovit | D. S. Perkins | K. R. Wener |
| J. F. Elwell | R. K. Plebuch | |

In addition, the assistance given by the following persons is gratefully acknowledged: Mr. R. L. Sohn, TRW Space Technology Laboratories; Mr. W. Houghton, Aerojet General Corporation; Dr. W. M. Jacobi, Westinghouse Astronuclear Laboratory; Mr. F. Smith, Lockheed Missile and Space Division; and the members of the NASA Technical Direction Committee, Mr. W. Y. Jordan, Jr., Chairman, and Messrs. R. H. Cavicchi, R. J. Harris, P. G. Johnson, W. L. Kirk, F. R. Nixon, C. Nevins, M. A. Page, and D. R. Saxton.

## ABSTRACT

The details of the study approach and basic guidelines and assumptions which were used in a comprehensive, parametric lunar and interplanetary mission analysis are given. The analyses performed and the analytic techniques generated in developing two mission analysis computer programs for the IBM 7094 are presented. These two programs, the SWingby Optimization Program (SWOP) and the FLyby Optimization Program (FLOP) were employed to generate over 20,000 mission simulations; the optimum trajectory and vehicle were determined for each simulation. An evaluation of the results is presented which establishes an optimum thrust range for the advanced nuclear engine, determines the design characteristics of a compromise advanced nuclear engine, and establishes the sensitivity of the vehicle to variations in mission, engine, and vehicle parameters and modes.

CONTENTS

# ILLUSTRATIONS

## ILLUSTRATIONS

# TABLES

# I INTRODUCTION

This final report presents the details of the mission and vehicle analyses conducted during Phases I, II, and III of the Mission Oriented Advanced Nuclear System Parameters Study performed by TRW/STL for the George C. Marshall Space Flight Center. A companion volume, Volume IV, is a similar final report for the nuclear rocket engine analysis performed during the study.

Included in this volume are the overall study approach and basic study guidelines, the analytic mission evaluation techniques developed, the analyses performed, and an evaluation of the mission performance results obtained together with specific conclusions and recommendations.

## STUDY OBJECTIVE

The basic overall objectives of this study consisted of the following:

- Derivation and computer programming of analytical models for evaluating the various nuclear engine, vehicle system, and mission parameters for nuclear propulsion system applications in the 1975-1990 time period.
- Produce the necessary propulsion and system parametric data and criteria based on probable missions to permit NASA to identify and define the essential design requirements for an operational nuclear propulsion system or systems for the 1975-1990 time period.
- Recommend to NASA preliminary design characteristics of the nuclear propulsion system which results in the best compromise for lunar, planetary flyby, and planetary stopover missions.

## STUDY APPROACH

It is evident that no simple criteria are readily available upon which the selection of the "optimum" engine may be based. The engine, or engines, should be a compromise for a large majority of possible missions in the chosen time period. The performance of the engine should be biased toward the performance requirements of the missions of greatest importance and the missions requiring the largest number of flights. Furthermore, the selected nuclear engines must meet the requirements of demonstrated technical feasibility and be capable of development by the time of operational application. In this assessment, it is necessary to review the state-of-the-art concerning materials and component technology in order to arrive at rational predictions of future development capability. Finally, the vehicle which utilizes the compromise engine must be compatible with the launch and payload constraints of the boost vehicles for this time period.

In order to analyze and evaluate the mission utility of a nuclear propulsion system, it was necessary to formulate a study approach that would reflect all of the complex interactions between the engine, mission, and vehicle parameters. Furthermore, parametric relationships had to be established with sufficient accuracy such that the results of the study would not be invalidated. The goal in this study was to develop, for the first time, efficient methods of carrying out parametric analyses which preserve the accuracy inherent in detailed calculations of individual subsystems.

Figure I-1 shows a graphical representation of the approach adopted for the overall study. The key elements of this approach are listed at the bottom of the chart.

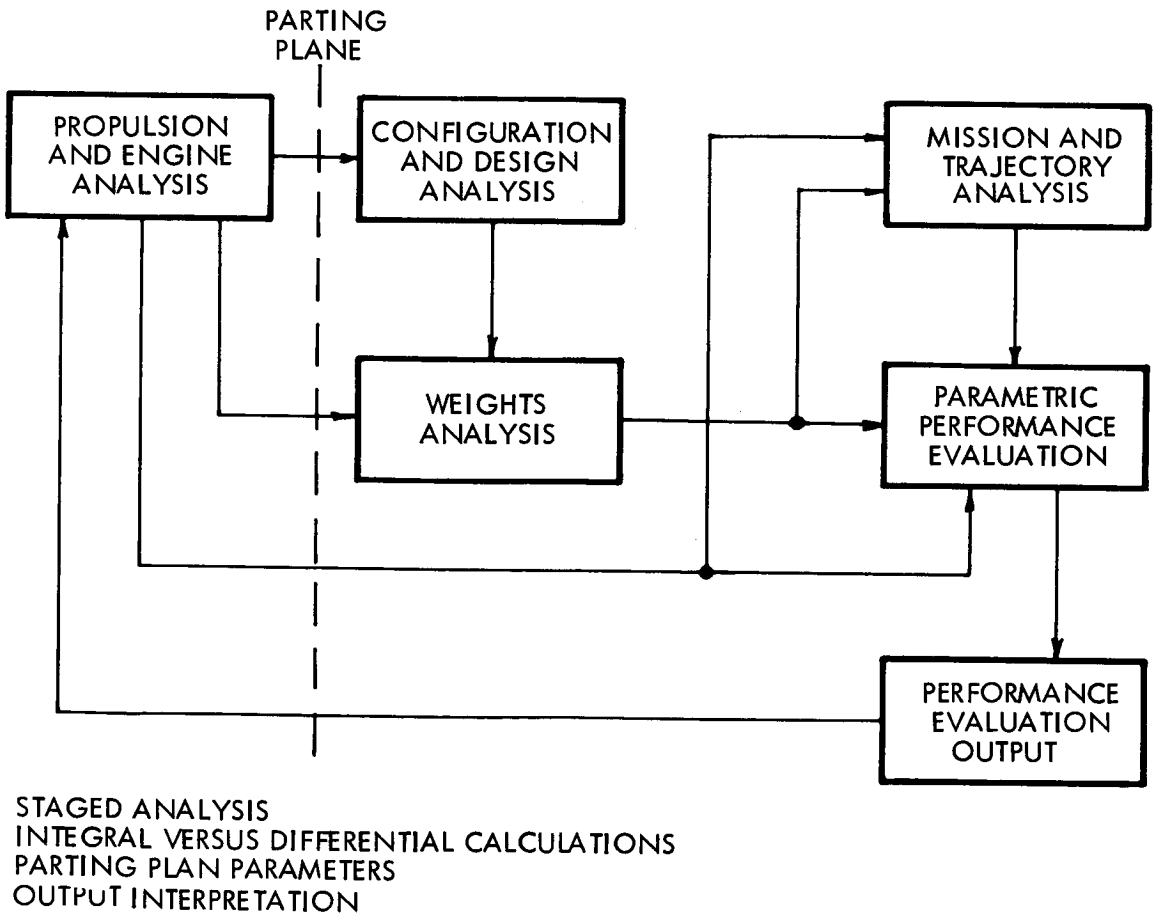


Figure I-1 Study Approach

First and foremost is the concept of "Staged Analysis". This concept refers to the separation of major subsystem parametric analyses into individual segments or stages for each major subsystem. In this way, each individual subsystem could be analyzed independently in order to derive the integral scaling laws so essential for the efficient parametric analysis of complex systems. The development of reliable integral scaling laws from detailed differential calculations allowed the treatment of each subsystem in a "black box" fashion, characterizing each subsystem solely by its principal input and output variables.

Figure I-1 shows each of these principal logic areas as boxes in a functional flow chain of information. However, the box concerning the nuclear propulsion system is separated from the remainder of the logic and information content by a "Parting Plane". All exchange of information between the engine analysis and system performance areas of effort must occur through this parting plane. Engine performance at the parting plane is characterized by three basic performance parameters; engine specific impulse, engine thrust, and engine weight. These three variables provide the principal links between the engine and the vehicle. The single parting plane parameter characterizing the vehicle performance is the total vehicle weight in Earth orbit required to deliver a given payload weight for the mission specified. The study approach outlined can be used to determine the sensitivity and interactions among the engine, vehicle, and mission parameters.

Figure I-2 is a functional diagram showing the interrelationships of the major task categories, task inputs and outputs, and computer programs. It is analogous on a functional level to the previous figure indicating the study approach.

The rectangular boxes represent the computer programs that were developed in the course of the study. The Nuclear Rocket Engine Optimization Program (NOP) produces the reactor and engine performance parameters while the mission analysis programs, the FLyby Optimization Program (FLOP) and SWingby Optimization Program (SWOP) determine the required minimum vehicle weight for any given set of engine performance parameters, vehicle configurations, or mission constraints. The hexagonal boxes represent the analyses performed in order to generate the required inputs from the configuration design, trajectory, and weight studies.

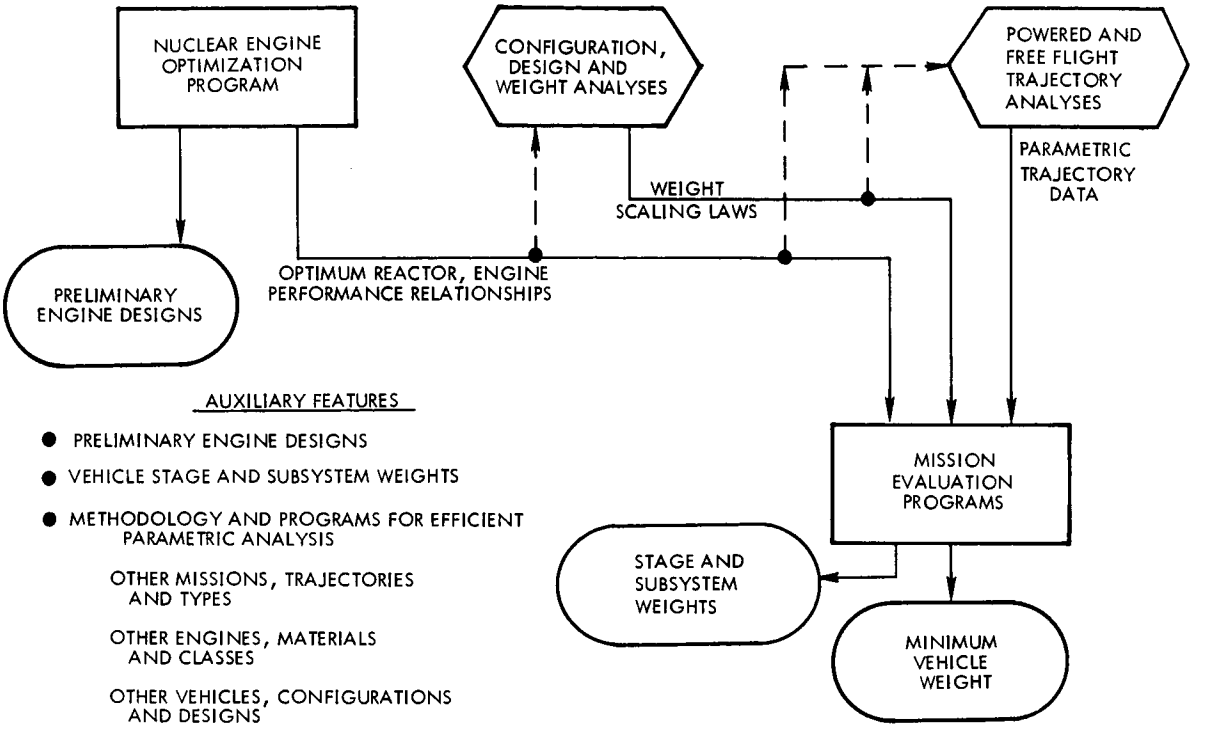


Figure I-2 Performance Evaluation of Nuclear Systems

The nuclear engine and mission analysis computer programs inherently produce outputs of considerable value quite apart from the basic objectives of the overall study. Not only do the programs give optimum nuclear engine and minimum vehicle weight information, but each yields preliminary weights, sizes, and designs for given sets of flight or operating specifications. In the operation of these programs, these outputs can be made optimum or non-optimum as desired. The considerable complexity of accurate determination of optimum interplanetary flight trajectories for any given set of engine performance and vehicle configuration criteria required the utilization of a new and unique method of analysis. The methods developed constitute a major advance in the methodology of mission and trajectory analysis. Similarly the overall design of nuclear rocket engines is an extremely complicated undertaking, compounded by numerous design constraints placed on the engine. The conception and construction of the Nuclear Rocket Engine Optimization Program marked a major step forward in improving the accuracy of parametric nuclear engine analysis and design capability by utilizing differentially calculated results.

The basic methodology, concepts, and computer programs developed during the study already have found application to a wide variety of other mission analyses of interest in the investigation of interplanetary space travel. The versatility and adaptability of the programs permitted, during the course of the study, the expansion of the scope of work to include non-nuclear propulsion configurations, powered and unpowered swingby trajectories, variable tank scaling laws, trip time constraints, upgrading existing engine designs, and the evaluation of different nuclear engine designs.

## STUDY PLAN

The implementation of the study approach required a study plan which when followed would realize the required study objectives. The tasks constituting the study plan were:

- Develop mission evaulation programs
- Develop engine optimization program
- Perform detailed trajectory, vehicle, and engine analysis
- Determine compromise thrust
- Determine vehicle and stage weight sensitivity to mission, vehicle, and performance parameters
- Utilize engine optimization program for engine analysis
- Determine mission performance as a function of engine design variables
- Identify engine size and major design criteria
- Point engine design analysis
- Point vehicle design check
- Parametric data books

These tasks were accomplished during three study phases, the first of which was the "identification" phase. During this phase, the principal objectives were 1) to develop an efficient and accurate methodology for the rapid analysis and comparison of advanced nuclear engine systems, 2) to establish the necessary constraints and guidelines to allow the successful application of this methodology in the second phase of this study, and 3) to evaluate the scope and level of effort appropriate to the second phase of work.

The second phase of the study was concerned with developing the computer programs which would be used to analyze the engine design parameters in terms of the engine thrust, specific impulse, and weight and then determining the influence of engine performance on the required vehicle weight. The development of these computer programs required detailed analyses of interplanetary trajectories, nuclear engines, and the spacecraft in order to determine the required scaling laws, data, and correlations which would relate the pertinent variables for each major subsystem of the complete engine and vehicle. The scaling laws and correlations were then coupled by appropriate calculational techniques and functional equations to provide the parametric description of the integrated mission/vehicle/engine system. Digital computer programs were developed in order to perform the large number of computations necessary for the parametric analyses required by the scope of this study.

In the third phase of the study, these computer programs were utilized to obtain the relationships existing among the parameters that define the mission, the vehicle configuration, the nuclear propulsion system, and the performance of the overall vehicle for interplanetary and lunar missions. These relationships clearly indicated the relative importance and sensitivity of the nuclear engine design parameters on the overall vehicle performance for the range of engine, vehicle, and mission parameters established in Phase I. The results obtained from the computer runs also showed the influence of 1) the various modes of engine usage, e.g. clustered vs single engines and nuclear engine aftercooling, 2) vehicle design and operation, e.g., propellant tank mass fractions, payload weight, and non-nuclear (chemical) propulsion stages, and 3) trajectory perturbations, e.g., planet destinations, trip times, and mission years.

The mission evaluation programs were utilized to analyze the parting plane parameters to determine the best compromise engine thrust level for interplanetary missions in the 1975 to 1990 time period. Primarily, the initial vehicle weight and maximum engine firing time were determined as a function of thrust level and various mission modes and mission years. Following the determination of this compromise thrust, a detailed analysis was made to determine the vehicle and stage weight sensitivity to variations in performance, vehicle, and mission parameters. These variations include payload weights,

stage mass fractions, engine weights, thrust, specific impulse, propellant types, aerodynamic braking, propellant boil-off, stopover time, and mission year. Concurrently, the nuclear engine optimization computer program was used for analyzing the detailed engine design parameters in terms of their effect on the parting plane parameters, i.e., the engine weight, thrust, and specific impulse.

In this manner, it was possible to determine within a narrow range the mission, vehicle, and engine performance requirements for future manned interplanetary missions. Within this narrow range, a more detailed analysis was then performed which related the vehicle and mission requirements to variations in specific engine design parameters. These parametric results permitted the determination and evaluation of the requirements for the design and development of the various optimum vehicle engine configurations. This portion of the study provided an assessment of the criteria for the successful development of optimum engine and vehicle combinations and determined the influence of various major or critical state-of-the-art advancements on engine and vehicle performance. Similarly, a definition and evaluation of vehicle design problems, requirements, criteria, and constraints were made as influenced by the range of nuclear engine design parameters.

The information obtained from these detailed assessments then permitted the identification of the design requirements for the engine of maximum utility together with major vehicle and mission criteria. A preliminary engine and vehicle design was then performed for the recommended engine and vehicle. The final result of this study is a detailed set of engine specifications which outline the basic engine and reactor performance and design requirements for the selected compromise nuclear propulsion system (Volumes IV and V). Additional specifications include a set of constraints and requirements for the remaining portions of the vehicle system for each specific mission of major interest (Volumes II and III). The combined set of engine and vehicle specifications in turn define the performance characteristics which can be expected from vehicles propelled by the selected nuclear engine for interplanetary flight missions in the 1975 to 1990 time period.

## STUDY ASSUMPTIONS AND CONSTRAINTS

A set of assumptions and constraints were postulated for the study in order to circumscribe the mission types and modes, the engine designs, the vehicle configurations, the mission operational criteria, and the scope of analyses and computational procedures.

Some of the assumptions and constraints listed in this section were formulated at the start of the study, while others were postulated in later study stages. In an advanced study such as this, which spans a period of over a year and a half, many of the initially established ground rules or guidelines will change or be invalidated during the course of the study. This will occur due to disclosures made in the study itself or in associated studies, or due to a change in study emphasis or scope prompted by technical, fiscal, or scheduling considerations on many levels. The assumptions and constraints presented here include only those which were finally used or incorporated in the analyses, computer programs, and results.

Many guidelines and criteria resulted from analyses conducted during the study. These are in the nature of study results and for the most part, do not appear in this chapter but rather in those chapters applicable to the analyses or study areas. The assumptions and constraints that are presented in this chapter are the result of initial study guidelines or NASA decisions and directives. Any exceptions to these criteria are noted wherever the exception occurs.

### Missions

The basic set of missions to be investigated consists of the following:

- Manned Mars stopover mission
- Manned Venus stopover mission
- Manned Mars flyby mission
- Manned Venus flyby mission
- Manned Mars/Venus swingby mission
- Lunar transfer mission

Stopover Mission - A typical stopover mission is shown on Figure I-3, which depicts the major operational phases that occur during the mission. Figure I-4 shows a typical stopover mission trajectory and the points along this trajectory at which major velocity and vehicle weight changes occur. Additional vehicle weight requirements are included for life support expendables, propellant boiloff, and attitude control. If an aerodynamic braking mode is employed at the target planet (Mars), a propulsive velocity change is used for circularizing or adjusting the resulting orbit. The earth braking propulsive retro can be eliminated by option and an all aerodynamic earth braking mode employed. All opposition years from 1975 to 1990 were considered for the Mars stopover missions; Venus stopover missions were analyzed only for the 1980 conjunction.

Stopover Mission Trajectory Type - Two types of trajectories were considered for the stopover missions, designated type IB and type IIB. The "B" denotes an inbound trajectory leg where the heliocentric angle traversed, $\theta$, is greater than $180^{\circ}$ and less than $360^{\circ}$; the "I" denotes an outbound trajectory leg where $180^{\circ} < \theta < 360^{\circ}$; the "II" designates an outbound trajectory leg where $0^{\circ} < \theta < 180^{\circ}$. The total trip time for a type IB mission is characteristically between 500 and 550 days; for type IIB between 400 and 450 days.

Swingby Mission - A swingby mission is essentially the same as a Mars stopover mission except the trajectory is constrained to pass in the vicinity of the planet Venus either during the outbound or inbound leg. The vehicle, therefore, performs a hyperbolic turn about Venus. For the swingby mission, a third midcourse correction propulsion maneuver is assumed. Typical inbound and outbound swingby trajectories are shown in Figures I-5 and I-6.

Flyby Mission - Characteristically, the operational sequence for the flyby mission is identical to that of the stopover mission except the vehicle does not go into orbit about Mars (See Figure I-7). Thus, the two velocity changes at the target planet are eliminated, i.e., the arrive planet braking and leave planet boost phases. Low energy trajectories were assumed for Mars flyby mission (600 to 700 days) and high energy for Venus. The years 1978 and 1980 were considered for Mars; 1980 for Venus.

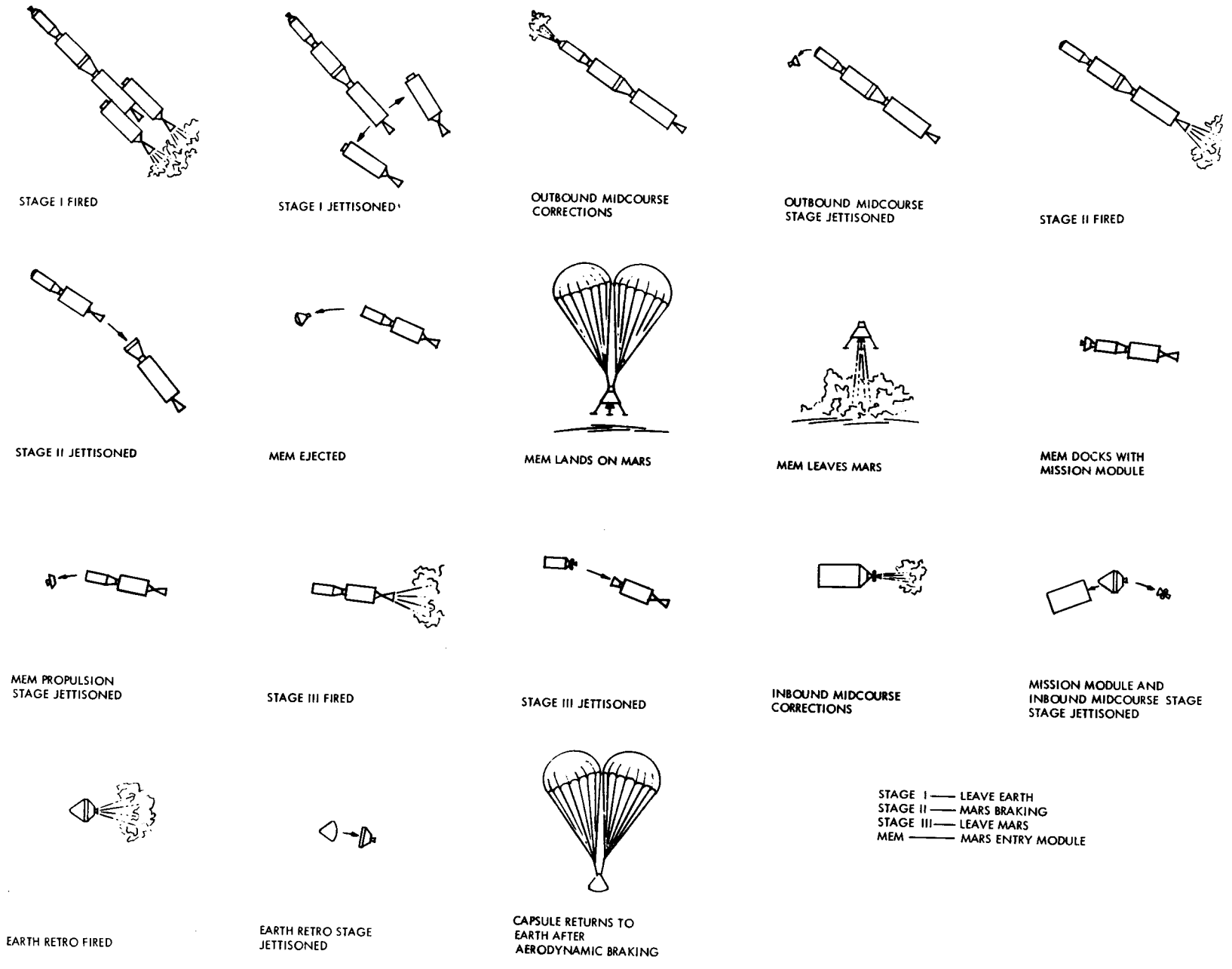


Figure I-3 Mars Stopover Mission Sequence

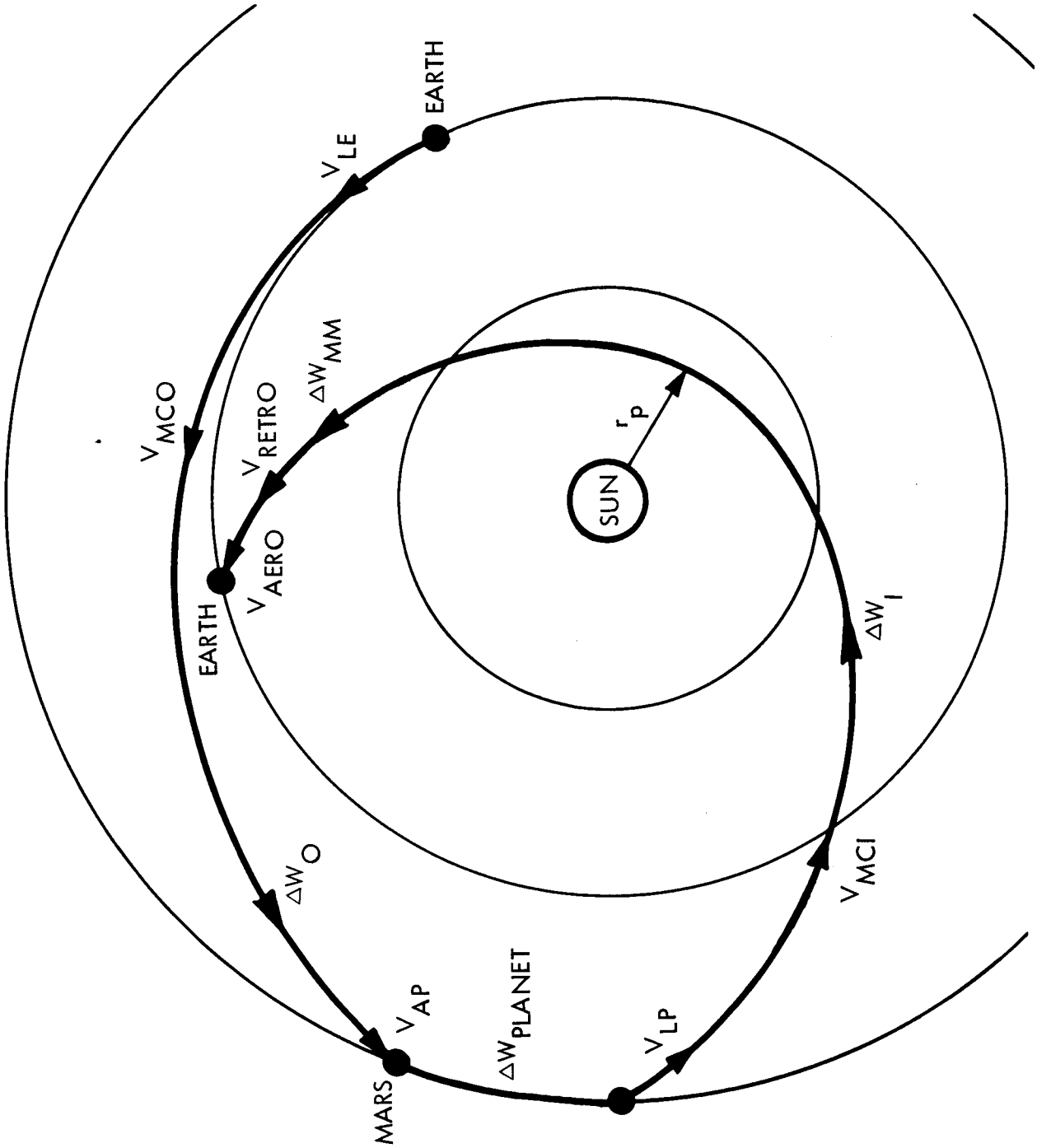


Figure I-4 Typical Stopover Mission Trajectory

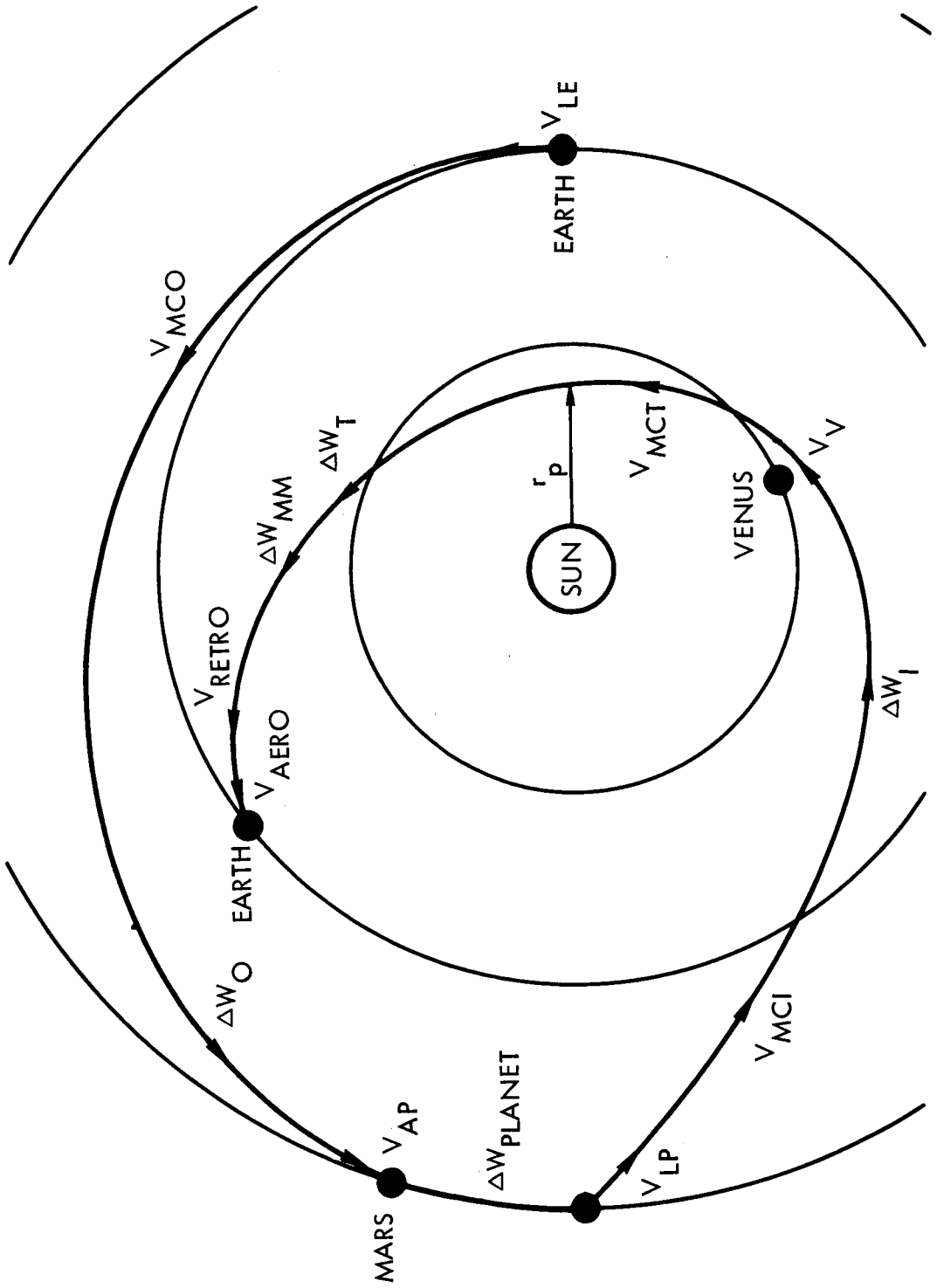


Figure I-5 Typical Venus Inbound Swingby Mission Trajectory

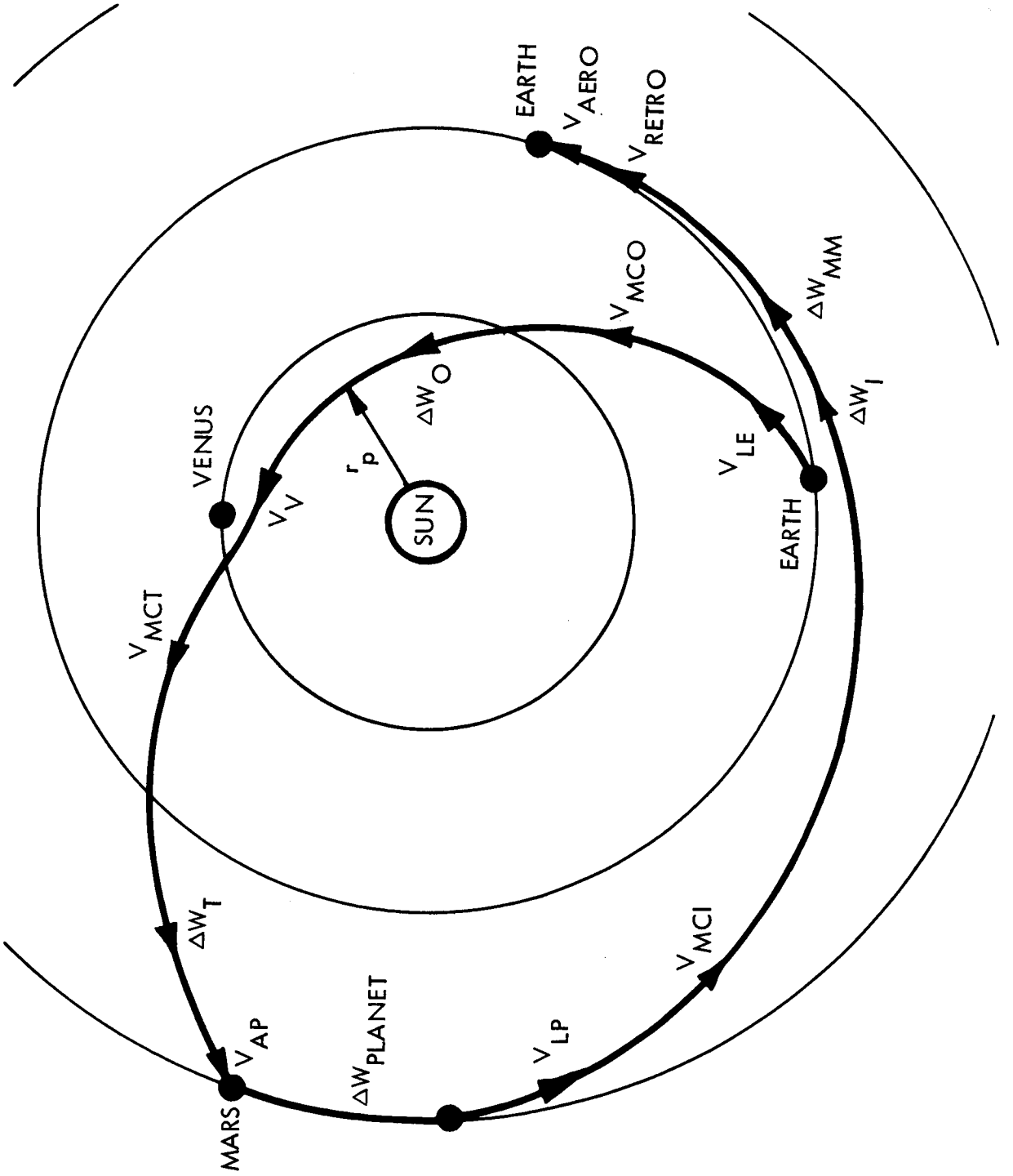


Figure I-6 Typical Venus Outbound Swingby Mission Trajectory

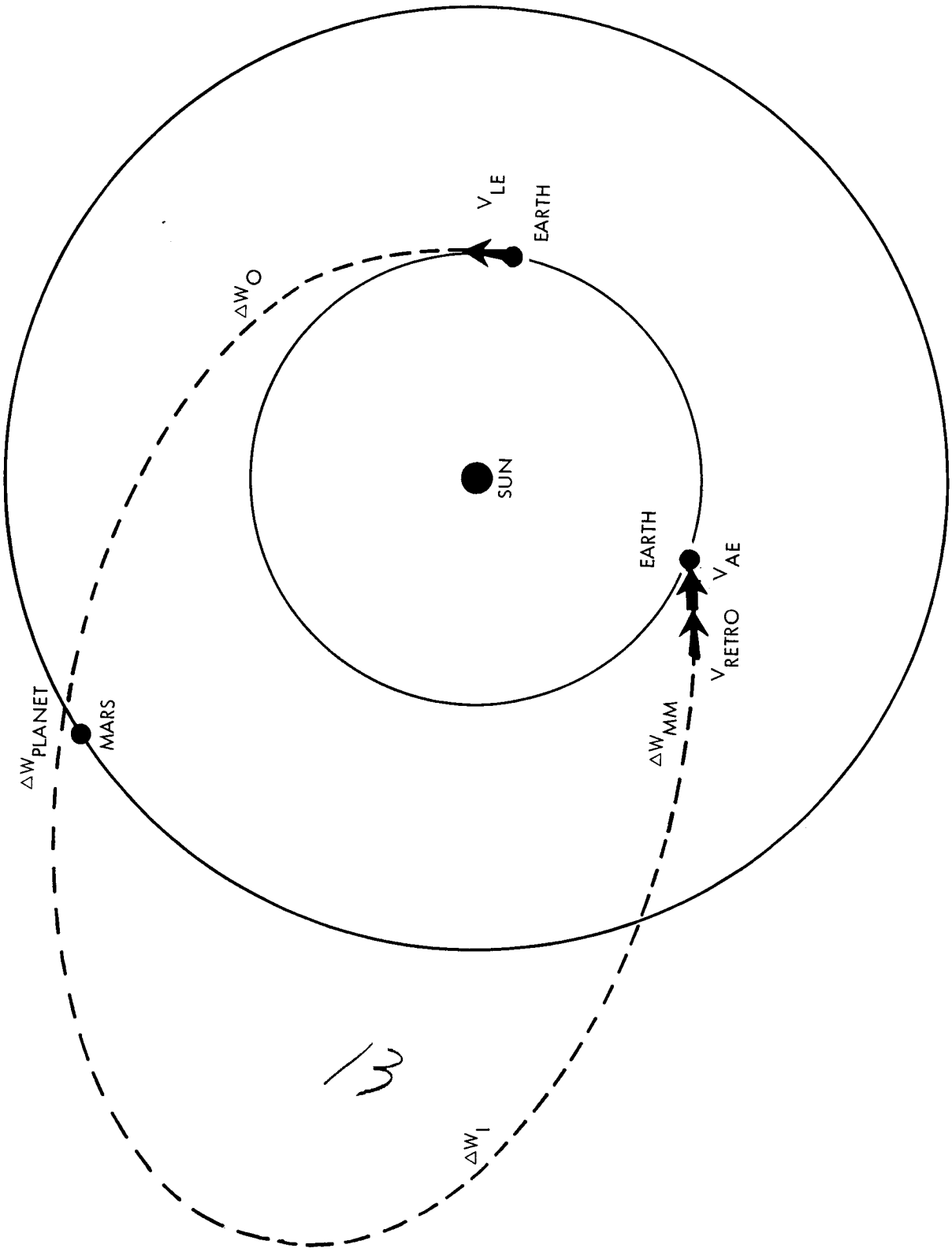


Figure I-7 Typical Mars Flyby Trajectory

Lunar Transfer Mission - A typical lunar transfer mission consists of the following major phases: boost out of Earth parking orbit, propulsive midcourse velocity correction, and a propulsive retro into a lunar orbit. Additional vehicle weight requirements are computed for life support expendables, propellant boil-off, and attitude control. A 70-hour transfer trajectory was assumed for apogee, perigee, and mean transfer trajectories.

Orbital Altitudes - The following altitudes were assumed for the planetary and lunar circular orbits for computing the vehicle velocity and trajectory requirements.

The orbital altitude above the Earth's surface is 500 km for all Mars and Venus stopover and flyby missions. The orbital altitude for the circular orbits about Mars and Venus is 600 km. The Earth orbit altitude for lunar missions is 485 km; a 100nm circular orbit altitude is used at moon. The planet peri-passage radius for all flyby missions is 1.05 times the radius of the planet.

## Nuclear Engine

Configuration - The study was confined to analysis and evaluation of beryllium-reflected, graphite-moderated nuclear rocket engines. Both topping and bleed cycle engines and single and counterflow tie rod cooling were to be investigated. The reactor core diameter ranges from 45 to 65 in. diameter.

Performance - The specific impulse varies parametrically from 700 to 900 seconds and the thrust from 50,000 to 500,000 pounds (approximately 1,000 to 12,000 Mw). The weight penalties associated with the clustering of engines for a given stage is based on data obtained from Aerojet General Corporation.

## Vehicle Configuration and Design

A number of assumptions and constraints were made concerning the mission payloads, propellant tanks, non-nuclear propulsion systems, secondary systems, and operational modes.

Payloads - The payloads for all planetary flyby and stopover missions include (1) an earth recovered module (ERM), (2) a mission module jettisoned prior to earth entry, and (3) a planet lander or probe jettisoned at the target planet (MEM). In addition, in the stopover mission, an ascent module is picked up before leaving the target planet. The payload for the lunar mission is a parametric, inert weight delivered into lunar orbit.

Propellant Tanks and Clustered Engines - All hydrogen (nuclear) propellant tanks are 33 feet in diameter. A modular approach is used in which all tanks clustered in any given stage are of the same capacity. The maximum capacity of each tank is set by the limitations imposed by the Saturn V booster and its launching equipment. In addition, the number of engines assigned to any given stage cannot be greater than the number of tanks for that stage.

Except as noted, the scaling laws which define the weight of the propellant tanks are based on data generated by Lockheed Missile and Space Company under NASA Contract, NAS8-9500, for the George C. Marshall Space Flight Center.

In order to increase the gross effective thrust and thereby reduce the velocity gravity losses, engine clustering, or the simultaneous use of two or more identical nuclear engines on a single stage, is used. Unless specifically stated, nuclear engine clustering is employed only for the depart earth stage. As an alternative mode, aftercooling of the nuclear engine for later restart is assumed possible for the braking propulsion phase at the target planet.

Non-Nuclear Propulsion Systems - In addition to the use of nuclear rocket engines for performing all of the major velocity changes, the use of nuclear and chemical engines in separate stages for the same mission, and all chemically propelled vehicles are also considered for evaluation and comparison purposes. Once a chemical stage is introduced into a particular mission (ignoring midcourse corrections), all remaining stages employ chemical propulsion. Separate chemical engines and stages are used for braking at and departing the target planet.

Both high energy cryogenic ($LO_2/LH_2$) and liquid storable chemical propulsion systems are considered with specific impulses of 440 sec and 330 sec, respectively.

Aerodynamic Braking Systems - The range of aerodynamic braking capability at earth to be investigated was assumed to vary parametrically from all aerodynamic braking to aerodynamic braking down to parabolic entry velocity. The scaling laws for sizing the required structure, ablative material, insulation, and landing and recovery aids for aerodynamic braking are based on results generated by TRW/STL under NASA Contract, NAS2-1409 for Ames Research Center.

Aerodynamic braking at Mars is also considered as an alternative mode. It was assumed that the vehicle is aerodynamically braked into a capture orbit about Mars, after which the orbit is circularized by a storable propellant stage. The scaling law used to size the Mars aerodynamic braking heat shield is based on data obtained from Lewis Research Center.

Secondary Systems - It was assumed that the vehicle for any mission contains a separate storable propellant midcourse correction stage for each major leg of the mission. Weight provisions are also included for attitude control of the vehicle.

Scaling laws are used to size the solar flare shield requirements as a function of assumed yearly solar activity and perihelion distance. The scaling laws are a compromise of data obtained from Lewis Research Center and the Marshall Space Flight Center.

Earth Ascent and Orbital Operations

It was assumed that all modules used in the spacecraft are boosted into earth orbit by the Saturn V vehicle. Thus, the maximum size and weight of any module are set by the limitations of the Saturn V and its launching equipment However, this assumption has little bearing on the vehicle weights and parametric data generated during the study.

In determining the vehicle configuration, its requirements, and its operation, no detailed considerations are given to the problems and requirements of ascent to orbit and orbital rendezvous, assembly, checkout, and propellant and personnel transfer. Therefore, the vehicle primarily is sized and configured for the mission phases and operations commencing with boost out of an earth parking orbit and terminating with earth recovery or retro into lunar orbit.

Computational Criteria

The possible combinations of mission types and modes, vehicle and engine configurations, and performance variations that could be formulated from the listed assumptions and constraints are extensive but obviously not all possible mission combinations could be considered in this study. Rather the mission combinations of most interest were determined during the course of the study by discussion with MSFC personnel. These are outlined and discussed later in detail.

Nevertheless, in order to enhance their future value, the mission evaluation computer programs were developed with the additional capability of analyzing many more mission, vehicle, and operational modes and types than those actually evaluated. In addition, a set of basic criteria was formulated defining some of the computational guidelines to be followed and objectives to be met. These criteria and additional computer program capabilities are outlined below.

1. Evaluation of the mission is based primarily on the total spacecraft weight. This weight is the minimum gross spacecraft weight that is required to perform a specified mission for specified vehicle, payload, and performance constraints. This weight corresponds to the overall vehicle weight at the point just prior to boost out of earth parking orbit. The vehicle weight in all cases is computed using trajectory characteristics that are optimum for the selected constraints, i.e., the particular launch dates and trip times used (with the corresponding characteristic velocities and perihelion distance) produce the minimum overall vehicle weight.

2. The initial vehicle weight data are based on calculations for the propellant weight in which the velocity losses due to operation in a gravity field are taken into account in an exact manner. The gravity losses can be determined by either specifying a) a fixed engine thrust, b) a fixed percentage increase of the impulsive velocity, or c) a fixed vehicle thrust-to-weight ratio.

   For vehicles employing nuclear propulsion stages, these losses are based on the required velocity change, the engine specific impulse, and the vehicle thrust-to-weight ratio obtained from the computed vehicle weight and the specified engine thrust.

For vehicles employing chemical propulsion systems, the characteristic velocity is obtained by increasing the required impulsive velocity change by a fixed percentage. The percentage values used are shown in the following schedule.

| Propulsive Phase | Propulsion Mode | Percentage Increase |
|---|---|---|
| Depart Earth | Cryogenic ($LO_2/LH_2$) | 2.3% |
| Arrive Planet | Cryogenic ($LO_2/LH_2$) | 0% |
| Depart Planet | Cryogenic ($LO_2/LH_2$) | 1% |
| Depart Planet | Storable | 1% |
| Arrive Earth Retro | Cryogenic ($LO_2/LH_2$) | 0% |
| Arrive Earth Retro | Storable | 0% |

However, with appropriate gravity loss data stored in the computer program for the lower specific impulse chemical propulsion systems, the actual velocity gravity losses experienced by the chemically propelled vehicle could be determined using one of the three options presently available.

3. The initial vehicle weight includes the weight of the propellant tank insulation and vaporized propellant. These are determined in an optimum manner which results in minimum initial vehicle weight requirements. The optimization procedure considers the length of storage time and the various propulsive velocity changes that each cryogenic stage undergoes. The propellant heat of vaporization, temperature difference across the insulation, and insulation density and thermal conductivity are specified input values.

4. The solar flare shield weight is sized and the perihelion distance determined so as to have a minimum effect on the initial vehicle weight. The dependence of the solar flare shield scaling law on perihelion distance permits this optimization.

5. All missions may be manned or unmanned.

6. The programs compute and output the vehicle weight before and after every powered phase of the mission as well as all propellant, insulation, and tank weights.

7. The jettisoning or pickup of miscellaneous payload weights (such as probes) can be included between every major velocity change phase.

8. Propulsive braking or full aerodynamic braking can be considered upon earth return for all mission modes. The computer programs also permit propulsive braking to any arbitrary velocity (maximum aerodynamic braking entry velocity) followed by aerodynamic entry.

9. Engines and/or tankage can be jettisoned after each firing. Wherever stages employing clustered engines and/or tanks are used for more than one phase of the overall mission profile, the engines and/or tanks can be partially jettisoned.

10. Staging of engines and/or tanks can be included in the propulsive earth depart phase.

11. The earth depart nuclear engines can be aftercooled in addition to the arrive planet engines. Either all or part of the clustered engines in the depart earth or arrive planet stage can be aftercooled. Recovery of the thrust during earth depart aftercooling can be accomplished.

12. The arrive and depart earth and planet dates and/or the leg or total trip times can be constrained to specific values in the optimization computations.

# II MISSION OPTIMIZATION PROCEDURE

## GENERAL

Within a given class of trajectories for any interplanetary flight, there usually exists one trajectory which requires the least initial vehicle weight to perform the mission. The problem is to find this trajectory for a particular vehicle configuration and performance.

The general approach and optimization procedure used to solve this problem for this study is discussed in this chapter. The next chapter describes in detail the vehicle scaling laws and constraints and the vehicle weight calculations. These analysis techniques, scaling laws, and procedures were programmed for the computer to permit rapid calculation of the large number of cases investigated.

The optimization procedure developed is based on a mission for which the propulsion system firing time is essentially instantaneous when compared with the trip time. That is, the vehicle is given a relatively high thrust velocity change followed by a long coast or free flight period. Since a free flight trajectory is independent of the vehicle size and weight, it is not necessary to calculate continually new trajectory parameters for the optimization procedure. Rather, a trajectory map is generated and stored within the computer program for continual reference.

The initial version of the Stopover Mission Optimization Program (SMOP) stored the trajectory data as curve fits. For each arrive planet date (at fixed 10-day intervals over a specified range of arrive planet dates) the leave earth and arrive planet characteristic velocities as a function of the outbound trip time, were fitted by 3rd order polynomials. The leave planet and arrive earth characteristic velocities and the perihelion distance were also fitted by 3rd order polynomials, but as a function of the inbound trip time for each depart planet date.

To find the optimum trajectory and the minimum vehicle weight, the curve fits were used in outbound and inbound trip time optimization equations to find the optimum trip times and the corresponding velocities for each arrive planet date. With these data, the total vehicle weight for each arrive planet date was calculated, using the vehicle scaling laws, payloads, etc.

described later in Chapter III. The arrive planet date corresponding to the minimum vehicle weight was found by curve fitting the three smallest vehicle weights as a function of the arrive planet date, differentiating the equation, and setting it equal to zero.

This procedure permitted an accurate determination of the minimum weight vehicle and the optimum trajectory. However, it required a large number of passes through the vehicle weight calculation procedure. Also, it was very troublesome developing 3rd order curve fits of the velocities and perihelion distance that were sufficiently accurate over the trip time range of interest. (This general procedure was retained and used for the FLyby Optimization Program (FLOP) since curve fitting of the trajectory data was not necessary; a description of this procedure is given later in this chapter.)

When the requirement was imposed to develop an optimization program for swingby missions, it was clear that attempting to optimize the mission by extending the initial SMOP procedure would be very cumbersome and costly in computer time. Since the powered swingby has one more independent trajectory parameter, which adds another dimension to the trajectory map on the swingby portion of the mission, it would be necessary to either curve fit trajectory data along two axes, solve the corresponding optimization equations and then calculate vehicle weight along one axis, or to continue to curve fit along only one axis, and calculate vehicle weight along two axes. In either case, a tremendous number of passes through the vehicle weight calculation portion of the program would be necessary. To get away from these problems, a basic change in the method of trajectory data storage and arrive planet date optimization was made.

The trajectory map is stored in the SWingby Optimization Program (SWOP) as discrete values of the dependent parameters at regular intervals of the independent parameters. No curve fit preprocessing is necessary. The curve fitting is done internally by the program, using 2nd order polynomials. Rather than calculating the initial vehicle weight for the stopover mission and unpowered swingby mission for each arrive planet

date to find the minimum vehicle weight, one weight calculation is made and an optimization equation used to determine the optimum arrive planet date. The optimum outbound and inbound leg times, as before, are found using optimization equations. For a powered swingby mission, an additional optimization equation is used to find the optimum third leg time. This procedure saves some effort over the original SMOP program by not calculating the vehicle weight as often (approximately 1/8 as often), but this advantage is offset by the need to solve a complicated optimization equation and to calculate a minimum of ten 2nd order polynomial curve fits every iteration. The computer time required per case has remained about the same, but now it is much easier to prepare the trajectory data for the program, and the program has the potential to handle increasing complicated missions. Also the powered swingby mission can be solved with only a slight increase in computer time.

In order to accurately account for the velocity losses due to finite firing time in a gravity field, the impulsive velocity data stored in the program are corrected for this effect by multiplying the velocities by gravity loss factors to obtain the characteristic velocity change. The gravity loss factors are also stored in the program, and were obtained by simulating powered flights for leaving earth, and arriving and leaving the target planet. These factors depend on the specific impulse of the propulsion system, the vehicle thrust-to-weight ratio, and the orbit altitude. Once generated, they can be used for any vehicle configuration and mission.

## FLYBY MISSION

The trajectory for a typical flyby mission has previously been shown in Chapter I by Fig. I-7. Only two independent trajectory parameters are needed to completely define a flyby mission. However, if the constraint of constant periplanet distance is imposed for a series of possible flights, only one independent parameter is left to specify. The FLyby Optimization Program (FLOP) uses the arrive planet date as the independent parameter. No trajectory curve fits are used. The dependent leave and arrive earth velocities and outbound and inbound leg times are supplied to the program for uniform intervals of the arrive planet date. The flyby trajectory data used for this study was supplied by Marshall Space Flight Center.

The flyby mission optimization procedure is shown in Fig. II-1. The overall optimization is divided into two parts. First, the initial vehicle weight is calculated for each arrive planet date over a range of dates that are specified by input. Starting with the arrive earth payload, the program works backward to the initial vehicle weight using the correct leave earth gravity loss factors and the scaling laws, payloads, and coefficients described in Chapter III. The calculation for the leave earth stage is repeated until consistent values of the initial weight in earth orbit (thrust-to-weight ratio) and the velocity gravity loss is obtained.

Second, once the initial vehicle weights for the range of arrive planet dates are obtained, the three lightest vehicle weights are curve fitted as a function of the arrive planet date. By differentiating the curve fit, the arrive planet date corresponding to the minimum weight vehicle is found. Then all trajectory parameters for this "optimum" arrive planet date are found by curve fitting the stored trajectory data. The vehicle component weights are then determined for the optimum date (and corresponding optimum velocities) by passing through the weight calculation portion of the program once more. Then some auxiliary output quantities are calculated. The equations and detail procedures employed in FLOP are completely outlined in the program documentation, Vol. VIII, of this series of final reports.

## STOPOVER AND SWINGBY MISSIONS

### Generalized Mission Analysis Procedure

The mission analysis for the stopover and swingby missions is split into two parts, a trajectory optimization and a vehicle weight calculation. Each part supplies the other with necessary trajectory or vehicle parameters. Figure II-2 shows the generalized mission analysis procedure employed by the SWingby Optimization Program (SWOP). This procedure is applicable to the optimization of stopover missions and both powered and unpowered, inbound and outbound, swingby missions.

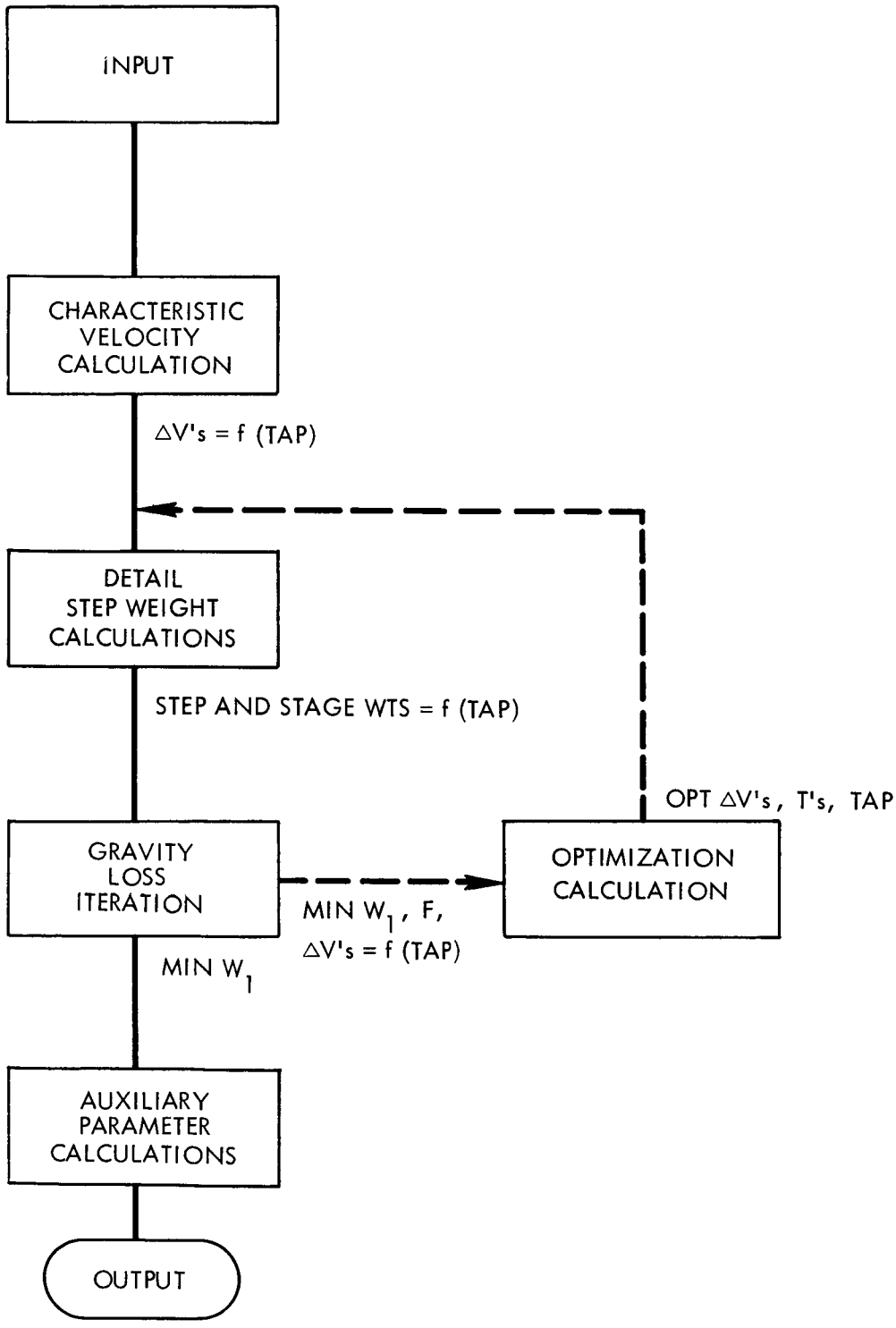


Figure II-1 Flyby Mission Optimization Procedure

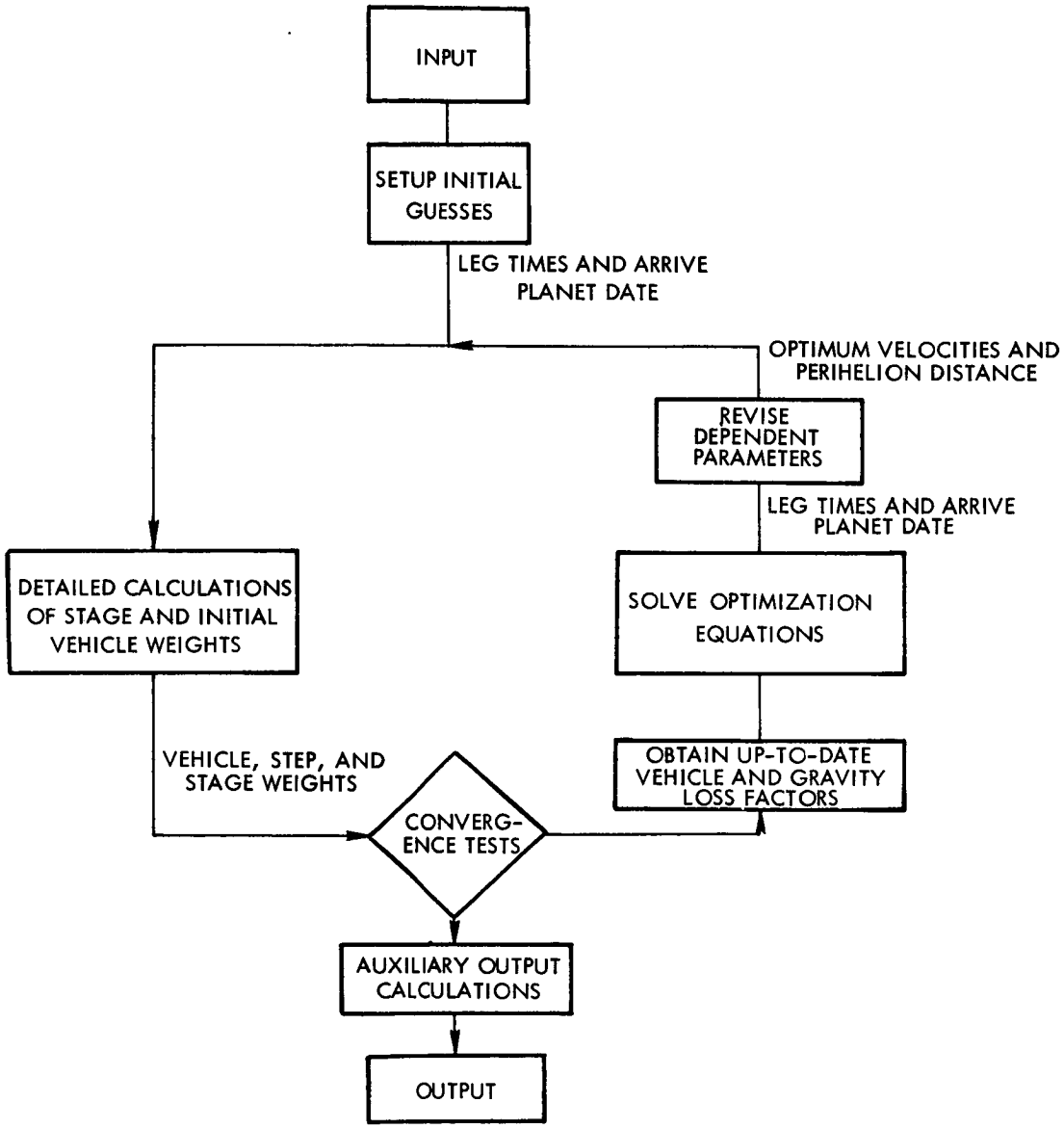


Figure II-2 Swingby Mission Optimization Procedure

The necessary scaling law coefficients and vehicle constraints are inputted and then initial guesses for the independent trajectory parameters are used to start a mission optimization. The stored trajectory data are used to determine the characteristic velocities corresponding to these initial guesses. Then a detailed calculation of the vehicle stage weights is made and the resulting vehicle stage weights are combined with calculated velocity gravity losses to form coefficients in the optimization equations. The optimization equations are then solved for the "optimum" leg times and arrive planet date. The characteristic velocities and perihelion distance corresponding to these "optimum" independent parameters are obtained from stored trajectory data.

These new values of velocities and perihelion distance are used in recalculating the stage and initial vehicle weights. When a sufficient number of interations are performed successive new values of vehicle weights and trajectory parameters no longer appreciably change. At that time, the calculated vehicle weights satisfy convergence tests and the computational procedure is terminated following the computation of required auxiliary output values. The pertinent mission, vehicle, and performance data are obtained on a three page printout. A typical mission analysis computer printout is shown in Fig. II-3.

Trajectory Data

Stopover and Unpowered Swingby Missions - The stopover and unpowered swingby mission requires three independent parameters to completely specify the trajectory. Figures I-4, I-5 and I-6 in Chapter I show these trajectories. The set of three independent parameters used in this study includes the arrive planet date and the outbound and inbound leg times. This selection permits all of the dependent trajectory parameters (leave and arrive earth velocities, arrive and leave target planet velocities, and the perihelion distance for the stopover mission, plus periplanet distance and the third leg time for the swingby mission) to be expressed as functions of only two of these independent trajectory parameters. This greatly eases the problems associated with the generation and storage of trajectory data. In addition, the leg time optimization equations are simplified.

TYPICAL OUTPUT FORMAT

```
POINT VEHICLE DESIGN  MANNED MARS MISSION 1982
850 SEC ISP  TWO ENGINE CLUSTER
 PROBLEM NO.   5

              SEQUENCE OF EVENTS, INCLUDING OPTIONS CHOSEN.

                   LEN - EARTH DEPART - NUCLEAR PROPULSION
                       - OUTBOUND MIDCOURSE CORRECTION - STORABLE PROPULSION
                   APN - PLANET BRAKING - NUCLEAR PROPULSION
                   LPN - PLANET DEPART - NUCLEAR PROPULSION
                       - INBOUND MIDCOURSE CORRECTION - STORABLE PROPULSION
                   AEC - EARTH BRAKING - AERO PLUS CRYOGENIC RETRO 00   0.78749999E 01 KM/SEC.

GENERAL RESULTS AND DATA              NO. ITERATIONS =     3

OPTIMUM JULIAN DATES FOR   LEAVING EARTH     ARRIVING PLANET    LEAVING PLANET     ARRIVING EARTH     ARE
                         0.24449667E 07    0.24451850E 07    0.24493208E 07    0.24496222E 07

TOTAL TRIP TIME, IN DAYS, IS   0.45540073E 03 .  THE LEG TIMES ARE
   OUTBOUND LEG 1    OUTBOUND LEG 2    STOP OVER TIME     INBOUND LEG 1     INBOUND LEG 2
   0.21909230E 03            *         0.20000000E 02    0.21630849E 03            *

PERIHELION DISTANCE, IN A.U., IS    0.52634771E 00

VARIOUS WEIGHTS, IN LB, OF INTEREST.

WT. AFTER AERO BRAKING AT PLANET              *       WT. HEAT SHIELD AT PLANET                  *

WT. PLANET LANDER                  0.80000000E 05  WT. PICKUP AT PLANET          0.15000000E 04

WT. OF MISSION MODULE IS SUM OF
SOLAR RADIATION SHIELD WT.         0.22939073E 05  AND CREW COMPARTMENT WT.       0.68733999E 05

WT. AFTER RETRO BRAKING AT EARTH    0.13825576E 05

ARBITRARY WT. DROPPED OUTBOUND     0.              ARBITRARY WT. DROPPED INBOUND   0.
```

Figure II-3 Typical Output Format

TYPICAL OUTPUT FORMAT (CONTINUED)

RESULTS AND DATA

| | LEAVE EARTH | OUTBOUND MIDCOURSE CORRECTION | ARRIVE PLANET | LEAVE PLANET |
|---|---|---|---|---|
| SPECIFIC IMPULSE (SEC) | 0.85000000E 03 | 0.850000000E 03 | 0.850000000E 03 | 0.850000000E 03 |
| THRUST (LB)-NUC | 0.45236199E 06 | | 0.22618099E 06 | 0.22618099E 06 |
| THRUST/WEIGHT-NUC | 0.22967221E-00 | | 0.23681882E-00 | 0.49211431E-00 |
| ENGINE WEIGHT (LB)-NUC | 0.77956999E 05 | | 0.37445000E 05 | 0.37445000E 05 |
| FIRING TIME (SEC)-NUC | 0.13584719E 04 | | 0.11504000E 04 | 0.61712332E 03 |
| AFTERCOOLING TIME (SEC)-NUC | * | | * | * |
| OPTIMUM VELOCITY (KM/SEC) | 0.38024227E 01 | | 0.32124463E 01 | 0.53264606E 01 |
| PROPULSION VELOCITY (KM/SEC) | 0.38024227E 01 | 0.09999999E-00 | 0.32124463E 01 | 0.53264606E 01 |
| GRAVITY LOSS FACTOR | 0.10482758E 01 | | 0.10250300E 01 | 0.10161722E 01 |
| MASS RATIO | 0.15799353E 01 | 0.10314601E 01 | 0.14716904E 01 | 0.18978214E 01 |
| TANK MASS FRACTION | 0.84590907E 00 | 0.84897889E 00 | 0.81663588E 00 | 0.81697331E 00 |
| NUMBER OF TANKS | 0.20000000E 01 | 0.09999999E 01 | 0.09999999E 01 | 0.09999999E 01 |
| PROPELLANT WEIGHT (LB) | 0.72296599E 06 | 0.31635582E 05 | 0.30611603E 06 | 0.21743266E 06 |
| PROPELLANT-AFTERCOOLING (LB) | * | * | * | * |
| TOTAL WEIGHT BEFORE (LB) | 0.19695982E 07 | 0.10369797E 07 | 0.85508032E 06 | 0.45961069E 06 |
| FINAL WEIGHT AFTER (LB) | 0.10369797E 07 | 0.99971662E 06 | 0.54114160E 06 | 0.15332090E 06 |
| JETTISON WEIGHT (LB) | 0.80965260E 06 | 0.56275143E 04 | 0.30768269E 06 | 0.30057214E 05 |
| STRUCTURAL WEIGHT (LB) | 0.13184561E 06 | 0.56275143E 04 | 0.42330099E 05 | 0.44825781E 05 |
| PROPELLANT VAPORIZED (LB) | | | 0.11548414E 05 | 0.12054775E 05 |
| FUEL VAPORIZED (LB) | | | * | * |
| OXIDIZER VAPORIZED (LB) | | | * | * |
| TANK INSULATION (LB) | | | 0.37445000E 04 | 0.44863240E 04 |
| FUEL INSULATION (LB) | | | * | * |
| OXIDIZER INSULATION (LB) | | | * | * |
| STAGE MASS FRACTION | 0.77520006E 00 | 0.84897889E 00 | 0.74659000E 00 | 0.72087754E 00 |

Figure II-3 Typical Output Format (Continued)

TYPICAL OUTPUT FORMAT (CONTINUED)

| | INBOUND MIDCOURSE CORRECTION | ARRIVE EARTH | INTERMEDIATE VELOCITY CHANGE | THIRD MIDCOURSE CORRECTION |
|---|---|---|---|---|
| SPECIFIC IMPULSE (SEC) | 0.33000000E 03 | 0.44000000E 03 | • | • |
| THRUST (LB)-NUC | | | • | |
| THRUST/WEIGHT-NUC | | | • | |
| ENGINE WEIGHT (LB)-NUC | | | • | |
| FIRING TIME (SEC)-NUC | | | • | |
| AFTERCOOLING TIME (SEC)-NUC | | | • | |
| OPTIMUM VELOCITY (KM/SEC) | | 0.10341997E 02 | • | |
| PROPULSION VELOCITY (KM/SEC) | 0.09999999E-00 | 0.29669978E 01 | • | • |
| GRAVITY LOSS FACTOR | | | | |
| MASS RATIO | 0.10314681E 01 | 0.19926280E 01 | • | • |
| TANK MASS FRACTION | 0.78937627E 00 | 0.75864427E 00 | • | • |
| NUMBER OF TANKS | 0.09999999E 01 | 0.09999999E 01 | • | • |
| PROPELLANT WEIGHT (LB) | 0.46774464E 04 | 0.21103316E 05 | • | • |
| PROPELLANT-AFTERCOOLING (LB) | | | | |
| TOTAL WEIGHT BEFORE (LB) | 0.15932090E 06 | 0.42868487E 05 | | |
| FINAL WEIGHT AFTER (LB) | 0.14739541E 06 | 0.09999999E 05 | | |
| JETTISON WEIGHT (LB) | 0.12480502E 04 | 0.74345640E 04 | • | • |
| STRUCTURAL WEIGHT (LB) | 0.12480502E 04 | 0.66723303E 04 | • | • |
| PROPELLANT VAPORIZED (LB) | | 0.22654656E 04 | • | |
| FUEL VAPORIZED (LB) | | 0.17109642E 04 | • | |
| OXIDIZER VAPORIZED (LB) | | 0.55450145E 03 | • | |
| TANK INSULATION (LB) | | 0.76223370E 03 | • | |
| FUEL INSULATION (LB) | | 0.57566734E 03 | • | |
| OXIDIZER INSULATION (LB) | | 0.18656636E 03 | • | |
| STAGE MASS FRACTION | 0.78937627E 00 | 0.75864427E 00 | • | • |

Figure II-3 Typical Output Format (Continued)

A discussion of the procedure used in generating the stopover trajectory data is useful to provide some insight into the optimization technique. The inbound and outbound legs are treated separately by selecting either an arrive planet or a depart planet date. A discrete set of outbound or inbound trip times are then considered, and the dependent velocities and perihelion distances obtained by free flight trajectory simulations as a function of the trip time, for the fixed arrive or depart date. For this arrive or depart date, the range of trip times that contains all possible optimum trajectories can be determined and the data within this range are processed for storage. The arrive planet or depart planet date is then changed by a uniform interval, and the process repeated for another set of trip times. In this manner, an entire set of maps of the dependent variables as functions of the independent parameters are obtained. The stopover trajectory data used in this study were taken from Ref. 1. The hyperbolic excess velocities were converted to characteristic velocities, based on a 500 km circular orbit at earth and a 600 km circular orbit at Mars and Venus.

Powered Swingby Mission - The powered turn swingby mission introduces two additional degrees of freedom to the trajectory specifications. However, it has been shown (Ref. 2) that there is an optimum relationship between the periplanet distance, PP, and the impulsive velocity change, VI, when passing the swingby planet. This relationship can be used while generating the trajectory data to obtain the optimum combination of PP and VI. If the optimum PP is less than the minimum pass distance, PPMIN, for any particular set of independent parameters, PP must be set equal to PPMIN and the corresponding VI calculated. Using this set of values results in only one new degree of freedom. The parameter selected as the additional independent parameter is the third leg time, which may be the leg time between earth and the swingby planet for an outbound swingby and between the swingby planet and earth for an inbound swingby.

The powered swingby trajectory data is generated much the same as for the stopover mission. For an inbound swingby, the depart planet date is set, the inbound leg time to the swingby planet is set, and the third leg time is then varied over a discrete set of values. The leave planet, optimum swingby, and arrive earth velocities, the optimum periplanet distance, and the perihelion

distance, are obtained as a function of the third leg time for the fixed planet date and inbound leg time. If PP < PPMIN, the VI corresponding to PPMIN is obtained.

The inbound leg time is then changed by a uniform interval, and the process repeated for another range of third leg times. This is continued over the desired inbound leg time range. The leave planet date is then incremented, and the entire process repeated for another inbound leg time range, and more third leg time ranges. These ranges may change every time so that only those trajectories giving minimum and near minimum velocities need be stored in the program.

Since no consistent set of powered swingby trajectory data was available, it was not possible to analyze any powered swingby missions during the study. Nevertheless, the powered swingby option of the SWOP program is fully developed and has been checked out as far as is feasible without actual trajectory data being available.

Derivation of Optimization Equations

There are several sets of optimization equations for the different combinations of stopover missions and powered and unpowered, inbound and outbound, swingby missions. In addition, different forms of the equations result when certain constraints are imposed, such as a specified or constrained total trip time. For the purposes of reporting, it is only necessary to derive the optimization equations for one of these sets. Therefore, only the optimization equations for the inbound powered swingby mission are derived in detail. However, the equations for all missions are listed at the end of this section.

The optimization of the trajectory to obtain minimum initial vehicle weight uses the calculus of maxima and minima theorem that states that a function, f, is at a maxima or minima point when the total differential is equal to zero. This occurs when each partial derivative of f is equal to zero. That is,

$$df = \frac{\partial f}{\partial X_1} dX_1 + \frac{\partial f}{\partial X_2} dX_2 + \text{-----}$$

$$= 0$$

if

$$\frac{\partial f}{\partial X_i} = 0, \; i = 1, 2, \text{----}$$

For the inbound powered swingby mission (SWOP - IB powered) there are four independent parameters. These are the outbound trip time, TO, the arrive planet date, TAP, the first inbound leg time, TI1, and the second inbound leg time, TI2. If the vehicle payload ratio is PLR = $W_{initial}/W_{final}$ the minimum vehicle weight (or maximum payload) occurs when

$$d(PLR) = \frac{\partial(PLR)}{\partial(TO)}\, d(TO) + \frac{\partial(PLR)}{\partial(TAP)}\, d(TAP) + \frac{\partial(PLR)}{\partial(TI1)}\, d(TI1) + \frac{\partial(PLR)}{\partial(TI2)}\, d(TI2) = 0 \tag{1}$$

or when

$$\frac{\partial(PLR)}{\partial(TO)} = 0 \tag{2}$$

$$\frac{\partial(PLR)}{\partial(TAP)} = 0 \tag{3}$$

$$\frac{\partial(PLR)}{\partial(TI1)} = 0 \tag{4}$$

$$\frac{\partial(PLR)}{\partial(TI2)} = 0 \tag{5}$$

Equations 2 to 5 must all equal zero simultaneously to satisfy Eq. 1.

The first step is deriving the four optimization equations is to set up the payload ratio equation, which defines the entire vehicle as a function of the trajectory parameters and vehicle constants.

The dependent trajectory parameters which affect the vehicle weight are the five major velocity changes and the perihelion distance, $r_p$, which are functions of two or three of the four independent trajectory parameters TO, TAP, TI1, and TI2. The functional dependence of these parameters is

$$VLE = f(TO, TAP)$$
$$VAP = f(TO, TAP)$$
$$VLP = f(TDP, TI1)$$
$$VI = f(TDP, TI1, TI2)$$
$$VAE = f(TDP, TI1, TI2)$$
$$r_p = f(TDP, TI1, TI2)$$

where the depart planet date, TDP, is simply related to the arrive planet date, TAP, by the stopover time, TSO.

The jettison weight of each stage of the vehicle is represented by the structure factor, obtained from the vehicle weight calculation. Figure II-4 shows the symbols used in the equations. The "W's" represent the vehicle weight throughout the mission before and after every velocity or payload change. The "V's" followed by two or three letters represent the following velocity changes: leave earth, outbound midcourse correction, arrive planet, circularizing orbit (if needed), leave planet, first inbound midcourse correction, planet swingby, second inbound midcourse correction, arrive earth retro, and arrive earth aero braking. The " $\Delta W$" symbols represent any abrupt weight changes, such as a planet lander or mission module, and the "R· T" symbols represent the time dependent weight changes, such as vaporizing propellant and life support expendables. Using these definitions, the vehicle payload ratio is

$$PLR = \frac{WBLE}{WAAE} = \frac{1}{WAAE}\,\frac{WBLE}{WALE}\,\frac{WALE}{WACO}\left(\Delta WO + RO\cdot TO + \frac{WBAP}{WAAP}\,\frac{WAAP}{WAAP'}\left\{\Delta WPLANET + \frac{WBLP}{WALP}\,\frac{WALP}{WACI1}\left[\Delta WI1 + RI1\cdot TI1 + \frac{WBVI}{WAVI}\,\frac{WAVI}{WACI2}\left(\Delta WI2 + RI2\cdot TI2 + \Delta WMM + \frac{WBAE}{WBAE'}\,WBAE'\right)\right]\right\}\right) \quad (6)$$

where

$\frac{WBLE}{WALE}$ = leave earth payload ratio

$= f(VLE)$

$= \left[\frac{r(1-\sigma)}{1-r\sigma}\right]_{LE}$

$\frac{WALE}{WACO}$ = Outbound midcourse correction payload ratio, assumed independent of trajectory parameters

$= KCO$

$\Delta WO$ = Net payload weight jettisoned during outbound leg

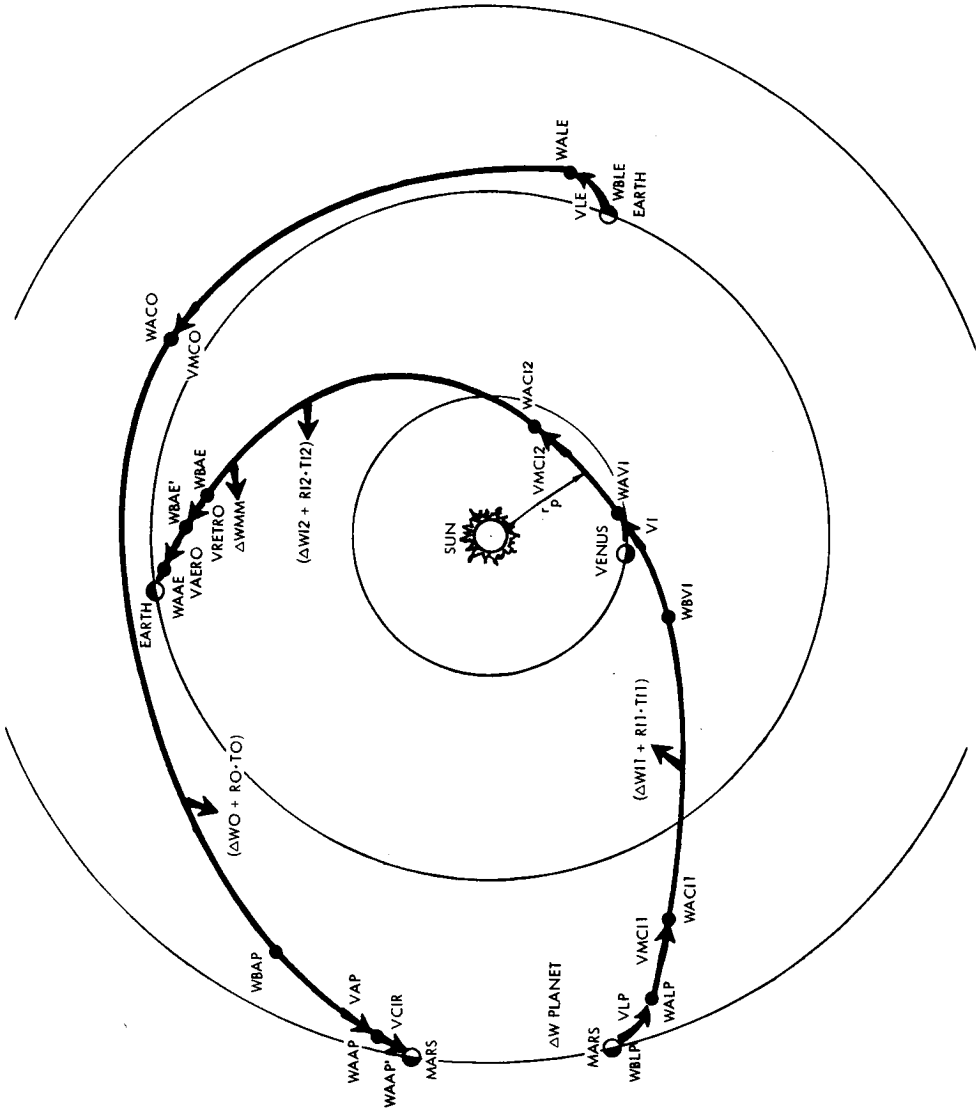


Figure II-4 SWOP Parameter Notation

$\frac{WBAP}{WAAP}$ = Arrive planet payload ratio

= f (VAP)

= $\left[\frac{r\,(1-\sigma)}{1-r\,\sigma}\right]_{AP}$ (for propulsive braking)

= $\left\{1-K\left[C\,(VAP)^2 + D\,(VAP) + E\right]\right\}^{-1}$ (for aero braking)

$\frac{WAAP}{WAAP'}$ = Orbit circularlizing stage, used only for arrive planet aerobraking, assumed independent of trajectory parameters

= KCR

$\Delta$WPLANET = Net weight change during planet stopover, including attitude control, vaporized propellant, etc.

$\frac{WBLP}{WALP}$ = Leave planet payload ratio

= f (VLP)

= $\left[\frac{r\,(1-\sigma)}{1-r\,\sigma}\right]_{LP}$

$\frac{WALP}{WACI1}$ = First inbound midcourse correction payload ratio, assumed independent of trajectory parameters

= KCI1

$\Delta$WI1 = Net payload weight jettisoned during first inbound leg

$\frac{WBVI}{WAVI}$ = Swingby velocity change payload ratio

= f (VI)

= $\left[\frac{r\,(1-\sigma)}{1-r\,\sigma}\right]_{VI}$

$\frac{WAVI}{WACI2}$ = Second inbound midcourse correction payload ratio, assumed independent of trajectory parameters

= KCI2

$\Delta$WI2 = Net payload weight jettisoned during second inbound leg

$\Delta$WMM = Mission module weight jettisoned before braking at earth. Includes crew compartment, WCC, and a solar flare shield

= $WCC + A + \frac{B}{r_p - C}$

$\frac{WBAE}{WBAE'}$ = Arrive earth retro stage payload ratio. Equal to unity for an all aero reentry

$$= f(VRETRO) = f(VAE\text{-}VAERO) = \left[\frac{r(1-\sigma)}{1-r\sigma}\right]_{VRETRO}$$

WBAE' = Arrive earth aero braking weight. Includes heat shield and earth landed weight. VAERO = VAE for all aero-braking; VAERO = maximum permissible aerobraking velocity DV9A for retro plus aerobraking.

$$= f(VAERO) = C(VAERO)^2 + D(VAERO) + E$$

and

r = Propulsion mass ratio

$$= \exp\left[\frac{\Delta V_{ch}}{g\ ISP}\right]$$

$\Delta V_{ch}$ = Characteristic velocity including losses for a propulsion stage

g = Gravitational constant

ISP = Specific impulse for propulsion stage

$\sigma$ = Stage structure factor

$$= \frac{W_{jettison}}{W_{jettison} + W_{propellant}}$$

$r_p$ = Perihelion distance

$P_p$ = Periplanet distance

The aerobraking and solar flare shield weight scaling laws and the values of their constants are discussed in separate sections in Chapter III. Only their functional form is of interest here.

The optimization equations are obtained by differentiating Eq. 6 with respect to each of the four independent trajectory parameters (Eqs. 2 to 5).

Outbound Leg Time Optimization Equation - The outbound leg for a SWOP-IB powered mission is the same as for a stopover mission. Thus, the same optimization equation is valid for both missions. Only the leave earth and arrive planet velocity changes are functions of the outbound leg time, TO. Differentiating Eq. 6 with respect to TO (Eq. 2) gives

$$\frac{\partial (PLR)}{\partial TO} = \frac{KCO}{WAAE} \left\{ (WACO) \frac{\partial (WBLE/WALE)}{\partial VLE} \frac{\partial VLE}{\partial TO} + \frac{WBLE}{WALE} \left[ RO + KCR\ (WAAP') \frac{\partial (WBAP/WAAP)}{\partial VAP} \frac{\partial VAP}{\partial TO} \right] \right\}$$

$$= 0$$

Therefore,

$$(WACO) \frac{1}{(WBLE/WALE)} \frac{\partial (WBLE/WALE)}{\partial VLE} \frac{\partial VLE}{\partial TO} + RO + (WBAP) \frac{1}{(WBAP/WAAP)} \frac{\partial (WBAP/WAAP)}{\partial VAP} \frac{\partial VAP}{\partial TO} = 0$$

In a later section, the weight derivatives or vehicle exchange ratios will be shown to have a relatively simple form. For the present, they will be represented by constants. Defining

$$GLE = (WACO) \frac{1}{(WBLE/WALE)} \frac{\partial (WBLE/WALE)}{\partial VLE} \tag{7}$$

and

$$GAP = (WBAP) \frac{1}{(WBAP/WAAP)} \frac{\partial (WBAP/WAAP)}{\partial VAP} \tag{8}$$

the optimization equation for the outbound trip time becomes

$$GLE \frac{\partial VLE}{\partial TO} + RO + GAP \frac{\partial VAP}{\partial TO} = 0 \tag{9}$$

The velocity derivatives are found by curve fitting the stored trajectory data. This will be discussed in a later section.

Inbound Leg 1 Optimization Equation - The leave planet, swingby, and arrive earth velocity changes and the perihelion distance are functions of the first inbound leg time, TI1. Differentiating Eq. 6 with respect to TI1 (Eq. 4) gives

$$\frac{\partial (PLR)}{\partial TI1} = \frac{KCO}{WAAE} \frac{WBLE}{WALE} \frac{WBAP}{WAAP} KCR\ KCI1 \left( (WACI1) \frac{\partial (WBLP/WALP)}{\partial VLP} \frac{\partial VLP}{\partial TI1} + \frac{WBLP}{WALP} \left\{ RI1 + KCI2\ (WACI2) \frac{\partial (WBVI/WAVI)}{\partial VI} \frac{\partial VI}{\partial TI1} + KCI2 \frac{WBVI}{WAVI} \left[ \frac{\partial \Delta WMM}{\partial r_p} \frac{\partial r_p}{\partial TI1} + \frac{\partial (WBAE/WBAE')\ WBAE'}{\partial VAE} \frac{\partial VAE}{\partial TI1} \right] \right\} \right)$$

$$= 0$$

Therefore,

$$(WACI1)\ \frac{1}{(WBLP/WALP)}\ \frac{\partial (WBLP/WALP)}{\partial VLP}\ \frac{\partial VLP}{\partial TI1}$$

$$+\ RI1\ +\ (WBVI)\ \frac{1}{(WBVI/WAVI)}\ \frac{\partial (WBVI/WAVI)}{\partial VI}\ \frac{\partial VI}{\partial TI1}$$

$$+\ KCI2\ \frac{WBVI}{WAVI}\left[\frac{\partial \Delta WMM}{\partial r_p}\ \frac{\partial r_p}{\partial TI1} + \frac{\partial (WBAE/WBAE')\ WBAE'}{\partial VAE}\ \frac{\partial VAE}{\partial TI1}\right]$$

$$=\ 0$$

As before, the constants that depend on the vehicle calculations are defined.

$$GLP = (WACI1)\ \frac{1}{(WBLP/WALP)}\ \frac{\partial (WBLP/WALP)}{\partial VLP} \tag{10}$$

$$GVI = (WBVI)\ \frac{1}{(WBVI/WAVI)}\ \frac{\partial (WBVI/WAVI)}{\partial VI} \tag{11}$$

$$GRP = \frac{\partial \Delta WMM}{\partial r_p} \tag{12}$$

$$GAE = \frac{\partial (WBAE/WBAE')\ WBAE'}{\partial VAE} \tag{13}$$

The optimization equation for the first inbound leg time thus becomes

$$GLP\ \frac{\partial VLP}{\partial TI1} + RI1 + GVI\ \frac{\partial VI}{\partial TI1}$$

$$+\ KCI2\ \frac{WBVI}{WAVI}\left(GRP\ \frac{\partial r_p}{\partial TI1} + GAE\ \frac{\partial VAE}{\partial TI1}\right) = 0 \tag{14}$$

Inbound Leg 2 Optimization Equation - The swingby and arrive earth velocity changes and the perihelion distance are functions of the second inbound leg time, TI2. Differentiating Eq. 6 with respect to TI2 (Eq. 5) results in

$$\frac{\partial(PLR)}{\partial TI2} = \frac{KCO}{WAAE}\ \frac{WBLE}{WALE}\ \frac{WBAP}{WAAP}\ KCR\ KCI1\ \frac{WBLP}{WALP}$$

$$KCI2\left\{(WACI2)\ \frac{\partial(WBVI/WAVI)}{\partial VI}\ \frac{\partial VI}{\partial TI2} + \frac{WBVI}{WAVI}\right.$$

$$\left.\left[RI2 + \frac{\partial \Delta WMM}{\partial r_p}\ \frac{\partial r_p}{\partial TI2} + \frac{\partial(WBAE/WBAE')WBAE'}{\partial VAE}\ \frac{\partial VAE}{\partial TI2}\right]\right\}$$

$$= 0$$

Using the definitions expressed by Eqs. 11 to 13, the optimization equation for the second inbound leg time is

$$GVI\ \frac{\partial VI}{\partial TI2} + KCI2\ \frac{WBVI}{WAVI}\left(RI2 + GRP\ \frac{\partial r_p}{\partial TI2} + GAE\ \frac{\partial VAE}{\partial TI2} = \right) 0 \qquad (15)$$

Arrive Planet Date Optimization Equation - Since all of the dependent trajectory parameters are functions of the arrive planet date, TAP, (Some through the depart planet date, TDP = TAP + TSO) the arrive planet date optimization equation is somewhat complicated. Differentiating Eq. 6 with respect to TAP (Eq. 3) gives

$$\frac{\partial(PLR)}{\partial TAP} = \frac{KCO}{WAAE}\left\{(WACO)\ \frac{\partial(WBLE/WALE)}{\partial VLE}\ \frac{\partial VLE}{\partial TAP}\right.$$

$$+ \frac{WBLE}{WALE}\ KCR\left[(WAAP')\ \frac{\partial(WBAP/WAAP)}{\partial VAP}\ \frac{\partial VAP}{\partial TAP}\right.$$

$$+ \frac{WBAP}{WAAP}\ KCI1\left((WACI1)\ \frac{\partial(WBLP/WALP)}{\partial VLP}\ \frac{\partial VLP}{\partial TAP}\right.$$

$$+ \frac{WBLP}{WALP}\ KCI2\left\{(WACI2)\ \frac{\partial(WBVI/WAVI)}{\partial VI}\ \frac{\partial VI}{\partial TAP}\right.$$

$$\left.\left.\left.\left.+ \frac{WBVI}{WAVI}\left[\frac{\partial \Delta WMM}{\partial r_p}\ \frac{\partial r_p}{\partial TAP} + \frac{\partial(WBAE/WBAE')WBAE'}{\partial VAE}\ \frac{\partial VAE}{\partial TAP}\right]\right\}\right)\right]\right\}$$

$$= 0$$

Using the definitions from Eqs. 7, 8, 10, 11, 12, and 13, the optimization equation for the arrive planet date is

$$GLE\ \frac{\partial VLE}{\partial TAP} + GAP\ \frac{\partial VAP}{\partial TAP} + \left(KCR\ \frac{WBAP}{WAAP}\right)\left(KCI1\ \frac{WBLP}{WALP}\right)\left[GLP\ \frac{\partial VLP}{\partial TAP}\right.$$

$$\left. + GVI\ \frac{\partial VI}{\partial TAP} + \left(KC12\ \frac{WBVI}{WAVI}\right)\left(GRP\ \frac{\partial r_p}{\partial TAP} + GAE\ \frac{\partial VAE}{\partial TAP}\right)\right] \qquad (16)$$

$$= 0$$

The above four optimization equations (Eqs. 9, 14, 15, and 16) are sufficient to find the optimum values of the four independent trajectory parameters, based on the best estimate of the vehicle weights as reflected in the "G" constants or weight derivatives.

## Weight Derivatives

The optimization equations contain derivatives of the payload ratio (vehicle exchange ratios) for each of the main stages (Eqs. 7, 8, 10, 11, and 13) and also, a derivative of the solar flare shield weight. These derivatives exist for both propulsion and aero-braking main stages.

These derivatives can be easily calculated, using the definitions following Eq. 6. All of the derivatives are shown here in terms of the performance parameters and vehicle scaling laws. The constants for the scaling laws are discussed in Chapter III.

For a propulsion stage, the payload ratio is

$$PLR = \frac{WB}{WA}$$

$$= \frac{r\,(1-\sigma)}{1-r\,\sigma}$$

where

$r$ = mass ratio

$= \exp\,(\Delta V/gISP)$

$\sigma$ = stage structure factor

and

$$= \frac{W_{jettison}}{W_{jettison} + W_{propellant}}$$

The normalized derivative of PLR with respect to the velocity change is

$$\frac{1}{PLR}\ \frac{\partial(PLR)}{\partial \Delta V} = \left[\frac{1 - r\sigma}{r\,(1-\sigma)}\right]\left[\frac{r\,(1-\sigma)}{(gISP)\,(1-r\sigma)^2}\right]$$

$$= \left[\frac{1}{(gISP)\,(1-r\sigma)}\right]_{\text{propulsion}} \tag{17}$$

It is assumed that $\sigma$ is a constant. However, since it is recalculated every iteration, its effect in the optimization is taken into account indirectly. The above equation can be used for any of the propulsion stages, using the appropriate values of the parameters, $\sigma$, r, and ISP. The equation is multiplied by the appropriate vehicle weight indicated in Eqs. 7, 8, 9, 10, 11, and 13 and defined on p. II-14 and Fig. II-4 to obtain GLE, GAP, GVI, and GAE for propulsive stages.

For the arrive Mars aerodynamic braking mode, the derivative of the aero braking scaling law is used for the payload derivative.

$$PLR_{AM_{aero}} = \frac{1}{1-K(CVAM^2 + DVAM + E)}$$

$$\frac{1}{PLR}\ \frac{\partial PLR}{\partial V_{AM}} = \left[\frac{K\,(2CVAM + D)}{1 - K(CVAM^2 + DVAM + E)}\right]_{\text{arrive Mars aero}} \tag{18}$$

the above equation is multiplied by WBAP to obtain GAP (Eq. 8).

The influence of the perihelion distance on the optimum trajectory and vehicle weight is expressed in the solar flare shield weight. For an assumed level of solar activity and approximate total trip time, the mission module weight is

$$\Delta WMM = WCC + A + \frac{B}{r_p - C}$$

thus

$$\frac{\partial\, \Delta WMM}{\partial r_p} = \frac{-B}{(r_p - C)^2} \tag{19}$$

The derivative of the arrive earth payload ratio can take two forms, one for an all aero entry mode and one for a mode employing a propulsive retro followed by aerobraking from a specified velocity, DV9A.

For the all aero mode, the vehicle weight before braking is

$$\frac{WBAE}{WBAE'} \quad WBAE' = C\ VAE^2 + D\ VAE + E$$

and GAE (Eq. 13) is

$$\frac{\partial\,(WBAE/WBAE')\ WBAE'}{\partial\ VAE} = 2\ C\ VAE + D \tag{20}$$

For the retro plus aero mode, the vehicle weight before braking is

$$\frac{WBAE}{WBAE'} \quad WBAE' = \left[\frac{r\,(1-\sigma)}{1 - r\sigma}\right] \quad \left[C\ VA^2 + D\ VA + E\right]$$

and GAE is

$$\frac{\partial(WBAE/WBAE')\ WBAE'}{\partial\ VAE} = \left[\frac{r(1-\sigma)}{gISP\,(1-r\sigma)}^2\right] \quad \left[C\ VA^2 + D\ VA + E\right] \tag{21}$$

where $r = \exp\left(\frac{VAE - DV9A}{g\ ISP}\right)$

and $VA = DV9A$

Trajectory Derivatives

Partial derivatives of all the dependent trajectory parameters are needed in the optimization equations. These are obtained by two or three dimensional curve-fitting of the stored trajectory data with 2nd order polynomials. Figure II-5 indicates the stored trajectory map for one of the velocities as a function of a leg time, TO, and the arrive planet date, TAP. For a two dimensional curve fit, the nine points (3 x 3 array) closest to the optimum TO and TAP are selected. For the partial derivative, $\partial V/\partial TAP$, the procedure in effect is to find the values of the velocity at the optimum TO, by three curve fits, for the three arrive planet dates. These velocity values are then curve-fitted in the TAP direction to get the equation for the velocity as a function of TAP.

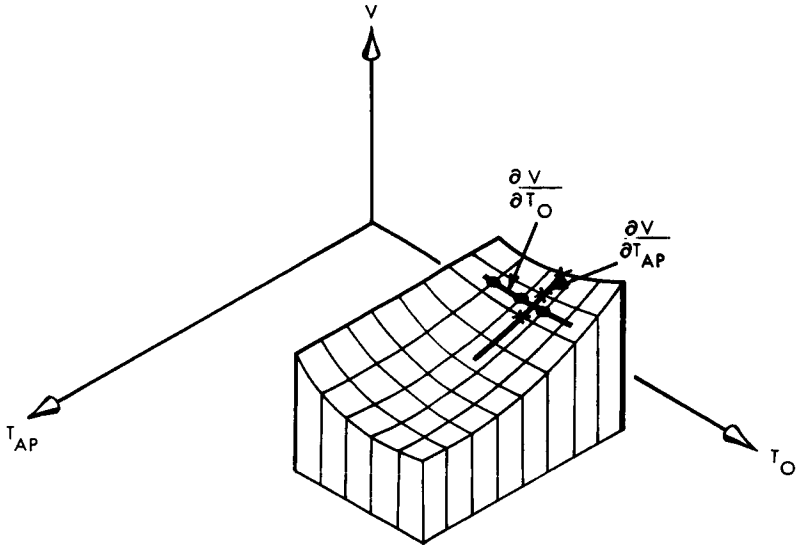


FINDING PARTIAL DERIVATIVES FROM STORED DATA

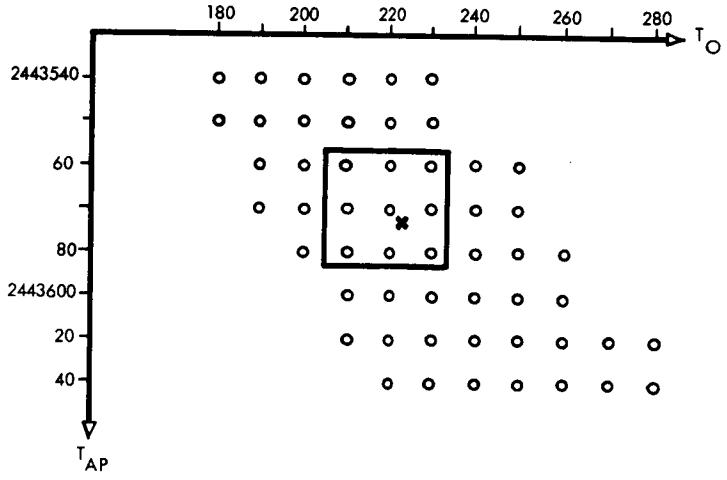


PLAN VIEW OF STORED TRAJECTORY DATA

Figure II-5 Stored Trajectory Data Map

$$V = A(TAP)^2 + B(TAP) + C$$

Thus

$$\frac{\partial V}{\partial TAP} = 2A(TAP) + B \tag{22}$$

For the parameters that are functions of the depart planet date, TDP rather than TAP, the 3 x 3 array is centered around the TDP = TAP + TSO. The resultant equation for the partial derivative is

$$\frac{\partial V}{\partial TAP} = 2A(TAP + TSO) + B \tag{23}$$

This procedure is repeated for all the partial derivatives needed, using the appropriate 3 x 3 or 3 x 3 x 3 arrays for curve-fitting.

The detailed equations used for the two and three dimensional curve fits are shown below.

Two-dimensional Curve Fits - The procedure used to obtain the partial derivative for a two-dimensional array is described in this section using $Y = f(X, Z)$ as an example. The coefficients of $Y(X, Z^*) = A X^2 + BX + C$ are found, where $X^*$ and $Z^*$ are the estimated optimum values of X and Z. The components in the 3 x 3 array around $X^*$ and $Z^*$ are numbered as shown.

| | | $\longrightarrow X$ | | |
|---|---|---|---|---|
| | | $(X_1)$ | $(X_2)$ | $(X_3)$ |
| ↓ | $Z_1$ | $Y_{11}$ | $Y_{12}$ | $Y_{13}$ |
| Z | $Z_2$ | $Y_{21}$ | $Y_{22}$ | $Y_{23}$ |
| | $Z_3$ | $Y_{31}$ | $Y_{32}$ | $Y_{33}$ |

Define

$$F_1 = \frac{Z^* - Z_1}{2\,\Delta Z}, \text{ where } \Delta Z = Z_3 - Z_2 = Z_2 - Z_1$$

$$F_2 = F_1 \frac{(Z^* - Z_1)}{\Delta Z}$$

and

$$G_1 = 1 - 3F_1 + F_2$$

$$G_2 = 4F_1 - 2F_2$$

$$G_3 = -F_1 + F_2$$

Also,

$$D_i = Y_{i3} - 2Y_{i2} + Y_{i1}, \; i = 1, 2, 3$$

and

$$E_i = Y_{i3} - 4Y_{i2} + 3Y_{i1}, \; i = 1, 2, 3$$

Then the A coefficient is

$$A = \frac{1}{2(\Delta X)^2} \sum_{i=1}^{3} G_i D_i, \text{ where } \Delta X = X_2 - X_2 = X_2 - X_1$$

An intermediate constant is

$$K = \frac{1}{2(\Delta X)} \sum_{i=1}^{3} G_i E_i$$

Thus, the B coefficient is

$$B = -2(X_1)\,A - K$$

and lastly, the C coefficient is

$$C = A(X_1)^2 + K(X_1) + \sum_{i=1}^{3} G_i Y_{i1}$$

To get the partial derivative in the Z direction ( $\partial Y(X^*, Z)/\partial Z$), the 3 x 3 array is reflected about the diagonal and the same equations used, with the new Z's.

Three-dimensional Curve Fits - For the powered swingby mission, a few of the trajectory variables are dependent on three independent parameters. The procedure used to obtain the partial derivative for a three dimensional array is described in this section. As an example, $Y = f(X, Z, T)$ is used to find the coefficients of

$$Y(X, Z^*, T^*) = A X^2 + BX + C$$

where

$X^*$, $Z^*$, and $T^*$ are the estimated optimum values of X, Z, and T. The components in the 3 x 3 x 3 array around $X^*$, $Z^*$, and $T^*$ are numbered as shown.

| | | | T | | |
|---|---|---|---|---|---|
| | | | $(T_1)$ | $(T_2)$ | $(T_3)$ |
| | ↓ Z | $(Z_1)$ | $Y_{111}$ | $Y_{112}$ | $Y_{113}$ |
| $X_1$ | | $(Z_2)$ | $Y_{121}$ | $Y_{122}$ | $Y_{123}$ |
| | | $(Z_3)$ | $Y_{131}$ | $Y_{132}$ | $Y_{133}$ |
| | ↓ Z | $(Z_1)$ | $Y_{211}$ | $Y_{212}$ | $Y_{213}$ |
| $X_2$ | | $(Z_2)$ | $Y_{221}$ | $Y_{222}$ | $Y_{223}$ |
| | | $(Z_3)$ | $Y_{231}$ | $Y_{232}$ | $Y_{233}$ |
| | ↓ Z | $(Z_1)$ | $Y_{311}$ | $Y_{312}$ | $Y_{313}$ |
| $X_3$ | | $(Z_2)$ | $Y_{321}$ | $Y_{322}$ | $Y_{323}$ |
| | | $(Z_3)$ | $Y_{331}$ | $Y_{332}$ | $Y_{333}$ |

Using the two dimensional curve fitting procedure, the values of $Y(X_i, Z^*, T^*)$ are found for i = 1, 2, 3, where the three 3 x 3 arrays have been used separately.

A curve fit of $Y_1$, $Y_2$, and $Y_3$ in the X direction now quickly yields the desired coefficients.

$$A = \frac{(Y_3 - 2Y_2 + Y_1)}{2(\Delta X)^2}$$

$$K = \frac{(Y_3 - 4Y_2 + Y_1)}{2(\Delta X)}$$

$$B = -2(X_1)A - K$$

$$C = A(X_1)^2 + K(X_1) + Y_1$$

The 3 x 3 x 3 array is rotated twice to obtain the curve coefficients along the other two axis.

Solution of Optimization Equations

Once the weight derivatives and trajectory derivatives are calculated, it is only necessary to substitute them into the optimization equations and solve for the respective independent parameters. As an illustration, the outbound leg time and arrive planet date equations for the inbound powered swingby are solved in this section. The other equations are solved in an analogous way.

Outbound Leg Time Optimization Equation - Referring back to Eq. 9, the solution of the optimization equation takes the following form when the curve fitted trajectory derivatives as a function of TO are used.

$$TO = \frac{-\left[GLE(B_{LE}) + RO + GAP(B_{AP})\right]}{2\left[GLE(A_{LE}) + GAP(A_{AP})\right]} \qquad (24)$$

where $A_{LE}$, $B_{LE}$, $A_{AP}$, and $B_{AP}$ are the trajectory curve fit constants.

The other leg time equations have similar solutions.

Arrive Planet Date Optimization Equation - Using the curve fitted trajectory derivatives as a function of TAP and TDP, the solution of Eq. 16 is

$$TAP = -\left( \begin{array}{l} GLE(B_{LE}) + GAP(B_{AP}) + KCR \ \frac{WBAP}{WAAP} \ KCI1 \ \frac{WBLP}{WALP} \left\{ GLP(B_{LP}) \right. \\ \left. + GVI(B_{VI}) + KCI2 \ \frac{WBVI}{WAVI} \left[ GRP(B_{RP}) + GAE(B_{AE}) \right] + 2\,(TSO) \ K \right\} \end{array} \right) \div 2\left[ GLE(A_{LE}) + GAP(A_{AP}) + KCR \ \frac{WBAP}{WAAP} \ KCI1 \ \frac{WBLP}{WALP} \ (K) \right] \quad (25)$$

where

$$K = GLP(A_{LP}) + GVI(A_{VI}) + KCI2 \ \frac{WBVI}{WAVI} \left[ GRP(A_{RP}) + GAE(A_{RP}) \right]$$

Optimization of the Inbound Powered Swingby Mission With Constraints on Independent Parameters

It is possible to constrain any or all of the independent trajectory parameters, as well as any of the related parameters, such as the leave earth date. For the four independent trajectory parameters, this is done simply by not solving the optimization equation corresponding to the constrained parameter. For a constraint on the leave or arrive earth date, the arrive planet date optimization equation is not solved, and the arrive planet date is set equal to either the leave earth date plus the outbound time or the arrive earth date minus the inbound and the stopover time.

A constraint on the total trip time is harder to handle. This reduces the number of independent parameters by one. For the inbound powered swingby mission, the outbound leg time equation is solved as usual, but the two inbound legs (TI1 and TI2) are related through the total trip time constraint. The total trip time is

$$TTT = TO + TSO + TI1 + TI2$$

choosing TI2 as the dependent parameter, for constant total trip time

$$\frac{\partial TTT}{\partial TI1} = 0 = 1 + \frac{\partial TI2}{\partial TI1}$$

or

$$\frac{\partial TI2}{\partial TI1} = -1 \quad (26)$$

Now, differentiating the vehicle payload ratio (Eq. 6) with respect to TI1, the optimization equation for TI1 becomes

$$\frac{\partial(PLR)}{\partial TI1} = \frac{KCO}{WAAE}\ \frac{WBLE}{WALE}\ \frac{WBAP}{WAAP}\ KCR\ KCI1 \Bigg( (WACI1)\ \frac{\partial(WBLP/WALP)}{\partial VLP}\ \frac{\partial VLP}{\partial TI1}$$

$$+ \frac{WBLP}{WALP} \Bigg\{ RI1 + KCI2\ (WACI2)\ \frac{\partial(WBVI/WAVI)}{\partial VI} \left( \frac{\partial VI}{\partial TI1} + \frac{\partial VI}{\partial TI2}\ \frac{\partial TI2}{\partial TI1} \right)$$

$$+ KCI2\ \frac{WBVI}{WAVI} \Bigg[ RI2\ \frac{\partial TI2}{\partial TI1} + \frac{\partial \Delta WMM}{\partial r_p} \left( \frac{\partial r_p}{\partial TI1} + \frac{\partial r_p}{\partial TI2}\ \frac{\partial TI2}{\partial TI1} \right)$$

$$+ \frac{\partial(WBAE/WBAE')\ WBAE'}{\partial VAE} \left( \frac{\partial VAE}{\partial TI1} + \frac{\partial VAE}{\partial TI2}\ \frac{\partial TI2}{\partial TI1} \right) \Bigg] \Bigg\} \Bigg)$$

$$= 0$$

using the "G" definitions, and Eq. 26, the leg one optimization equation is

$$GLP\ \frac{\partial VLP}{\partial TI1} + RI1 + GVI \left( \frac{\partial VI}{\partial TI1} - \frac{\partial VI}{\partial TI2} \right)$$

$$+ KCI2\ \frac{WBVI}{WAVI} \Bigg\{ - RI2 + GRP \left( \frac{\partial r_p}{\partial TI1} - \frac{\partial r_p}{\partial TI2} \right) \qquad (27)$$

$$+ GAE \left( \frac{\partial VAE}{\partial TI1} - \frac{\partial VAE}{\partial TI2} \right) \Bigg\} = 0$$

This equation is now solved for TI1 using the calculated vehicle exchange ratios and the curve fitted trajectory data. The partials with respect to TI1 are used as usual, but the partials with respect to TI2 are

$$\frac{\partial V}{\partial TI2} = 2A\ (TTT - TO - TSO - TI1) + B$$

List of All Optimization Equations

The basic nomenclature defined in Figure II-4 is used for all of the equations. For the stopover mission, the second inbound leg and the swingby parameters do not exist. For the outbound swingby, the swingby parameters are switched into the outbound leg, and the first outbound leg TO1 with its associated phases occurs between earth and the swingby planet. For the unpowered swingby mode, there is no VI stage.

For each of the five mission modes, the optimization equations and the total trip time constraint equation are presented.

Stopover Mission - There are three independent parameters for a stopover mission. These are the outbound leg time, TO, the arrive planet date, TAP, and the inbound leg time, TI. The dependent parameters are

$$\begin{aligned} VLE &= f(TO, TAP) \\ VAP &= f(TO, TAP) \\ VLP &= f(TI, TDP) \\ VAE &= f(TI, TDP) \\ r_p &= f(TI, TDP) \end{aligned}$$

TO Equation

$$GLE \frac{\partial VLE}{\partial TO} + RO + GAP \frac{\partial VAP}{\partial TO} = 0 \qquad (28)$$

TAP Equation

$$GLE \frac{\partial VLE}{\partial TAP} + GAP \frac{\partial VAP}{\partial TAP} + \frac{WBAP}{WAAP} KCR \frac{WBLP}{WALP} KCI \left( GLP \frac{\partial VLP}{\partial TAP} + GRP \frac{\partial r_p}{\partial TAP} + GAE \frac{\partial VAE}{\partial TAP} \right) = 0 \qquad (29)$$

TI Equation

$$GLP \frac{\partial VLP}{\partial TI} + RI + GRP \frac{\partial r_p}{\partial TI} + GAE \frac{\partial VAE}{\partial TI} = 0 \qquad (30)$$

Constant Total Trip Time

Choosing TI as the dependent parameter,

$$TTT = TO + TSO + TI$$

thus

$$\frac{\partial TTT}{\partial TO} = 0 = 1 + \frac{\partial TI}{\partial TO}$$

and

$$\frac{\partial TI}{\partial TO} = -1$$

The optimization equation for TO becomes

$$GLE\ \frac{\partial VLE}{\partial TO} + RO + GAP\ \frac{\partial VAP}{\partial TO} + \frac{WBAP}{WAAP}\ KCR\ \frac{WBLP}{WALP}\ KCI \left( - GLP\ \frac{\partial VLP}{\partial TI} - RI - GRP\ \frac{\partial r_p}{\partial TI} - GAE\ \frac{\partial VAE}{\partial TI} \right) = 0 \qquad (31)$$

with $\frac{\partial V}{\partial TI} = 2A\ (TTT - TO - TSO) + B$

Outbound Gravity Turn Swingby Mission - There are three independent parameters for this mission. These are the second outbound leg time, TO2, the arrive planet date, TAP, and the inbound trip time, TI. The dependent parameters are

$$\begin{aligned} VLE &= f(TO2, TAP) \\ VAP &= f(TO2, TAP) \\ VLP &= f(TI, TDP) \\ VAE &= f(TI, TDP) \\ r_p &= f(TO2, TAP) \\ TO1 &= f(TO2, TAP) \\ P_p &= f(TO2, TAP) \end{aligned}$$

TO2 Equation

$$GLE\ \frac{\partial VLE}{\partial TO2} + RO1\ \frac{\partial TO1}{\partial TO2} + KCO2 \left( RO2 + GAP\ \frac{\partial VAP}{\partial TO2} + \frac{WBAP}{WAAP}\ KCR\ \frac{WBLP}{WALP}\ KCI\ GRP\ \frac{\partial r_p}{\partial TO2} \right) = 0 \qquad (32)$$

TAP Equation

$$GLE\ \frac{\partial VLE}{\partial TAP} + RO1\ \frac{\partial TO1}{\partial TAP} + KCO2 \left[ GAP\ \frac{\partial VAP}{\partial TAP} + \frac{WBAP}{WAAP}\ KCR\ \frac{WBLP}{WALP}\ KCI \left( GLP\ \frac{\partial VLP}{\partial TAP} + GRP\ \frac{\partial r_p}{\partial TAP} + GAE\ \frac{\partial VAE}{\partial TAP} \right) \right] = 0 \qquad (33)$$

TI Equation

$$GLP \frac{\partial VLP}{\partial TI} + RI + GAE \frac{\partial VAE}{\partial TI} = 0 \qquad (34)$$

Constant Total Trip Time

Choosing TO2 as the independent leg time parameter, both TO1 and TI are dependent parameters.

$$TTT = TO1 + TO2 + TSO + TI$$

thus

$$\frac{\partial TTT}{\partial TO2} = 0 = \frac{\partial TO1}{\partial TO2} + 1 + \frac{\partial TI}{\partial TO2}$$

and

$$\frac{\partial TI}{\partial TO2} = -\left(1 + \frac{\partial TO1}{\partial TO2}\right)$$

The optimization equation for TO2 is

$$GLE \frac{\partial VLE}{\partial TO2} + RO1 \frac{\partial TO1}{\partial TO2} + KCO2 \left[ RO2 + GAP \frac{\partial VAP}{\partial TO2} + \frac{WBAP}{WAAP} KCR \frac{WBLP}{WALP} KCI \left( GLP \frac{\partial VLP}{\partial TI} \frac{\partial TI}{\partial TO2} + RI \frac{\partial TI}{\partial TO2} + GRP \frac{\partial r_p}{\partial TO2} + GAE \frac{\partial VAE}{\partial TI} \frac{\partial TI}{\partial TO2} \right) \right] = 0 \qquad (35)$$

with

$$\frac{\partial V}{\partial TI} = 2A\,(TTT - TO1 - TO2 - TSO) + B$$

Inbound Gravity Turn Swingby Mission - There are three independent parameters for this mission. These are the outbound leg time, TO, the arrive planet date, TAP, and the first inbound leg time, TI1. The dependent parameters are

$$
\begin{aligned}
VLE &= f(TO, TAP) \\
VAP &= f(TO, TAP) \\
VLP &= f(TI1, TDP) \\
VAE &= f(TI1, TDP) \\
r_p &= f(TI1, TDP) \\
TI2 &= f(TI1, TDP) \\
P_p &= f(TI1, TDP)
\end{aligned}
$$

TO Equation

$$GLE \frac{\partial VLE}{\partial TO} + RO + GAP \frac{\partial VAP}{\partial TO} = 0 \quad \text{(same as Eq. 28)}$$

TAP Equation

$$GLE \frac{\partial VLE}{\partial TAP} + GAP \frac{\partial VAP}{\partial TAP} + \frac{WBAP}{WAAP} KCR \frac{WBLP}{WALP} KCI1 \left[ GLP \frac{\partial VLP}{\partial TAP} + KCI2 \left( RI2 \frac{\partial TI2}{\partial TAP} + GRP \frac{\partial r_p}{\partial TAP} + GAE \frac{\partial VAE}{\partial TAP} \right) \right] = 0 \quad (36)$$

TI1 Equation

$$GLP \frac{\partial VLP}{\partial TI1} + RI1 + KCI2 \left( RI2 \frac{\partial TI2}{\partial TI1} + GRP \frac{\partial r_p}{\partial TI1} + GAE \frac{\partial VAE}{\partial TI1} \right) = 0 \quad (37)$$

Constant Total Trip Time

Choosing TO as the independent parameter, both TI1 and TI2 are dependent parameters

$$TTT = TO + TSO + TI1 + TI2$$

thus $$\frac{\partial TTT}{\partial TO} = 0 = 1 + \frac{\partial TI1}{\partial TO} + \frac{\partial TI2}{\partial TI1} \quad \frac{\partial TI1}{\partial TO}$$

and $$\frac{\partial TI1}{\partial TO} = \frac{-1}{1 + \frac{\partial TI2}{\partial TI1}}$$

The optimization euqation for TO is

$$GLE \frac{\partial VLE}{\partial TO} + RO + GAP \frac{\partial VAP}{\partial TO} + \frac{WBAP}{WAAP} KCR \quad \frac{WBLP}{WALP} KCI1 \left[ GLP \frac{\partial VLP}{\partial TI1} \quad \frac{\partial TI1}{\partial TO} \right.$$

$$+ RI1 \frac{\partial TI1}{\partial TO} + KCI2 \left( RI2 \frac{\partial TI2}{\partial TI1} \quad \frac{\partial TI1}{\partial TO} + GRP \frac{\partial r_p}{\partial TI1} \quad \frac{\partial TI1}{\partial TO} + GAE \frac{\partial VAE}{\partial TI1} \quad \frac{\partial TI1}{\partial TO} \right) \Bigg]$$

$$= 0 \qquad (38)$$

with

$$\frac{\partial V}{\partial TI1} = 2A\,(TTT - TO - TSO - TI2) + B$$

Outbound Powered Turn Swingby Mission - There are four independent parameters for this mission. These are the first outbound leg time, TO1, the second outbound leg time TO2, the arrive planet date, TAP, and the inbound leg time TI. The dependent parameters are

$$VLE = f(TO1, TO2, TAP)$$

$$VI = f(TO1, TO2, TAP)$$

$$VAP = f(TO2, TAP)$$

$$VLP = f(TI, TDP)$$

$$VAE = f(TI, TDP)$$

$$r_p = f(TO1, TO2, TAP)$$

$$P_p = f(TO1, TO2, TAP)$$

TO1 Equation

$$GLE \frac{\partial VLE}{\partial TO1} + RO1 + GVI \frac{\partial VI}{\partial TO1} +$$

$$+ \frac{WBVI}{WAVI} KCO2 \frac{WBAP}{WAAP} KCR \frac{WBLP}{WALP} KCI GRP \frac{\partial r_p}{\partial TO1} = 0 \quad (39)$$

TO2 Equation

$$GLE \frac{\partial VLE}{\partial TO2} + GVI \frac{\partial VI}{\partial TO2} + \frac{WBVI}{WAVI} KCO2 \left( RO2 + \right.$$

$$\left. + GAP \frac{\partial VAP}{\partial TO2} + \frac{WBAP}{WAAP} KCR \frac{WBLP}{WALP} KCI GRP \frac{\partial r_p}{\partial TO2} \right) = 0 \quad (40)$$

TAP Equation

$$GLE \frac{\partial VLE}{\partial TAP} + GVI \frac{\partial VI}{\partial TAP} + \frac{WBVI}{WAVI} KCO2 \left[ GAP \frac{\partial VAP}{\partial TAP} \right.$$

$$\left. + \frac{WBAP}{WAAP} KCR \frac{WBLP}{WALP} KCI \left( GLP \frac{\partial VLP}{\partial TAP} + GRP \frac{\partial r_p}{\partial TAP} + GAE \frac{\partial VAE}{\partial TAP} \right) \right] =$$

(41)

TI Equation

$$GLP \frac{\partial VLP}{\partial TI} + RI + GAE \frac{\partial VAE}{\partial TI} = 0 \qquad \text{(same as Eq. 34)}$$

Constant Total Trip Time

This constraint still leaves two leg times as independent parameters. Solve for TI the usual way, and choose TO1 as a dependent parameter of TO2.

$$TTT = TO1 + TO2 + TSO + TI$$

$$\frac{\partial TTT}{\partial TO2} = \frac{\partial TO1}{\partial TO2} + 1$$

or $$\frac{\partial TO1}{\partial TO2} = -1$$

The optimization equation for TO2 is

$$GLE\left(\frac{\partial VLE}{\partial TO2} - \frac{\partial VLE}{\partial TO1}\right) - RO1 + GVI\left(\frac{\partial VI}{\partial TO2} - \frac{\partial VI}{\partial TO1}\right)$$
$$+ \frac{WBVI}{WAVI} KCO2 \left[RO2 + GAP \frac{\partial VAP}{\partial TO2}\right.$$
$$\left. + \frac{WBAP}{WAAP} KCR \frac{WBLP}{WALP} KCI GRP\left(\frac{\partial r_p}{\partial TO2} - \frac{\partial r_p}{\partial TO1}\right)\right] = 0 \quad (42)$$

with $\frac{\partial V}{\partial TO1} = 2A\ (TTT - TO2 - TSO - TI) + B$

Inbound Powered Turn Swingby Mission - This mode has been used to demonstrate the derivation of the optimization equations. There are four independent parameters, which are the outbound trip time, TO, the arrive planet date, TAP, the first inbound leg time, TI1, and the second inbound leg time, TI2. The dependent parameters are

$$VLE = f(TO, TAP)$$
$$VAP = f(TO, TAP)$$
$$VLP = f(TI1, TDP)$$
$$VI = f(TI1, TI2, TDP)$$
$$VAE = f(TI1, TI2, TDP)$$
$$r_p = f(TI1, TI2, TDP)$$
$$P_p = f(TI1, TI2, TDP)$$

TO Equation

$$GLE \frac{\partial VLE}{\partial TO} + RO + GAP \frac{\partial VAP}{\partial TO} = 0 \quad \text{(same as Eq. 28)}$$

TAP Equation

$$GLE \frac{\partial VLE}{\partial TAP} + GAP \frac{\partial VAP}{\partial TAP} + \left(KCR \frac{WBAP}{WAAP}\right)\left(KCI1 \frac{WBLP}{WALP}\right)\left[GLP \frac{\partial VLP}{\partial TAP}\right.$$
$$\left. + GVI \frac{\partial VI}{\partial TAP} + \left(KCI2 \frac{WBVI}{WAVI}\right)\left(GRP \frac{\partial r_p}{\partial TAP} + GAE \frac{\partial VAE}{\partial TAP}\right)\right] = 0$$

(same as Eq. 16)

TI1 Equation

$$GLP \frac{\partial VLE}{\partial TI1} + RI1 + GVI \frac{\partial VI}{\partial TI1} + KCI2 \frac{WBVI}{WAVI} \left( GRP \frac{\partial r_p}{\partial TI1} + GAE \frac{\partial VAE}{\partial TI1} \right) = 0$$

(same as Eq. 14)

TI2 Equation

$$GVI \frac{\partial VI}{\partial TI2} + KCI2 \frac{WBVI}{WAVI} \left( RI2 + GRP \frac{\partial r_p}{\partial TI2} + GAE \frac{\partial VAE}{\partial TI2} \right) = 0$$

(same as Eq. 15)

Constant Total Trip Time

$$GLP \frac{\partial VLP}{\partial TI1} + RI1 + GVI \left( \frac{\partial VI}{\partial TI1} - \frac{\partial VI}{\partial TI2} \right) + KC12 \frac{WBVI}{WAVI} \left\{ - RI2 + GRP \left( \frac{\partial r_p}{\partial TI1} - \frac{\partial r_p}{\partial TI2} \right) + GAE \left( \frac{\partial VAE}{\partial TI1} - \frac{\partial VAE}{\partial TI2} \right) \right\} = 0$$

(same as Eq. 27)

GRAVITY LOSSES

The free flight trajectory data stored in the program contains the required velocity changes for an impulsive change from one trajectory to another. However, since the propulsion system fires for a finite time, the propellant used is lifted within a gravity field as the vehicle accelerates. This propellant acceleration imposes a penalty on the vehicle, making the actual or characteristic velocity change greater than the impulsive velocity change. The ratio of the characteristic velocity to the impulsive velocity is defined as the gravity loss factor. The magnitude of the gravity loss factor is equal to or greater than one, its value depending on the vehicle thrust-to-weight ratio, the required impulsive velocity change, and the specific impulse of the propulsion system. Also affecting the gravity loss factor is, of course, the planet involved and whether the vehicle is arriving or leaving the planet.

In this study, the gravity loss factors for leaving Earth and arriving and leaving Mars or Venus were calculated using a generalized, two-dimensional, powered-flight program. The Runge-Kutta integration method was used to solve the equations of motion for a vehicle leaving or arriving a spherical body, with the thrust directed along the velocity vector. Fig. II-6 is a typical example of the gravity loss factors.

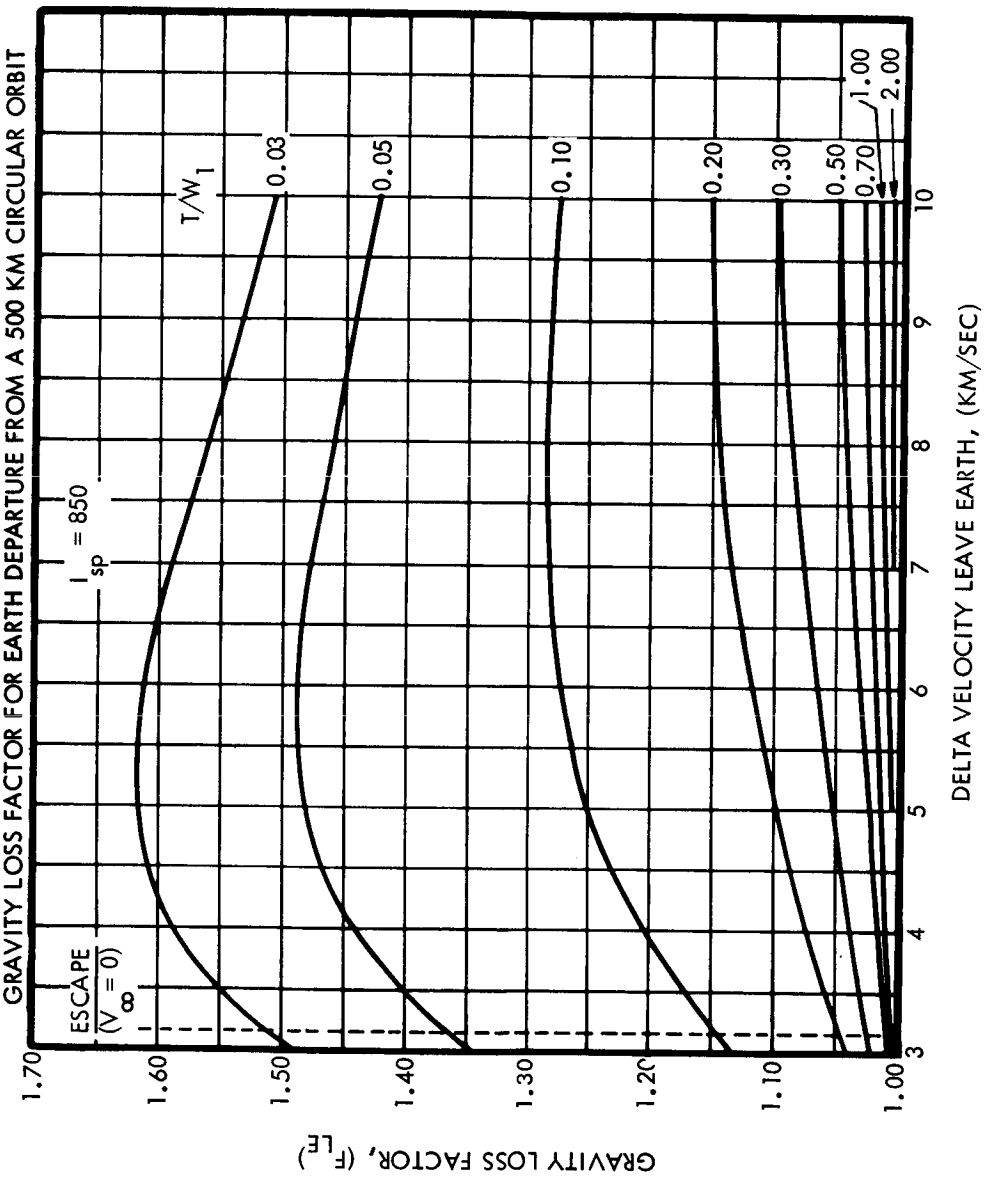


Figure II-6 Typical Gravity Loss Factors

# III VEHICLE AND PERFORMANCE ANALYSIS

This chapter presents the analyses that were conducted to determine the vehicle and performance scaling laws, constraints, and procedures which were incorporated in the computer programs and used in the mission evaluations.

## STAGE WEIGHT SCALING LAWS

Final stage weight scaling laws encompassing both nuclear and chemical propulsion systems are presented as a function of two variables, usable propellant weight and total propellant storage time in days. Scaling laws for the nuclear stage were based primarily on LMSC data from Ref. 3. Chemical stage weight scaling laws were derived from current empirical data.

The weight scaling laws presented for the various stages or "propulsion modules" are essentially independent of the overall vehicle configuration. Integration of the various "propulsion modules" into a vehicle to perform a specific interplanetary mission is investigated in the representative vehicle design section of this chapter.

The weight required for micrometeoroid protection is subject to wide variation depending upon the theoretical and experimental criteria assumed. Structural weight in this area was evaluated independently of other structural requirements. A separate equation was derived for micrometeoroid protection weight in terms of the time exposed and protected area. Weight was a direct function of time to the one-third power and protected area to the four-thirds power. The low density of hydrogen compared to chemical propellants, results in large areas and therefore, large protection weights for the nuclear stage. Reduction of micrometeoroid protection criteria would improve the nuclear stage capability with respect to the chemical systems.

### Weight and Area Scaling Laws

The scaling laws used to relate the weight and area of the propellant tanks to the total usable propellant weight and trip time are given below for the various propellants and mission phases. Also included are the primary assumptions used in formulating these equations.

The stage jettison weight equations are the summation of two separate equations. One equation was derived for stage jettison weight less micrometeoroid protection weight. This equation was obtained by computing numerous points from the individual subsystem and structure equations discussed in the section on subsystem weights. These points were plotted and several linear equations derived for the particular propellant range under consideration. The second equation provides for micrometeoroid protection weight. Derivation of this equation is discussed in the section on micrometeoroid protection. An example equation derivation is shown which details the approach employed.

Primary Assumptions - The primary assumptions made in deriving the propellant tank scaling laws are listed below.

- Except for the depart earth phase, all equations for cryogenic propellant tanks do not contain the weight provisions required for tank insulation.
- All equations include the weight provisions required for micrometeoroid protection.
- The equations for the depart earth phase contain tank insulation and micrometeoroid weight provisions sufficient for 90 days.
- The equations for hydrogen propellant tanks do not include the nuclear engine weight, the engine shielding, or the thrust structure.
- The equations for all chemical propellant tanks (non-nuclear) include the required engine weight. The engine, structure, and accessories have been sized to maintain a constant thrust-to-initial stage weight ratio of approximately 0.7.
- No overall vehicle attitude control system weight is included in the stage weight equations. Vehicle attitude control requirements are accounted for in the mission optimization by including a propellant and system weight allowance based on a percentage of the controlled vehicle weight.
- A weight allowance is provided for attitude maneuvering during the earth orbit assembly and docking phase.

The following define the nomenclature used in the scaling law equations:

| | | |
|---|---|---|
| $W_{p\ max}$ | - | The maximum usable propellant capacity for a single tank module (lbs) |
| $W_j$ | - | Final tank or stage jettison weight; total empty stage weight including propellant residuals (lbs) |
| $W_p$ | - | Usable propellant weight (lbs) |
| T | - | Total time exposed to micrometeoroids (days) |
| $A_t$ | - | Propellant tank surface area ($ft^2$) |
| $A_{t_{ox}}$ | - | Oxidizer tank surface area ($ft^2$) |
| $A_{t_f}$ | - | Fuel tank surface area ($ft^2$) |

Depart Earth Stage

Propellant - $LH_2$

Tank Dia. - 33 ft.

$W_{p\ max}$ - 342,540 lbs.

$$W_j = 0.1644\ W_p + 6420$$

Depart Earth Stage

Propellant - $LO_2/LH_2$

Tank Dia. - 33 ft. (common bulkhead)

$W_{p\ max}$ - 1,540,000 lbs.

$$W_j = 0.0485\ W_p + 18,564$$

Arrive Planet and Depart Planet Stage

Propellant - $LH_2$

Tank Dia. - 33 ft.

$W_{p\ max}$ - 342,540 lbs.

$$W_j = 0.12\ W_p + 0.01492\ T^{1/3}\ (0.02577\ W_p + 493)^{4/3} + 8368$$

$$A_t = 0.0292\ W_p + 1003$$

Arrive Planet and Depart Planet Stage

Propellant - $LO_2/LH_2$

Tank Dia. - 21.67 ft. (common bulkhead)

$W_{p\ max}$ - 700,000 lbs.

$$W_j = 0.0469\ W_p + 0.01492\ T^{1/3}\ (0.01021\ W_p - 104)^{4/3} + 11,904$$

$$A_{t_{ox}} = 0.0023\ W_p - 74$$

$$A_{t_f} = 0.00774\ W_p + 594$$

Depart Planet Stage

Propellant - $N_2O_4/A\text{-}50$

Tank Dia. - 21.67 ft. (separate tandem tanks)

$W_{p\ max}$ - 800,000 lbs.

$$W_j = 0.0284\ W_p + 0.01492\ T^{1/3}\ (0.0027\ W_p + 1374)^{4/3} + 12,646$$

Arrive Earth Retro Stage

Propellant - $LO_2/LH_2$

Tank Dia. - 21.67 ft. (internal tanks, spherical and cylindrical)

$W_{p\ max}$ - 150,000 lbs.

$$W_j = 0.0855\ W_p + 0.01492\ T^{1/3}\ (0.0186\ W_p + 972)^{4/3} + 2865$$

$$A_{t_{ox}} = 0.00656\ W_p + 210$$

$$A_{t_f} = 0.0198\ W_p + 301$$

Arrive Earth Retro Stage

Propellant - $N_2O_4/A\text{-}50$

Tank Dia. - 21.67 ft. (internal tanks, four cylindrical tanks with 2 elliptical bulkheads)

$W_{p\ max}$ - 150,000 lbs.

$$W_j = 0.0427\ W_p + 0.01492\ T^{1/3}\ (0.00595\ W_p + 505)^{1/3} + 3094$$

Outbound Leg Midcourse Correction and Planet Capture Orbit Circularizing Stage

Propellant - $N_2O_4$/A-50

Tank Dia. - 21.67 ft. (internal tanks)

$W_{p\ max}$ - 100,000 lbs.

$$W_j = 0.1154\ W_p + 0.0259\ T^{1/3}\ (0.00656\ W_p + 489)^{4/3} + 1190$$

Inbound Leg Midcourse Correction Stage

Propellant - $N_2O_4$/A-50

Tank Dia. - 21.67 ft. (internal tanks)

$W_{p\ max}$ - 25,000 lbs.

$$W_j = 0.0665\ W_p + 937$$

The above jettison weight equations are graphically presented in Figs. III-1 to III-6.

Example Derivation - Stage Jettison Weight Equation

An example of the approach used in deriving the stage jettison weight equation is presented below. The scaling law for the arrive planet and depart planet stage was selected. This equation is valid for $LO_2/LH_2$ within a total propellant weight range of 100,000 to 700,000 lbs. The stage diameter is 260 inches with $\sqrt{2}$ elliptical forward and aft bulkheads and a common center bulkhead. Final form of the equation is repeated below:

$$W_j = 0.0469\ W_p + 0.01492\ T^{1/3}\ (0.01021\ W_p - 104)^{4/3} + 11,904 \quad (1)$$

$$W_j = W_{j_1} + W_m \quad (2)$$

and

$$W_{j_1} = 0.0469\ W_p + 9,864 \quad (3)$$

$$W_m = 0.01492\ T^{1/3}\ (.01021\ W_p - 104)^{4/3} + 2,040 \quad (4)$$

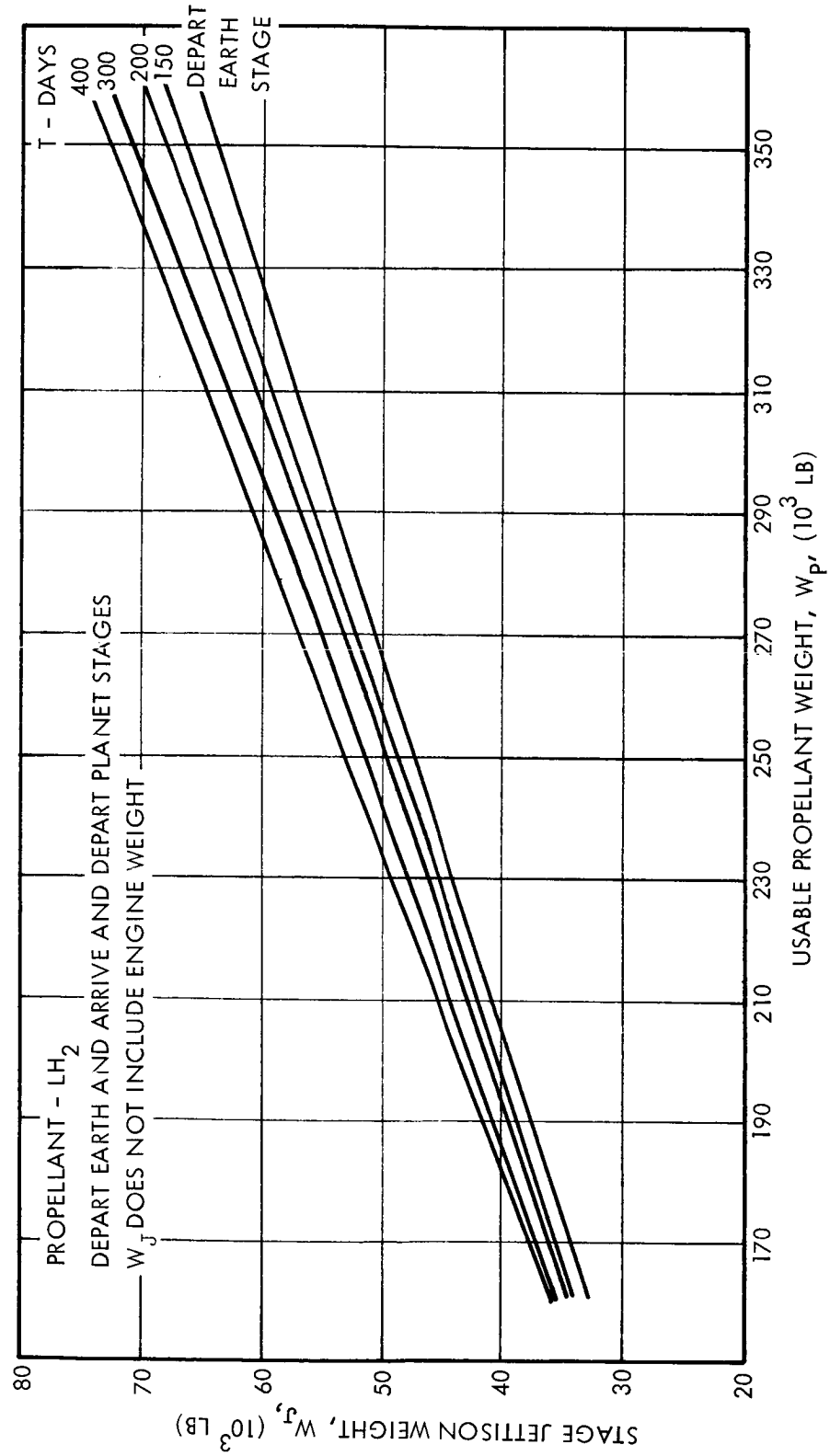


Figure III-1 Hydrogen Tank Weight Scaling Laws

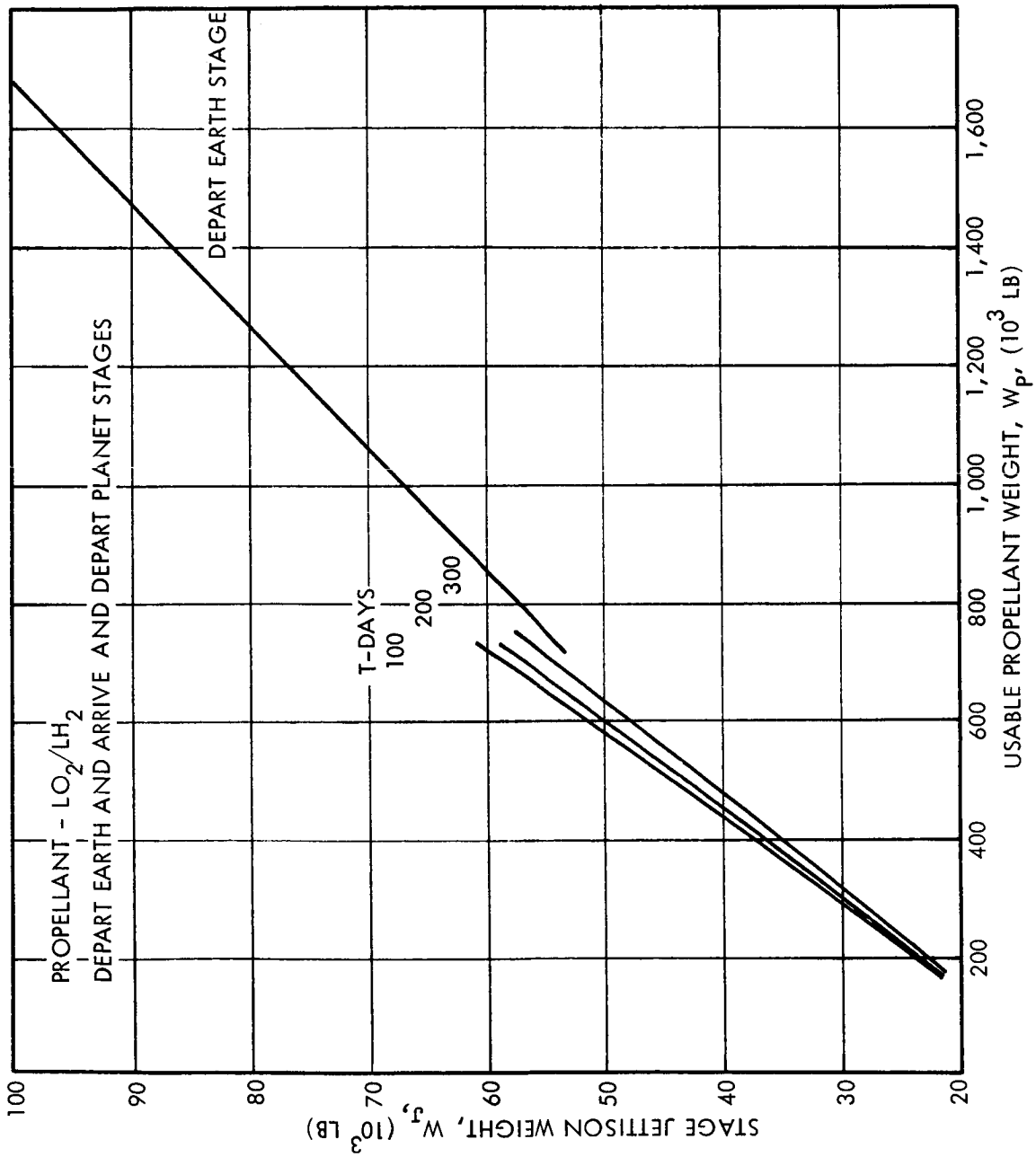


Figure III-2 $LO_2/LH_2$ Tank Weight Scaling Laws

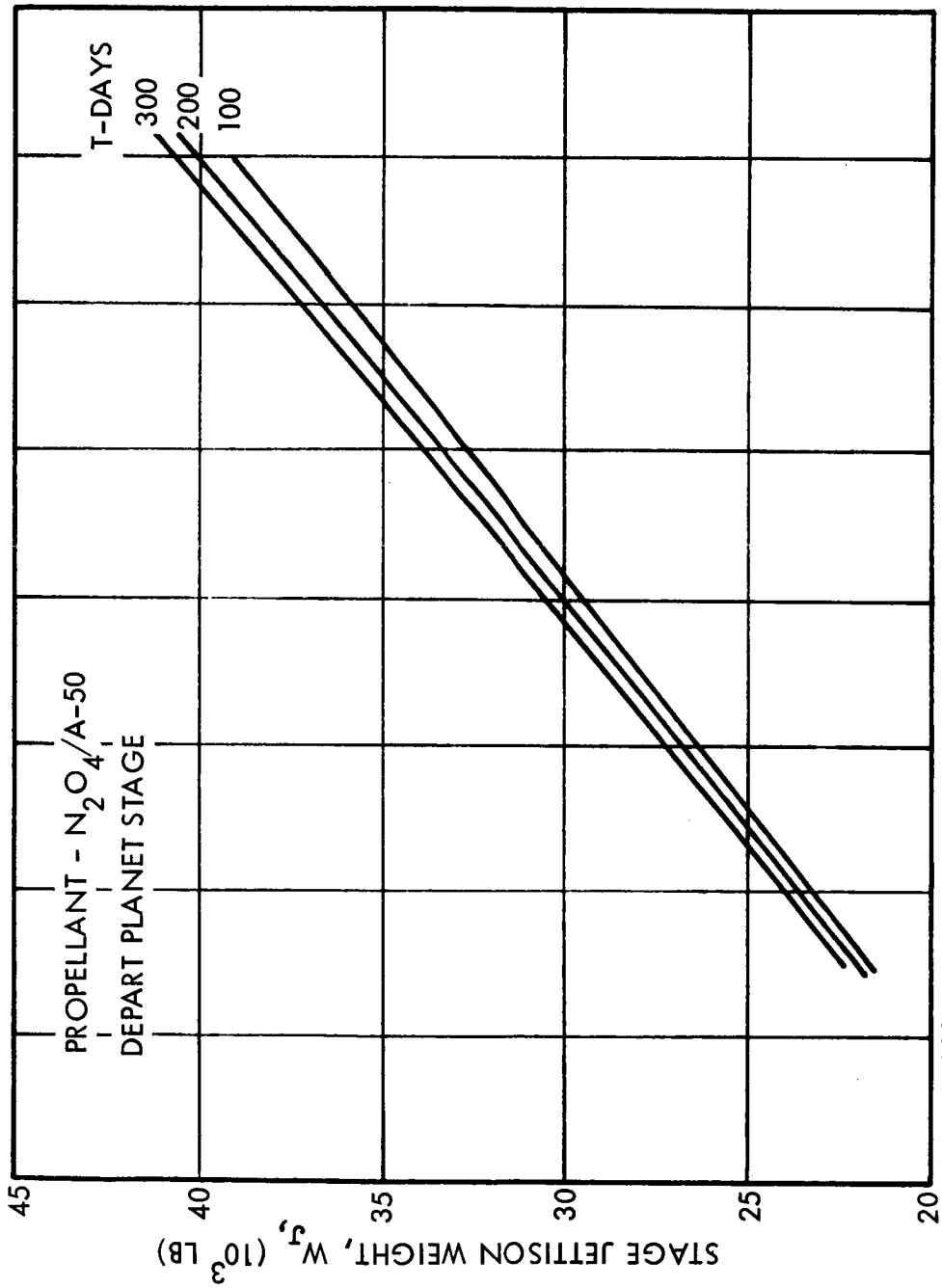


Figure III-3 Storable Tank Weight Scaling Laws

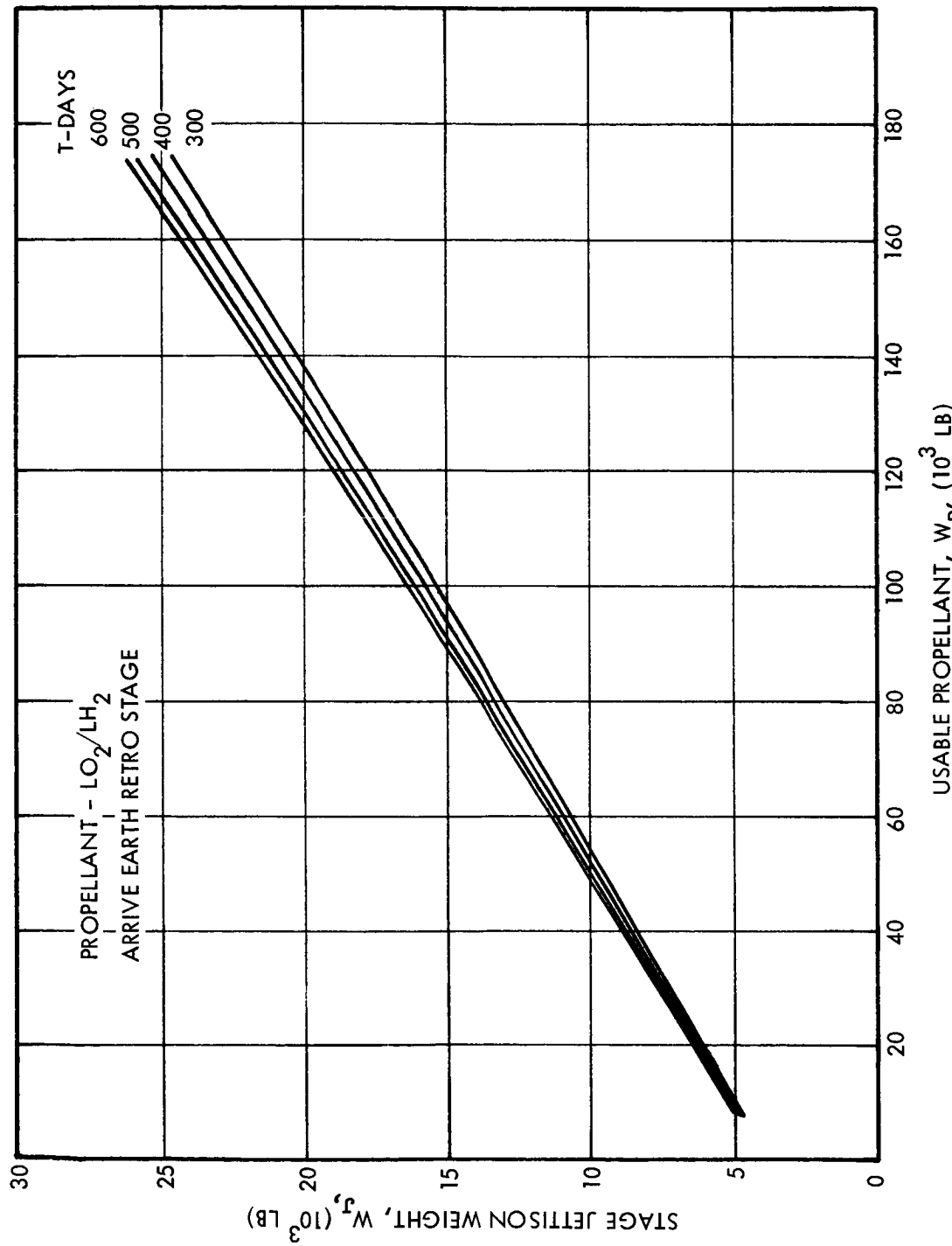


Figure III-4 $LO_2/LH_2$ Retro Weight Scaling Laws

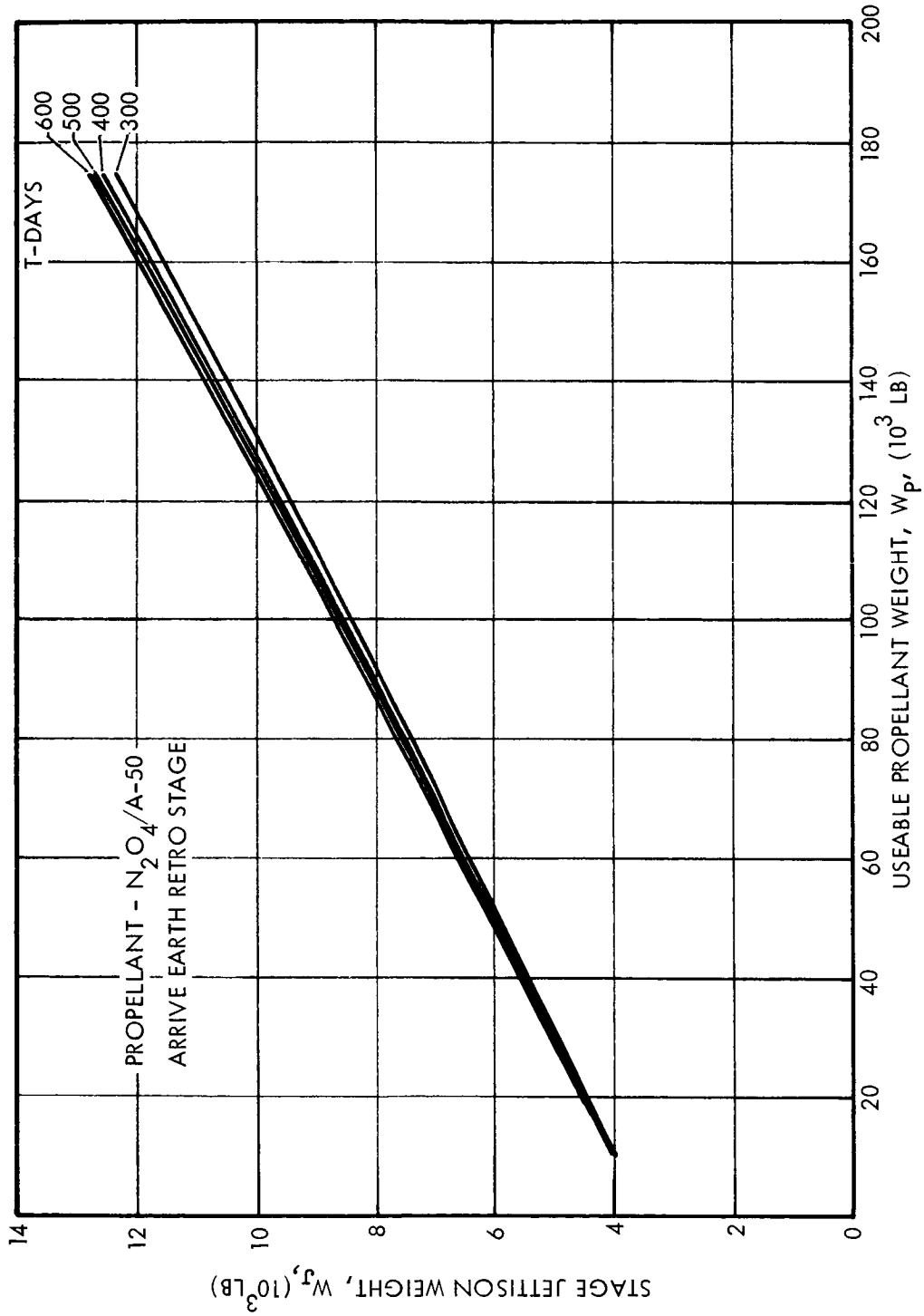


Figure III-5 Storable Retro Weight Scaling Laws

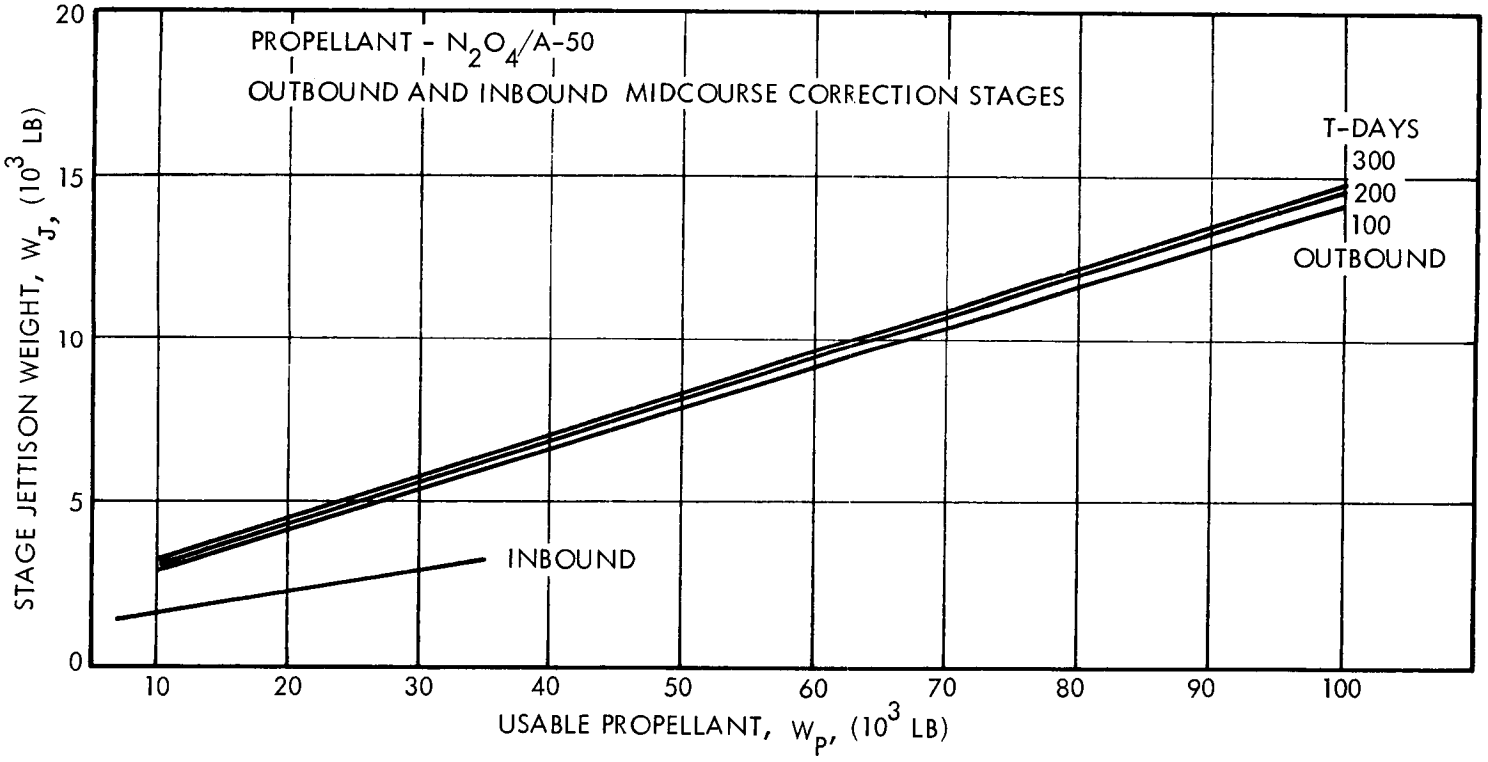


Figure III-6 Midcourse Correction Stage Weight Scaling Laws

$W_j$ = Final stage jettison weight (less insulation), lbs.

$W_{j_1}$ = $\sum$ subsystem weights excluding micrometeoroid protection and insulation, lbs.

$W_m$ = Micrometeoroid protection weight, lbs.

$W_p$ = Usable propellant weight, lbs.

T = Total time exposed to micrometeoroids, days

Derivation of $W_j$ - $W_{j_1}$ was computed for three points based on the appropriate subsystem equations presented in a later section. The calculated subsystem weights are summarized in Table III-1. The equation for $W_{j_1}$ was obtained by a linear curve fit using the stage jettison weights and propellant weights shown in Table III-1 for 400,000 lbs. and 700,000 lbs. total propellant weight.

$$W_{j_1} = 0.0469\, W_p + 9,864 \qquad (3)$$

Two iterations were made for each assumed tank capacity in order to evaluate several of the subsystems that are a function of the initial stage weight ($W_o$). Micrometeoroid protection weight for 90 days was assumed for this case. Additional stage data as required for computation of the individual subsystems are tabulated in Table III-1.

Derivation of $W_m$ - The detailed derivation of the micrometeoroid protection weight equation in terms of total mission time and protected surface area is presented below. The following equation is obtained from the section on micrometeoroid protection which is discussed in a later section.

$$W_m = 1.492 \times 10^{-2}\, T^{1/3}\, A_m^{4/3} + 2,040 \qquad (5)$$

The stage surface area ($A_m$) which is protected from micrometeoroids was calculated for each of the three points shown in Table III-1. An equation for $A_m$ was derived by a linear curve fit using $A_m$ and the propellant weights from Table III-1.

$$A_m = 0.01021\, W_p - 104 \qquad (6)$$

Combining Eqs. 5 and 6 results in the micrometeoroid weight (Eq. 4).

$$W_m = 0.01492\, T^{1/3}\, (0.01021\, W_p - 104)^{4/3} \quad 2,040 \qquad (4)$$

# TABLE III-1
## SUBSYSTEM WEIGHT CALCULATIONS
## MAIN PROPULSION STAGE-PROPELLANT - $LO_2/LH_2$
## 21.67 FT. DIA. TANK - COMMON BULKHEAD

| Sub* Systems | $W_{p_t}$ = 101,000 lb. | $W_{p_t}$ = 400,000 lb. | $W_{p_t}$ = 700,000 lb. |
|---|---|---|---|
| $W_1$ | 4,282 | 4,282 | 4,282 |
| $W_2$ | 5,210 | 11,650 | 18,310 |
| $W_3$ | 0 | 0 | 0 |
| $W_4$ | 2,478 | 6,507 | 9,823 |
| $W_5$ | 123 | 488 | 854 |
| $W_6$ | 814 | 1,039 | 1,262 |
| $W_7$ | 331 | 470 | 834 |
| $W_8$ | 1,010 | 4,000 | 7,000 |
| $W_{j_1}$ | 14,248 | 28,436 | 53,387 |
| $W_m$** | 2,636 | 6,258 | 11,022 |
| $W_p$ | 99,990 | 396,000 | 693,000 |
| $W_o$ | 116,874 | 430,694 | 746,387 |
| | Stage Data | Stage Data | Stage Data |
| $V_t$ | 5,780 $ft^3$ | 22,221 $ft^3$ | 32,281 $ft^3$ |
| $A_t$ | 1,580 $ft^2$ | 4,590 $ft^2$ | 7,544 $ft^2$ |
| $H_t$ | 20 ft | 65 ft | 109.7 ft |
| $H_t/D_s$ | 0.92 | 3.0 | 5.06 |
| $C_t$ | 1.028 | 1.008 | 1.002 |
| $D_s$ | 21.67 ft | 21.67 ft | 21.67 ft |
| $H_t$ + 1 ft | 21.0 ft | 66.0 ft | 110.7 ft |
| $H_t$ + D | 42.7 ft | 87.7 ft | 132.4 ft |
| $A_m$ | 917 $ft^2$ | 3,979 $ft^2$ | 6,972 $ft^2$ |
| $W_m/A_m$ | 2.8 $lb/ft^2$ | 1.6 $lb/ft^2$ | 1.6 $lb/ft^2$ |
| $W_p/W_o$ | 0.855 | 0.919 | 0.928 |
| $1 - W_p/W_o$ | 0.145 | 0.081 | 0.072 |

*See section on subsystem weights and micrometeoroid protection for definition of symbols

**Micrometeoroid protection for T = 90 days

Combining Eqs. 3 and 4 produces the final stage jettison weight, Eq. (1).

$$W_j = 0.0469\, W_p + 0.01492\, T^{1/3} (0.01021\, W_p - 104)^{4/3} + 11,904 \qquad (1)$$

No insulation weight is included in the final equation, $W_j$. Insulation weight is a function of mission time and is evaluated and added later in the program.

Subsystem Weight Equations.

Stage subsystems were separated into two categories, fixed and variable as shown below.

Fixed Subsystems

- Thrust Structure and Docking
- Stage Control
- Control Electronics
- Environmental Control
- Guidance
- Telemetry and Measuring Equipment
- Propellant Utilization
- Range Safety Equipment

Variable Subsystems

- Propellant Tanks
- Structure
- Propulsion
- Ullage Pressurization
- Electrical Power
- Stage Separation
- Residual and Trapped Propellant

Equations were derived for each variable subsystem. Stage jettison weights for the chemical stages were computed for several points within anticipated propellant ranges. Several linear jettison weight equations were then derived from the computed points. The nuclear stage jettison weights were based on data from Ref. 3.

The balance of this section includes a detailed discussion of the fixed subsystem weights and derivation of the individual subsystem equations.

Fixed Subsystem Weights - The items and corresponding weights as shown below for the nuclear stage are taken directly from the LMSC study (Ref. 3). These items were also assumed constant for the chemical stages except for the revisions as noted.

| Items | Nuclear Stage | Chemical Stage | |
|---|---|---|---|
| | | * | ** |
| Thrust Structure-Docking | 2,500 | 2,500 | 0 |
| Stage Control System | 797 | 797 | 300 |
| Control System Electronics | 20 | 20 | 20 |
| Environmental Control | 316 | 316 | 316 |
| Guidance | 186 | 186 | 186 |
| Telemetry and Measuring Equipment | 155 | 155 | 155 |
| Propellant Utilization | 58 | 58 | 58 |
| Range Safety Equipment | 1,049 | 250 | 250 |
| Fixed Weight, $W_1$ | 5,081 | 4,282 | 1,285 |

* Applies to all chemical stages except storable retros.
** Applies to storable retro stage only.

No docking thrust structure weight is included for the storable retro stage since all the stages considered could be placed in orbit with a full load of propellant thereby eliminating the need for docking thrust structure for propellant transfer.

Propellant Tank Weight - The equations used for evaluating the tank weight, $W_2$, of the various chemical stage configurations were based on an empirical equation presented in Ref. 4. The empirical equation was modified in some instances depending on the particular tank geometry. The equations used are summarized below for each stage.

Common Bulkhead

Diameter - 33.0 ft.

$$W_{2_a} = 0.241\ C_t\ V_t + 0.287\ A_t^{1.129} + 6,050$$

Diameter - 21.67 ft.

$$W_{2_b} = 0.241\ C_t\ V_t + 0.287\ A_t^{1.129} + 2,607$$

Separate Tandem Tanks

Diameter - 21.67 ft.

$$*W_{2_c} = 0.241\ C_t\ V_t + 0.287\ A_t^{1.129}$$

* Oxidizer and fuel tanks computed separately

Multiple Internal Tanks

Cylindrical Tanks

$$W_{2_d} = 0.241\ C_t\ V_t + 0.287\ A_t^{1.129}$$

Spherical

Spherical tanks were computed individually based on a pressure of 30 psi, safety factor of 1.4, and ultimate tensile strength for 2219T62 of 60,300 psi. Minimum material thickness of 0.032 inches was assumed.

The basic empirical equation from Ref. 4 is shown below.

$$W_2 = k\ C_t\ V_t + 0.287\ A^{1.129}$$

where

$C_t$ - Non-dimensional factor based on tank fineness ratio and bulkhead combination

$V_t$ - Total tank volume, $ft^2$

A - Total tank surface area, $ft^2$

k - $2 \times SF \times P \times \frac{\rho}{\sigma\ ult.}$

SF - Safety factor

P - Nominal tank pressure, psf

$\rho$ - Material density, $lb/ft^3$

$\sigma ult$ - Material ultimate tensile strength, psf

Values used for k are tabulated below with comparable design criteria from the LMSC Study, Ref. 3.

| | LMSC Criteria | STL Criteria | |
|---|---|---|---|
| | | Mtl. Ult. | Mtl. Yield |
| Material | 2219T87 | 2219T62 | Al. |
| Tensile-Ultimate-psi | - | 60,300 | - |
| Tensile-Yield-psi | 77,500 | - | 53,770 |
| Density-lb/in$^3$ | 0.10 | 0.10 | 0.10 |
| Nominal Tank Pressure-psi | 30 | 30 | 30 |
| Safety Factor | 1.25 | 1.4 | 1.25 |
| Material Temperature-$^oF$ | -375 | 70 | ? |
| k | 0.167 | 0.241 | 0.241 |

A lower material yield strength and a larger safety factor were used for the chemical propellant tanks for two reasons. First, boosting the stage into the earth orbit in an "off loaded" condition would induce the possibility of having an empty oxidizer or fuel tank when using a bipropellant and therefore, the material would not be at cryogenic temperature. Second, a safety factor of 1.4 was used assuming a man rated system.

As a matter of interest, a comparison was made between the LMSC tank weight and calculated tank weight using equation $W_{2_a}$. The weight comparison is shown below for comparable tank structure.

| | LMSC* Weight | STL Calculated Weight |
|---|---|---|
| Propellant Tank | 23,176 | |
| Skirt-Fwd | 912 | |
| Skirt-Aft | 2,135 | 30,894 |
| Baffles | ? | |
| Plumbing | 256 | |
| Paint and Sealer | 158 | |
| TOTALS | 26,637 | 30,894 |

*Based on the LMSC DI stage.

Considering the tank structure only, a 33 foot diameter chemical stage with a total volume equal to the LMSC DI stage would weight approximately 10,300 lbs. more. This is based on the above weight difference of 4,257 lbs. plus the common bulkhead of 6,050 lbs. required for the bipropellant chemical stage.

Intertank Structure - The intertank structural weight, $W_{3_a}$, for the storable separate tandem tank configuration was derived based on weight per unit area for the structure. The resulting weight per unit area was:

Sketch A

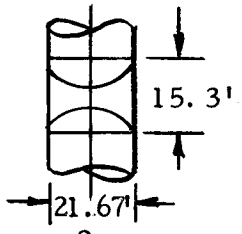


$$W/ft^2 = 1.67 \times 10^{-6} W_f + 1.733$$

$W_f$ = Weight of fuel above the interstage, lbs.

Multiplying the above equation by the intertank surface area (1,041 $ft^2$) per sketch A results in the following equation:

$$W_{3_a} = 1.74 \times 10^{-3} W_f + 1,804$$

Outer Shell Structure - The stage configurations utilizing internal tanks includes outer shell weight, $W_{3_b}$. For this type of stage, it was assumed that the micrometeoroid protection material also carries primary loads. The weight of the rings, longerons, and stringers was based on the following equation.

Sketch B

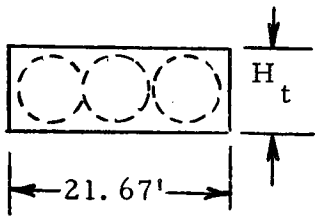


Stage Dia. - 21.67 ft.

$$W_{3_b} = 42 H_t + 490$$

Where $H_t$ is overall stage height in feet as shown in Sketch B.

The above equation provides for approximately one pound of shell weight per square foot of outer shell surface area excluding micrometeoroid protection weight.

Propulsion System - The propulsion system weight, $W_4$, shown below applies only to pump-fed chemical propulsion systems. An empirical equation was used to obtain propulsion system weight as a function of initial stage weight. The equation is based on a constant thrust-to-initial stage weight ratio of 0.7.

$$W_4 = 0.356\, W_o^{\,0.754}$$

where

$W_4$ - Propulsion system weight including the thrust chamber assembly and accessories, feed systems, and supports, lbs.

The above equation applies to both the main and retro propulsion systems. A check of the above equation was made based on SIV-B weights presented in Ref. 5. The weights are tabulated below.

| Items | Weight |
|---|---|
| Engine plus accessories | 3,586 |
| Purge system | 160 |
| Fuel system | 485 |
| Oxidizer system | 796 |
| TOTAL | 5,027 lbs. |

The value obtained by using the above equation results in a propulsion system weight of approximately 4,120 pounds. The SIV-B thrust-to-initial stage weight ratio is slightly greater than 0.7, which would contribute to the weight difference.

Ullage Pressurization System - The ullage pressurization weight for all pump-fed chemical stages, $W_5$, was based on a fixed percentage of total propellant weight.

$$W_5 = 1.22 \times 10^{-3}\, W_{p_t} + 84$$

where

$W_5$ - Pressurization system inert weight, lbs.

$W_{p_t}$ - Total propellant weight, lbs.

The pressurizing gas weight was considered part of residuals and is accounted for under "Residuals and Trapped Propellant".

Electrical Power System - It was assumed for this study that primary power would be supplied by an advanced type of thermoelectric or thermonic generator utilizing a radioisotope heat source. The major portion of the electrical system weight, $W_6$, would serve power distribution functions. A fixed weight allowance was provided for power required during launch, rendezvous, and docking in earth orbit. The following weight equation was used for the stage electrical system.

$$W_6 = 5 (H_t + D_s) + 600$$

where

$W_6$ - Total stage electrical system weight, lbs.

$H_t$ - Overall stage height excluding engine, ft.

$D_s$ - Stage diameter, ft.

The weight obtained from the above equation closely checks with the electrical system weight used in the LMSC Study (Ref. 3).

LMSC Study (DI Stage)

Electrical System Weight = 1,271 lbs.

$H_t$ (Less nuclear engine) = 106.7 ft.

Equation

$$W_6 = 5 (106.7 + 33) + 600 = 1,299 \text{ lbs.}$$

Stage Separation System - The stage separation system weight, $W_7$, was based on the assumption that retro thrust is applied to the expended stage to insure relative displacement after separation. Two equations were derived as a function of the stage jettison weight for systems utilizing solid propellant rockets for separation. The equations apply to the derived stage jettison weight for the chemical systems.

for $W_j \leq 100,000$ lbs.

$$W_7 = 7.5 \times 10^{-3} W_j + 205$$

for $W_j \geq 100,000$ lbs.

$$W_7 = 5.6 \times 10^{-3} W_j + 392$$

where

$W_7$ - Total separation system weight, lbs.

$W_j$ - Stage jettison weight, lbs.

The constant in the above equations includes a fixed allowance of 140 pounds for separation equipment required in addition to the solid propellant rockets.

Residual and Trapped Propellants - The residual and trapped propellant weight, $W_8$, was based on an allowance of 1 percent of the total propellant weight. for both the nuclear chemical stages.

$$W_8 = 0.01 W_{p_t}$$

where

$W_8$ = Residual and trapped propellant weight, lbs.

$W_{p_t}$ = Total stage propellant weight, lbs.

No provision was made in the LMSC (Ref. 3) stage weight breakdown for residual and trapped propellant. The above 1 percent allowance was applied to the LMSC data to maintain compatibility of stage jettison weights.

Tank Insulation Weight and Propellant Boiloff - No insulation weight or propellant boiloff allowance was considered in the derivation of the stage jettison weight equations since these items are a function of the mission time and vehicle velocity changes as well as tank surface area. Tank surface area equations were derived for stages utilizing cryogenic propellents. These equations are subsequently used to calculate the tank insulation and propellant boiloff weights in the overall mission and vehicle analysis.

The propellant tank surface area equations accompany the respective stage jettison weight equations previously presented.

Micrometeoroid Protection

The LMSC study presented micrometeoroid protection weight for single point designs based on a fixed time of 90 days and a 95 percent probability of zero penetration. Using the criterion of 95 percent probability of zero penetration, an equation was derived for micrometeoroid protection weight as a function of time and stage protected area. Weights were then computed for the LMSC design points using the derived equation. The derived equation was then modified to agree with the LMSC weights by adding a constant term. Final form of the resulting micrometeoroid weight equation is shown below.

$$W_m = 0.01492\, T^{1/3} A_m^{4/3} + 2,040 \qquad (7)$$

where

$W_m$ - Total micrometeoroid protection weight, lbs.

$T$ - Total time exposed to micrometeoroids, days

$A_m$ - Total surface area protected, $ft^2$

The above equation assumes non directional normal impacts. The protected area used for each particular stage is defined in the next section on stage geometry.

The derived equation for $W_m$ as a function of time and protected area is shown below.

$$W_m = 0.01492\, T^{1/3} A_m^{4/3} \qquad (8)$$

Total stage micrometeoroid protection weight is equal to:

$$W_m = 144\, A_m\, \rho\, t = 14.4\, A_m\, t \qquad (9)$$

where

$A_m$ - Total surface area protected, $ft^2$

$\rho$ - Material density (0.1 $lb/in^3$)

$t$ - Equivalent material thickness, inches

Equivalent Material Thickness - The equivalent material thickness from Ref. 6 is based on Nysmith and Summers penetration theory where

$$t = 1.67\, M^{1/3}\, \rho_m^{1/3} \left(\frac{V_m}{\rho_t\, S_t}\right)^{2/3} \frac{1}{R} \qquad (10)$$

where

- $t$ - Equivalent material thickness that barely resists the micrometeoroid, in.
- $M$ - Particle mass, gm.
- $\rho_m$ - Particle density (0.4 gm/cm$^3$)
- $V_m$ - Particle Velocity (80,000 ft/sec)
- $\rho_t$ - Target density (2.7 gm/cm$^3$)
- $S_t$ - Speed of sound in target material (16,800 ft/sec)
- $R$ - Protection efficiency increase for double wall construction (3)

Using the above values, the equivalent material thickness in terms of particle mass is:

$$t = 0.598\, M^{1/3} \qquad (11)$$

Micrometeoroid Flux - Values defining micrometeoroid flux (Whipple 1957 data) as presented in Ref. 6 suggested the following as a probable and conservative value.

$$NM = 8 \times 10^{-9}$$

where

- $N$ - Number of micrometeoroids of mass M, or larger, per ft$^2$ per day.
- $M$ - Micrometeoroid mass, gm.

The above value was arbitrarily reduced to the following for outer space application.

$$NM = 2.67 \times 10^{-10} \qquad (12)$$

Penetration Probability - The relationship between exposed area, time, and hit probability from Ref. 7 was used. Based on a Poisson distribution, the probability of receiving n hits is defined by the following equation.

$P_{(n)}$ is the probability of n hits in an $A_m$ $ft^2$ area exposed T days.

$$P_{(n)} = \frac{(NA_mT)^n \; e^{-NA_mT}}{n\,!}$$

$P_{(n)}$ should be near 1.0 when n = 0 for a high probability of zero hits. For 95% probability of zero hits;

$$P_{(o)} = \frac{(NA_mT)^o \; e^{-NA_mT}}{0\,!}$$

$$= \frac{1}{e^{NA_mT}}$$

$$= 0.95$$

$$NA_mT = \ln 1.0526$$

$$= 0.0513 \qquad (13)$$

where

N = Hits per $ft^2$ per day

$A_m$ = Total exposed area, $ft^2$

T = Total exposure time, days

Solving for M from Eqs. 12 and 13

$$M = 0.5205 \times 10^{-8} A_m T \qquad (14)$$

Therefore, from Eq. 11, the equivalent material thickness becomes

$$t = 1.036 \times 10^{-3} A_m^{1/3} T^{1/3} \qquad (15)$$

Solving Eq. 9 using the above value for t reduces to the derived equation previously presented, i.e.

$$W_m = 1.492 \times 10^{-2} A_m^{4/3} T^{1/3} \qquad (8)$$

LMSC Data - No micrometeoroid weight derivation was included in the LMSC study, consequently no direct comparison of equations was possible. However, a weight comparison was made by calculating micrometeoroid weight using the derived equation, Eq. 8, based on protected surface areas for the AI and DI stage configurations from the LMSC study. Results of the weight check are tabulated below.

| LMSC Data (Ref. 3) | | | Calculated Weight (lb) (T = 90 days) | Weight Difference (lb) |
|---|---|---|---|---|
| Stage | $A_m(ft^2)$ | $W_m$(lbs) | | |
| AI | 4,869 | 7,791 | 5,516 | -2,275 |
| DI | 9,320 | 14,913 | 13,110 | -1,803 |

An average of the above weight differences was added to the derived equation to obtain the final equation previously presented and repeated below.

$$W_m = 1.492 \times 10^{-2} T^{1/3} A_m^{4/3} + 2,040 \qquad (7)$$

Stage Geometry

The stage configurations used for the study are shown in Fig. III-7. Nuclear stage geometry for the 33 foot diameter tanks is identical to LMSC design from Ref. 3. Chemical stage diameters were limited to 33 and 21.67 (SIVB) feet in order to restrict the configurations to a reasonable number.

Tank surface area and micrometeoroid area equations were also required for evaluation of propellant boiloff, tank insulation, and micrometeoroid protection weight. Propellant tank surface area equations were derived from computed single point values in terms of usable propellant weight.

Area equations for evaluating micrometeoroid protection weight were based on the assumption that the entire cylindrical surface plus one end of the stage would require protection.

At the lower end of the storable propellant weight range, the small volumes involved were not compatible with the minimum stage diameter of 21.67 feet. Below a certain storable weight, it was assumed that propellant tanks could be located somewhere on the vehicle so that no additional structure would be required.

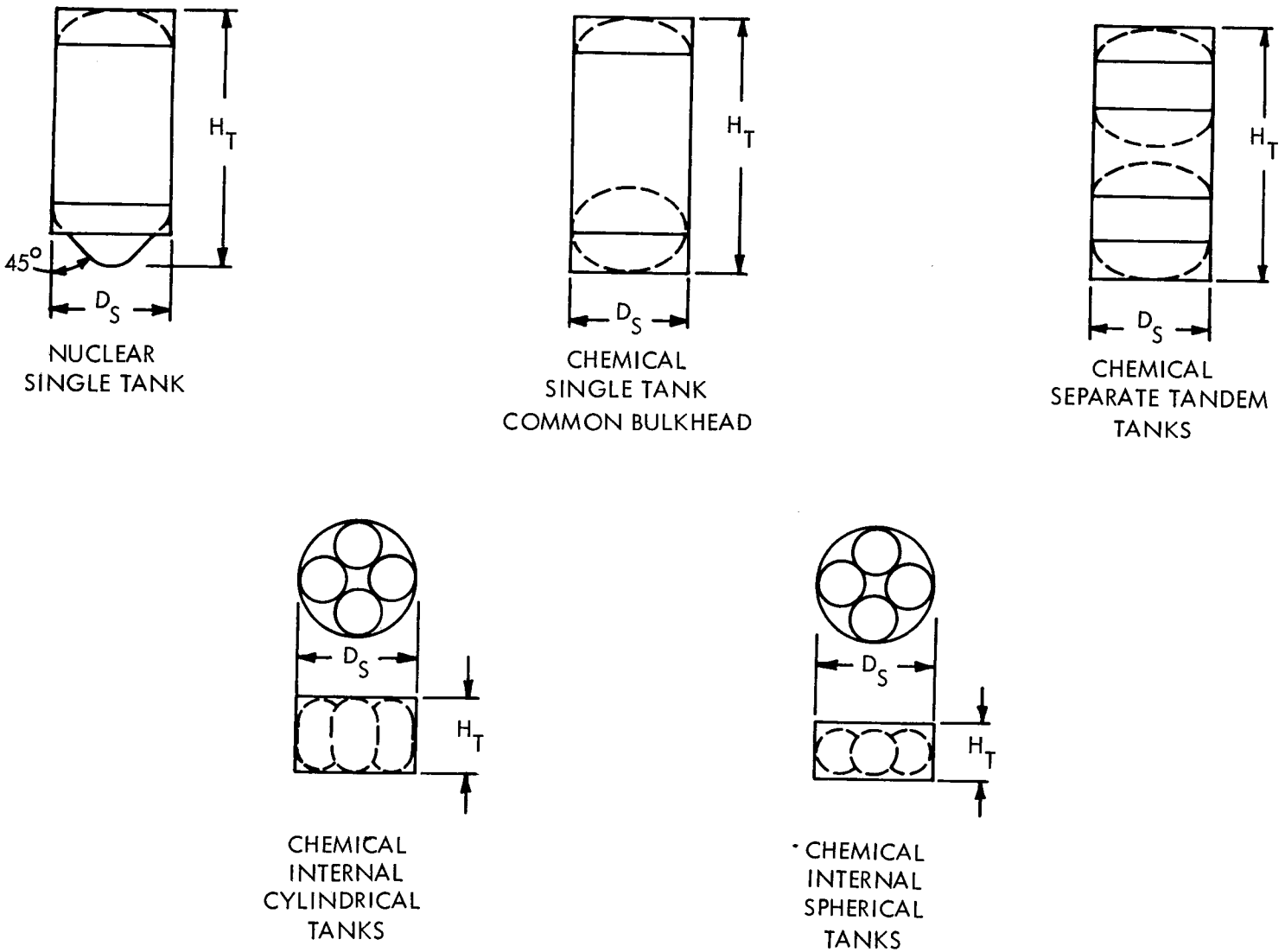


Figure III-7 Stage Geometry

Supplementary Scaling Laws

Four additional classes or "levels" of scaling laws were used for a supplementary set of mission evaluations which were defined during the latter part of the study. These four sets of scaling laws permitted the parametric evaluation of the effect of propellant tank jettison weights or mass fractions (ratio of total usable propellant-to-total gross stage weight) for various missions, configurations, and performance criteria. These four sets are designated as mass fraction case numbers 1 through 4. The average mass fractions given by the scaling laws decrease in an approximate linear fashion with increasing case number. The equations used for these four sets of scaling laws are given in Tables III-2 to III-5 for the various propellants and mission phases. Note that the equations and average mass fractions for nuclear stages do not include the weight of the nuclear engine.

These equations were obtained by linear curve fits of point data obtained from MSFC.

NUCLEAR ENGINE WEIGHTS

The weights of the nuclear engines used in the computations of vehicle weights are shown in the Table III-6, as a function of the thrust per engine and number of clustered engines.

Table III-6 Nuclear Engine Weights

| | NUCLEAR ENGINE WEIGHT - LBS | | | | | | |
|---|---|---|---|---|---|---|---|
| Thrust - lbs. / No Engines Clustered | 50,000 | 100,000 | 200,000 | 230,000 | 300,000 | 400,000 | 500,000 |
| Single | 15,000 | 18,300 | 31,000 | 34,200 | 40,800 | 48,800 | 56,000 |
| 2 | 31,560 | 39,256 | 64,780 | 71,200 | 84,400 | 100,000 | 114,800 |
| 3 | 50,550 | 63,075 | 102,225 | 111,900 | 131,820 | 155,850 | 177,450 |
| 4 | 72,800 | 91,200 | 144,600 | 157,600 | 184,900 | 217,500 | 246,600 |
| 5 | -- | -- | -- | 200,000 | -- | -- | -- |
| 7 | 134,400 | 168,700 | 264,075 | -- | 335,860 | 394,100 | 446,250 |

Table III-2 Mass Fraction Case No. 1

| Mode | Equation | Average Mass Fraction |
|---|---|---|
| Earth Depart | | |
| Nuclear Propulsion | $W_j = .11330\ W_p + 5791$ | .88 |
| Cryogenic Propulsion | $W_j = .05056\ W_p + 16,653$ | .94 |
| Midcourse Correction Outbound | | |
| Storable Propulsion | $W_j = .05732\ W_p + 1442$ | .92 |
| Planet Braking | | |
| Nuclear Propulsion | $W_j = .14674\ W_p + 1410$ | .87 |
| Cryogenic Propulsion | $W_j = .07097\ W_p + 9841$ | .92 |
| Aero Capture Orbit Circularizing | | |
| Storable Propulsion | $W_j = .05732\ W_p + 1442$ | .92 |
| Planet Depart | | |
| Nuclear Propulsion | $W_j = .14674\ W_p + 1410$ | .87 |
| Cryogenic Propulsion | $W_j = .07097\ W_p + 9841$ | .92 |
| Storable Propulsion | $W_j = .03121\ W_p + 15,187$ | .94 |
| Midcourse Correction Inbound | | |
| Storable Propulsion | $W_j = .03310\ W_p + 888$ | .92 |
| Earth Braking | | |
| Cryogenic Propulsion | $W_j = .09255\ W_p + 4282$ | .79 |
| Storable Propulsion | $W_j = .05312\ W_p + 3491$ | .91 |

Notes:

1. Includes micrometeoroid protection
2. Includes insulation for earth depart stages
3. Does not include insulation for all other stages
4. Includes engine weight for all non-nuclear stages
5. Does not include engine weight for all nuclear stages

Table III-3 Mass Fraction Case No. 2

| Mode | Equation | Average Mass Fraction |
|---|---|---|
| Earth Depart | | |
| Nuclear Propulsion | $W_j = .16520\ W_p + 6357$ | .84 |
| Cryogenic Propulsion | $W_j = .09622\ W_p + 18,184$ | .90 |
| Midcourse Correction Outbound | | |
| Storable Propulsion | $W_j = .09193\ W_p + 1541$ | .89 |
| Planet Braking | | |
| Nuclear Propulsion | $W_j = .19088\ W_p + 3198$ | .83 |
| Cryogenic Propulsion | $W_j = .13154\ W_p + 11013$ | .87 |
| Aero Capture Orbit Circularizing | | |
| Storable Propulsion | $W_j = .09193\ W_p + 1541$ | .89 |
| Planet Depart | | |
| Nuclear Propulsion | $W_j = .19088\ W_p + 3198$ | .83 |
| Cryogenic Propulsion | $W_j = .13154\ W_p + 11,013$ | .87 |
| Storable Propulsion | $W_j = .07554\ W_p + 16,561$ | .91 |
| Midcourse Correction Inbound | | |
| Storable Propulsion | $W_j = .06596\ W_p + 951$ | .89 |
| Earth Braking | | |
| Cryogenic Propulsion | $W_j = .15470\ W_p + 4901$ | .74 |
| Storable Propulsion | $W_j = .09931\ W_p + 3828$ | .87 |

Notes:

1. Includes micrometeoroid protection
2. Includes insulation for earth depart stages
3. Does not include insulation for all other stages
4. Includes engine weight for all non-nuclear stages
5. Does not include engine weight for all nuclear stages

Table III-4 Mass Fraction Case No. 3

| Mode | Equation | Average Mass Fraction |
|---|---|---|
| Earth Depart | | |
| Nuclear Propulsion | $W_j = .22208\ W_p + 7010$ | .80 |
| Cryogenic Propulsion | $W_j = .14692\ W_p + 19,921$ | .86 |
| Midcourse Correction Outbound | | |
| Storable Propulsion | $W_j = .12888\ W_p + 1652$ | .86 |
| Planet Braking | | |
| Nuclear Propulsion | $W_j = .25043\ W_p + 3531$ | .79 |
| Cryogenic Propulsion | $W_j = .19937\ W_p + 12,404$ | .82 |
| Aero Capture Orbit Circularizing | | |
| Storable Propulsion | $W_j = .12888\ W_p + 1652$ | .86 |
| Planet Depart | | |
| Nuclear Propulsion | $W_j = .25043\ W_p + 3531$ | .79 |
| Cryogenic Propulsion | $W_j = .19937\ W_p + 12,404$ | .82 |
| Storable Propulsion | $W_j = .12385\ W_p + 18,131$ | .87 |
| Midcourse Correction Inbound | | |
| Storable Propulsion | $W_j = .10094\ W_p + 1021$ | .86 |
| Earth Braking | | |
| Cryogenic Propulsion | $W_j = .22422\ W_p + 5668$ | .69 |
| Storable Propulsion | $W_j = .14973\ W_p + 4215$ | .83 |

Notes:

1. Includes micrometeoroid protection
2. Includes insulation for earth depart stages
3. Does not include insulation for all other stages
4. Includes engine weight for all non-nuclear stages
5. Does not include engine weight for all nuclear stages

Table III-5 Mass Fraction Case No. 4

| Mode | Equation | Average Mass Fraction |
|---|---|---|
| Earth Depart | | |
| Nuclear Propulsion | $W_j = .28485\ W_p + 7770$ | .76 |
| Cryogenic Propulsion | $W_j = .20204\ W_p + 21,926$ | .82 |
| Midcourse Correction Outbound | | |
| Storable Propulsion | $W_j = .16841\ W_p + 1775$ | .83 |
| Planet Braking | | |
| Nuclear Propulsion | $W_j = .31626\ W_p + 3917$ | .75 |
| Cryogenic Propulsion | $W_j = .27585\ W_p + 14,076$ | .77 |
| Aero Capture Orbit Circularizing | | |
| Storable Propulsion | $W_j = .16841\ W_p + 1775$ | .83 |
| Planet Depart | | |
| Nuclear Propulsion | $W_j = .31626\ W_p + 3917$ | .75 |
| Cryogenic Propulsion | $W_j = .27585\ W_p + 14,076$ | .77 |
| Storable Propulsion | $W_j = .17671\ W_p + 19,934$ | .83 |
| Midcourse Correction Inbound | | |
| Storable Propulsion | $W_j = .13832\ W_p + 1099$ | .83 |
| Earth Braking | | |
| Cryogenic Propulsion | $W_j = .30224\ W_p + 6640$ | .64 |
| Storable Propulsion | $W_j = .20497\ W_p + 4665$ | .79 |

Notes:

1. Includes micrometeoroid protection
2. Includes insulation for earth depart stages
3. Does not include insulation for all other stages
4. Includes engine weight for all non-nuclear stages
5. Does not include engine weight for all nuclear stages

These engine weights include the weight of the reactor, pressure vessel, nozzle, shielding, reflector, feed system, thrust structure, and auxiliary engine components. The weights are based on and extrapolated from data obtained from Aerojet General Corporation and include appropriate shielding and structural weight penalties for clustering arrangements and nucleonic interactions.

These weights were used in generating the vehicle weight data for all missions that employed nuclear rocket engines except those for the point vehicle design and for the vehicle weights that appear in Volumes IV and V, the nuclear engine analyses and results. The engine weights used to generate the vehicle weight data in these two volumes were obtained from the NOP computer calculations for specified engine power, specific impulse, and engine design constraints and parameters.

## NUCLEAR ROCKET ENGINE AFTERCOOLING

If a nuclear engine is to be saved for later reuse, the residual energy stored in the reactor core as radioactive fission products must be removed. This is accomplished by flowing propellant through the core until the energy generation rate decreases to the point where radiation cooling is adequate to keep the reactor temperature below its melting point. In actual practice, the propellant flow rate is varied as the decay power decreases, in an attempt to maintain as high an exit gas temperature and hence, specific impulse, as possible. However, when the flow rate is decreased below the point at which there is sonic velocity in the throat of the exhaust nozzle, a pulsed mode of aftercooling is necessary to maintain a reasonable specific impulse.

For this study, it is assumed that the aftercooling propellant flow rate is varied in such a way that the aftercooling propellant energy rise is constant throughout the aftercooling phase. Thus, the specific impulse and enthalpy increase of the propellant are represented by average values that are reasonable approximations to the actual aftercooling procedure.

In order to calculate the aftercooling requirements, the propellant, WPF, and burn time, TF, required for full power operation are first estimated. Then the total aftercooling time, TS, is calculated based on an inputted value of the ratio of the power at which aftercooling is terminated-to-the power during full operation, PRTS. The equations expressing the power ratio as a

function of the full power burn time and aftercooling time is based on data by J. J. Taylor. The constants in the equation have been refined by using data generated by the Nuclear Engine Optimization Program.

$$PRTS = 1.6 \exp(-TS/13.48) - 0.6 \exp(-TS/8.45) - 0.05598 \left[TS^{-0.2} - (TS + TF)^{-0.2}\right] \quad (16)$$

An iterative procedure is used to solve Eq. (16) for TS.

With the aftercooling time estimated, the amount of afterccoling propellant needed can be determined from the ratio of the total energy generated during aftercooling-to-the energy generated during full power operation, ERAT, and the ratio of the propellant enthalpy rise during full power operation-to-the aftercooling enthalpy rise, HR. The energy ratio equation is

$$ERAT = \frac{1}{TF}\left\{0.119\left[1. - \exp(-TS/13.48)\right] - 0.071\left[1. - \exp(-TS/8.45)\right] + 0.07\left[TS^{0.8} + TF^{0.8} - (TS+TF)^{0.8}\right]\right\} \quad (17)$$

and the required aftercooling propellant, WPS, is given by

$$WPS = WPF \cdot HR \cdot ERAT \quad (18)$$

where WPF is the propellant used during full power operation. The enthalpy ratio, HR, is an inputted value generally obtained from NOP results.

For an arrive planet aftercooled stage, the above equations are adequate to define the aftercooling and full power operation parameters, since it is assumed that the vehicle must achieve injection velocity during full power operation and the thrust generated during aftercooling is not used. However, for a depart earth aftercooled stage, the aftercooling thrust can be used to accelerate the vehicle. Recovery of the aftercooling thrust reduces the velocity change required during full power operation, thus reducing the burn time and the amount of propellant used during full power operation. For this thrusting condition, the aftercooling requirements are found by an iterative technique in which successive calculations are made of the full

power and aftercooling propellant requirements and the velocity changes associated with each phase until the total velocity change equals the required velocity change. The incorporation of this procedure into the overall stage design calculations is discussed in the next section.

The procedure and equations employed for calculating the total aftercooling time and propellant requirements for the aftercooled thrusting mode are identical to those for the nonthrusting mode, Eqs. (16), (17), and (18). However, it is assumed that thrust is not generated during the total aftercooling phase, since the flow rate (and thrust) becomes negligible at some point during this phase. Thus, in order to calculate the time and propellant expended during the thrusting period of the aftercooling phase, the value of the vehicle thrust-to-weight ratio at which useful aftercooling thrust is terminated is specified by input. An estimate of the vehicle weight is used to calculate the aftercooling thrust cutoff level, THTS. Then the ratio of the power at which aftercooled thrusting is terminated-to-the power during full operation, PRTST, is calculated.

$$PRTST = \frac{THTS \cdot ISPS}{THTF \cdot ISPF}$$

where THTF is the full power thrust and ISPF and ISPS are the specific impulses for the full power and aftercooled phases respectively. The aftercooled thrusting time, TST is obtained from

$$PRTST = 1.6 \exp(-TST/13.48) - 0.6 \exp(-TST/8.45) - 0.05598 \left[TST^{-0.2} - (TST + TF)^{-0.2}\right] \quad (19)$$

The ratio of total energy generated during aftercooled thrusting-to-the energy generated during full power operation, ERATT, is obtained

$$ERATT = \frac{1}{TF} \left\{0.119 \left[1. - \exp(-TST/13.48)\right] - 0.071 \left[1. - \exp(-TST/8.45)\right] + 0.07 \left[TST^{0.8} + TF^{0.8} - \left(TST + TF\right)^{0.8}\right]\right\} \quad (20)$$

and the propellant expended during aftercooled thrusting, WPST, is given by

$$WPST = WPF \cdot HR \cdot ERATT$$

In order to determine the velocity gravity loss errors introduced by the use of the low aftercooling thrust and long aftercooling thrusting time, powered flight trajectories were flown for two conditions. First, a powered flight profile was constructed in which the required characteristic velocity was attained by full power burn of the nuclear engine. After full power cutoff the vehicle was allowed to coast. A second trajectory was flown for the aftercooling thrust case. For this case, full power cutoff occurred at less than the required characteristic velocity and aftercooling thrusting initiated and continued to a thrust-to-weight ratio of approximately 0.001. At this point, the required characteristic velocity was attained. The trajectory flight parameters at this point of aftercooling thrust cutoff were then compared with the trajectory flight parameters for the nonaftercooling case at equal radius vectors. (See Figure III-8)

Comparative sets of trajectories were flown for a range of vehicle weights, characteristic velocities, and engine powers and thrusts. The maximum errors over the study range of interest were less than $0.1^{o}$ in flight path angle and less than 40 ft per second in hyperbolic excess velocity. The magnitudes of these errors were considered to be within the accuracy desired for the vehicle weight calculations. Therefore, the velocity gravity losses for the aftercooled depart earth mode are approximated by using the gravity losses for a nonaftercooled mode.

The procedure and equations outlined in this section are incorporated into the propulsion and stage design computations whenever an aftercooled mode is selected. The following section details these computations.

## PROPULSION AND STAGE DESIGN COMPUTATIONS

The analyses associated with specific components of an overall stage have been discussed in the previous sections. In this section, all of the analyses and the procedures used in designing a propulsion stage will be incorporated into a propulsion and stage design procedure.

The parameters of interest about a stage include the following: the propellant weight, WP; the vaporized propellant weight, WPV; the aftercooling propellant weight, if used, WPS; the stage structure weight, WS; the stage thermal insulation weight, WI; and the stage jettison weight, WJ,

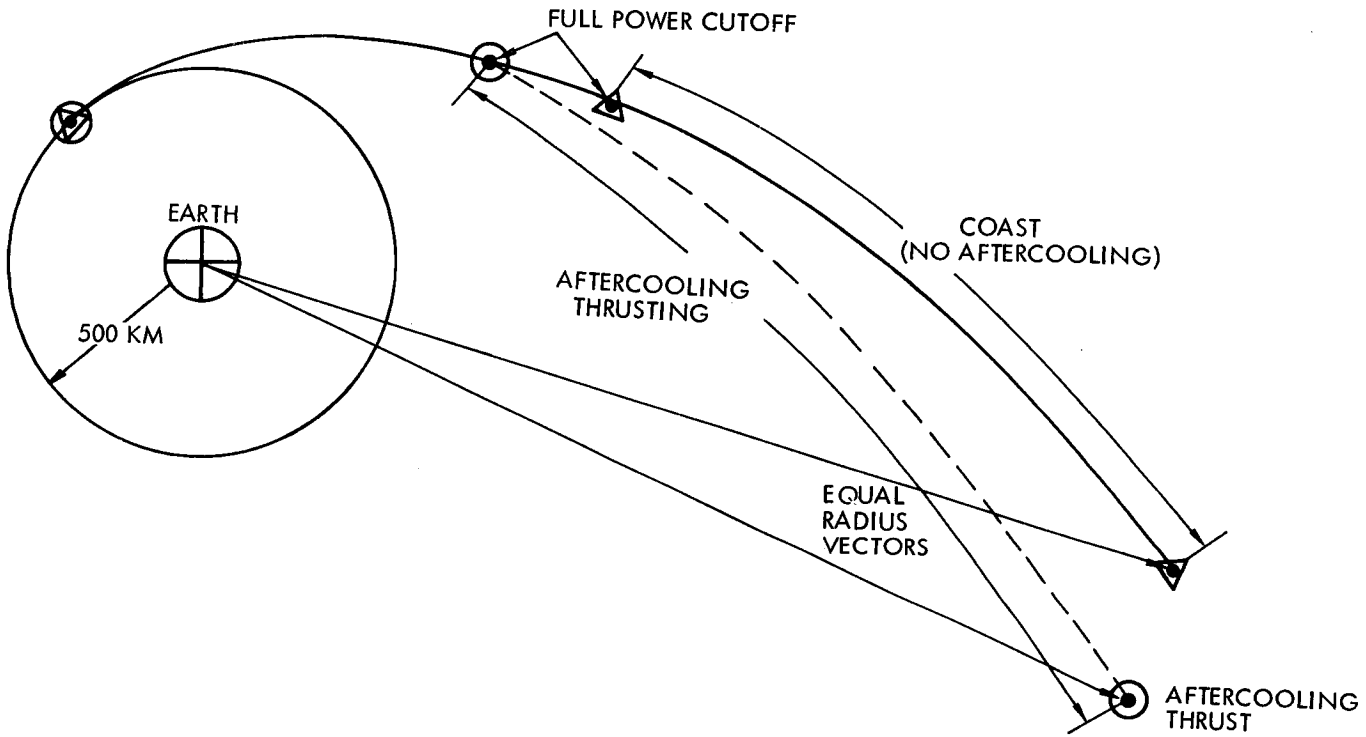


MAXIMUM ERRORS OVER RANGE OF INTEREST
(TRAJECTORY PARAMETERS AT EQUAL RADIUS VECTORS)

| | RADIUS VECTOR | FLIGHT PATH ANGLE | TOTAL $\Delta V$ | $V_\infty$ |
|---|---|---|---|---|
| △ NO AFTERCOOLING | 6.6 EARTH RADII | 14.44 DEG | 18,000 FT/SEC | 23,831 FT/SEC |
| ○ AFTERCOOLING THRUST TO F/W≤0.001 | 6.6 EARTH RADII | 14.52 DEG | 18,000 FT/SEC | 23,792 FT/SEC |

Figure III-8 Engine Aftercooling Gravity Loss Errors

which includes the tank structure, WS, insulation, and engine weight, WE. The vehicle thrust-to-weight ratio, the engine full power firing time, TF, and if applicable, the engine aftercooling time, TS, are also of interest.

The magnitude of the above items depends not only on the previously discussed scaling laws and optimum insulation relationships, but also on the stage payload, WPL, the thrust, THT, the specific impulse, ISP, of the propulsion system, and the characteristic velocity change, V, that the propulsion system must impart to the vehicle. Using the above parameters, the following procedure is employed to size the stage.

First an estimate of the propellant weight is made, based on the stage structure factor, $\sigma$, the stage payload, and the mass ratio, r. The stage structure factor is estimated or calculated using data from a previous iteration.

$$\sigma = \frac{WJ}{WJ + WP} \tag{21}$$

$$r = \exp(V/gISP) \tag{22}$$

$$WP = WPL \frac{(r-1)(1-\sigma)}{(1-r\sigma)} \tag{23}$$

As the program cycles through the main iteration loop (see Chapter II), the mass ratio and the stage structure factor converge on their final values, permitting an accurate estimate of WP.

For an aftercooled stage, the general stage design procedure is interrupted at this point, and the full power burn time, TF, the aftercooling time, TS, the energy ratio ERAT, and the estimated aftercooling propellant weight, WPS, are found using the equations described in the previous section. For a depart earth stage, the amount of aftercooling propellant that can be usefully employed for thrust, WPST, is also estimated, together with the energy ratio, ERATT, at which useful thrusting ceases.

The propellant used for full power operation, WP, or WPF for the aftercooled mode, the vaporized propellant WPV, (from the previous iteration), and the aftercooling propellant, WPS, if applicable, are summed to estimate the total propellant capacity required for the stage propellant tanks. The

number of tanks are then found based on the specified maximum propellant per tank. The remainder of the calculations are now put on a "per tank" basis by dividing the payload weight, engine weight, propellant weight, etc. by the number of tanks.

The total propellant per tank is used to determine the tank surface area, the propellant insulation weight, and the vaporized propellant weight, based on the equations discussed in the section on cryogenic propellant storage. The vaporized propellant, of course, is not carried through the current velocity change, but is expended over the previous portions of the trip.

It is now possible to complete the stage tank design, using the propellant tank scaling laws for single tanks. A stage jettison weight iteration loop is started, to converge on the correct value of WJ. Based on the current best estimates (per tank) of WP, WPV, and WPS, if applicable, the tank structure weight, WS, is determined using the appropriate propellant tank scaling law. Adding the single tank engine weight and insulation weight to WS, the single tank jettison weight, WJ, is obtained. Then a new estimate of WP can be made

$$WP = (r - 1)\ (WPL + WJ) \tag{24}$$

For an aftercooled stage, a new estimate of WPS is also made. These new estimates of propellant are used to resize the tank, and the stage jettison weight iteration loop is continued until convergence is obtained.

The stage jettison weight iteration loop is slightly different if the stage is an aftercooled, depart earth stage. The effect of the useful aftercooling thrust must be included.

The aftercooling thrust accelerates the vehicle through a velocity change VS. Once WPST is estimated as described in the previous section, an estimate of VS can be made based on the vehicle weight, W2, at the end of full power operation, but before aftercooling begins. At this point all engines not to be aftercooled are jettisoned, but the tanks and aftercooled engines remain, as well as the aftercooling propellant, WPS. The mass ratio is

$$r_S = \frac{W2}{W2 - WPST} \tag{25}$$

and

$$VS = gISPS \log_e (r_S) \tag{26}$$

Thus the full power velocity change, VF, is reduced to

$$VF = V - VS \tag{27}$$

with a corresponding decrease in the full power mass ratio, $r_F$

$$r_F = \exp(VF/gISPF) \tag{28}$$

Using $r_F$ in Eq. 24, the full power propellant estimate is recalculated. The stage jettison weight iteration loop is continued until convergence is obtained.

## AERODYNAMIC BRAKING SCALING LAWS

As part of the mission analyses it was necessary to express the weight of the aerodynamic heat shield as a function of entry velocity for the operational modes employing aerodynamic braking for the earth entry module and for arriving at Mars. The analysis and derivation of scaling laws for earth aerodynamic braking were previously considered by TRW/STL on another NASA contract, NAS 2-1409, for Ames Research Center. The data presented here are based on this previous work which is detailed in Section 6 of the final study report, Ref. 8.

The scaling laws for Mars aerodynamic braking were based on data developed by Lewis Research Center.

### Earth Aerodynamic Braking

The aerodynamic heating encountered for the extreme velocities considered in this study for earth entry is beyond the present state-of-the-art. Thus, it was necessary to use reasonable assumptions based on known data and analyses to arrive at representative weights.

Radiant and Convective Heating - The heating computations were based on an undershoot trajectory to pullout at 10 g's followed by constant altitude flight to orbital velocity (see Fig. III-9). Convective heating computations were made for conditions from the entry velocities to 40,000 ft/sec.

Heating calculations were performed for a recovered vehicle weight, exclusive of heat shield and insulation of 9034 lb for a vehicle with a L/D=1. For purposes of providing heating calculations, the major and minor axes of the ellipsoidal nose of the vehicle were taken as 25.5 in. and 14.6 in.

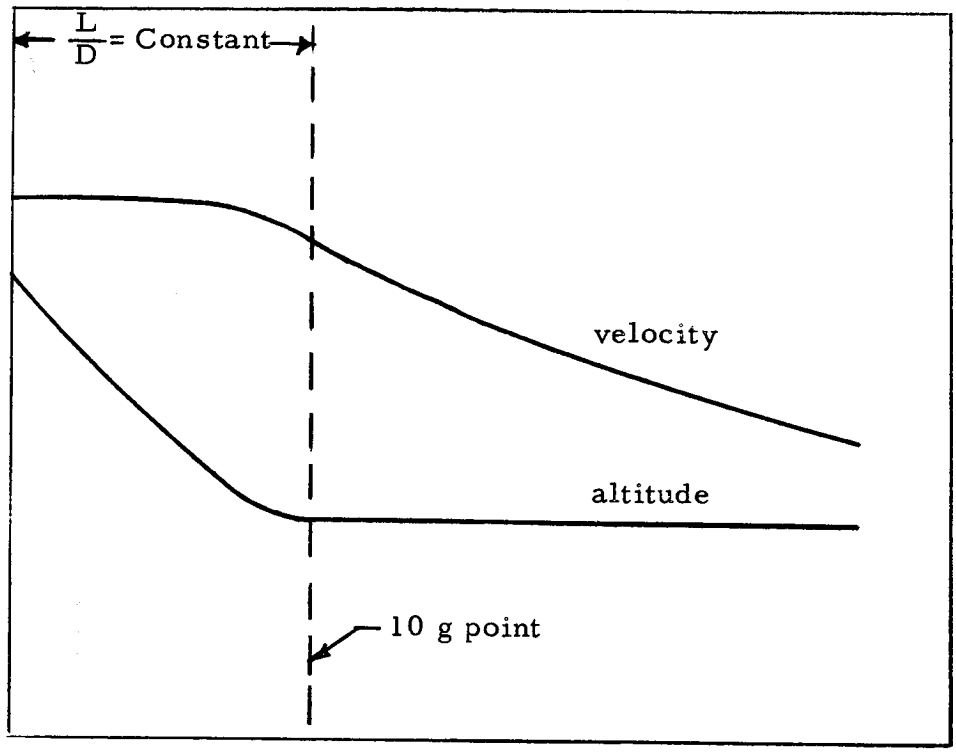


Figure III-9 Trajectory Type for Heating Calculations

Heat Protection Design - In the design of a heat shield for the earth entry module it was necessary to extrapolate the knowledge of material behavior in lower velocity environments to the conditions of interest for return from Mars. With increasing velocity, the relative importance of many factors affecting heat of ablation, such as surface temperature, free stream enthalpy, and radiant heat rates, is changed. Although quantitative data on ablation materials are not available for the very high velocity regimes, approximate design values can be estimated.

As a conservative preliminary design figure, a value of heat of ablation of 10,000 Btu/lb was chosen along with a material density of 120 $lb/ft^3$. A typical material would be phenolic refrasil. It is recognized that much uncertainty exists regarding the heat of ablation value, but this represents a best estimate at this time.

Insulation weights were estimated on the basis of an analytical approximation of Baer and Ambrosia (Ref. 9 ). The earth entry module weight breakdown is shown in Table III-7.

Table III-7 Earth Entry Module Weight Breakdown

| | | | |
|---|---|---|---|
| $V_E$ (ft/sec)* | 70,000 | 60,000 | 50,000 |
| Ballistic Coefficient (psf) | 865 | 744 | 665 |
| ABLATED HEAT SHIELD WEIGHT (LBS) | | | |
| Nose Region | | | |
| Convective | 814 | 450 | 195 |
| Radiant | 1,012 | 511 | 148 |
| Total | 1,826 | 961 | 343 |
| Lower Curved Surface | | | |
| Convective | 2,670 | 1,478 | 735 |
| Radiant | 0 | 0 | 0 |
| Total | 2,670 | 1,478 | 735 |
| Top Surface (Convective) | 1,043 | 576 | 286 |
| TOTAL | 5,539 | 3,015 | 1,364 |
| INSULATION WEIGHT | 3,500 | 3,500 | 3,500 |
| TOTAL HEAT SHIELD | 9,039 | 6,515 | 4,864 |
| RECOVERED VEHICLE WEIGHT | 9,034 | 9,034 | 9,034 |
| TOTAL VEHICLE WEIGHT | 18,073 | 15,549 | 13,898 |

*The velocity, $V_E$, used in this table is relative to the earth's atmosphere with the vehicle entering to the east at the equator.

Parametric Scaling Laws - Since several parametric values of earth recovered weight were to be investigated, it was necessary to estimate the heat shield weights for several vehicle weights.

The previous analysis considered a vehicle having a weight (less heat shield) of 9,034 lb. The entire range of interest of recovered vehicle weights was between 7,000 lb. and 20,000 lb. Therefore, additional designs were provided at weights of 7,000, 16,000, and 22,000 lb. Calculations were made at entry velocities of 50,000, 60,000, and 70,000 ft/sec. The following assumptions were made for these supplementary calculations.

- The vehicle density (less heat shield) is constant. Therefore, the lengths of the vehicles scale as the cube root of the weights.
- The nose shape and size is held constant. This simplifies the procedure for scaling convective and radiant heat rates.
- The drag and lift coefficients are constant and are not significantly affected by the preceding assumption of holding the nose size fixed. This is a valid assumption for this shape for which the ratio of nose radius-to-base radius is relatively small.

The results of the calculations are presented in Table III-8. In addition, the data were extrapolated to the velocity region of 35,000 ft/sec by considering minimum insulation requirements.

The data on Table III-8 were crossplotted to obtain correlated weight and velocity data for four discrete earth recovered weights (less heat shield) 7,000, 10,000, 15,000, and 20,000. The velocity units were changed from ft/sec to km/sec and the data converted to velocities with respect to a non-rotating earth, i.e.,

$$V_E = V_{AE} - V_{ER_{100}}$$

$$= V_{AE} - 0.471$$

where

$V_E$ = Velocity relative to earth's atmosphere, entering to east at the equator at 100 km (km/sec)

$V_{AE}$ = Velocity relative to non-rotating earth at 100 km (km/sec)

$V_{ER_{100}}$ = Earth's rotational velocity at 100 km (km/sec)

## Table III-8 Summary of Earth Entry Module Weights

| Weight Less Heat Shield (lb) | 7,000 | | | 9,034 | | | 16,000 | | | 22,000 | | |
|---|---|---|---|---|---|---|---|---|---|---|---|---|
| $V_E$ (ft/sec)* | 50,000 | 60,000 | 70,000 | 50,000 | 60,000 | 70,000 | 50,000 | 60,000 | 70,000 | 50,000 | 60,000 | 70,000 |
| Ballistic Coefficient (psf) | 640 | 720 | 845 | 665 | 744 | 865 | 750 | 815 | 920 | 810 | 875 | 970 |
| Heat Shield Weight (lb) | 4,180 | 5,690 | 7,900 | 4,864 | 6,515 | 9,039 | 7,000 | 9,000 | 12,210 | 8,430 | 10,950 | 14,500 |
| Total Vehicle Weight (lb) | 11,180 | 12,690 | 14,900 | 13,898 | 15,549 | 18,073 | 23,000 | 25,000 | 28,210 | 30,430 | 32,950 | 36,500 |

*The velocity, $V_E$, used in this table is relative to the earth's atmosphere with the vehicle entering to the east at the equator.

A second order polynomial was analytically fitted to the data points for the various recovered vehicle weights to yield the following scaling law equations relating the earth entry module weight to the arrival velocity at an altitude of 100 km.

$$W_R = 7000 \text{ lbs}$$

$$W_{ERM} = 36.92\ V_{AE}^2 - 767.9\ V_{AE} + 14,162$$

$$W_R = 10,000 \text{ lbs}$$

$$W_{ERM} = 46.71\ V_{AE}^2 - 1042.3\ V_{AE} + 20,122$$

$$W_R = 15,000 \text{ lbs}$$

$$W_{ERM} = 55.82\ V_{AE}^2 - 1237.7\ V_{AE} + 27,384$$

$$W_R = 20,000 \text{ lbs}$$

$$W_{ERM} = 55.83\ V_{AE}^2 - 1164.6\ V_{AE} + 32,480$$

where

$W_R$ - Recovered or usable payload weight after earth entry (lbs)

$W_{ERM}$ - Gross vehicle weight or earth entry module weight (lbs)

Graphs of these scaling law equations are shown in Fig. III-10.

In order to derive scaling law constants for earth aerodynamic braking that are amenable to the FLOP and SWOP programs, it was necessary to perform other velocity tranformations. First the velocity data stored in these programs are normalized to an earth altitude of 500 km. Second, the stored velocities are in the form of characteristic velocities with respect to the circular earth orbital velocity at 500 km. That is, the characteristic velocity is the impulsive velocity change required to retro into a 500 km circular orbit for the earth arrive phase (or boost out of orbit for an earth depart phase). Therefore, the preceding equations required transformation by the following velocity substitution.

$$V_{AE}^2 = (\Delta V_{AE} + V_{c_{500}})^2 + 2(V_{c_{100}}^2 - V_{c_{500}}^2)$$

$$= \Delta V_{AE}^2 + 15.232\ \Delta V_{AE} + 65.175$$

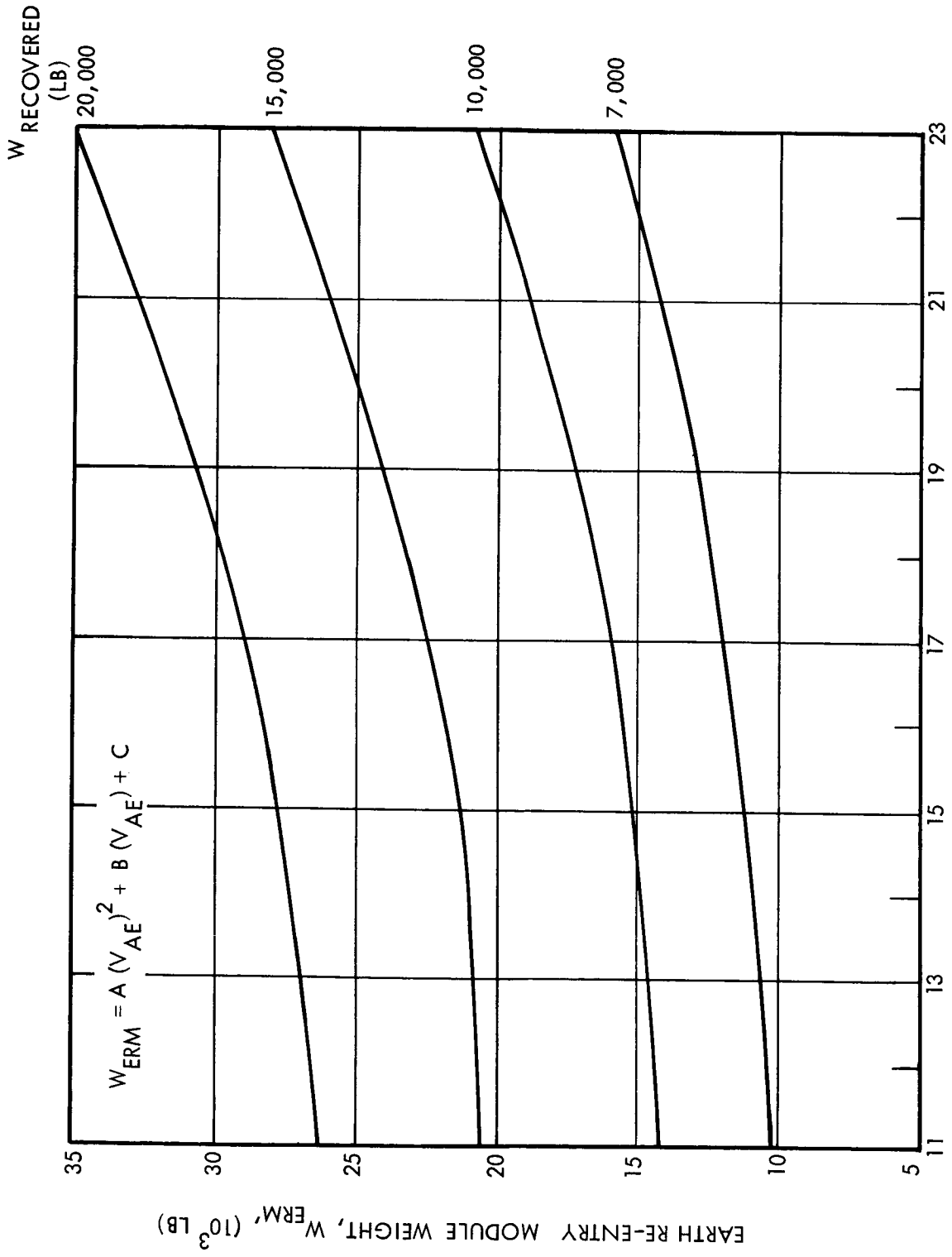


Figure III-10 Earth Aerodynamic Braking Scaling Laws

where

$\Delta V_{AE}$ - Characteristic velocity corresponding to velocity data stored in computer programs (km/sec)

$V_{c_{100}}$ and $V_{c_{500}}$ - Circular orbital velocity at 100 and 500 km altitude, respectively (km/sec)

This substitution was made numerically in the scaling law equations for discrete values of $\Delta V_{AE}$ and the resulting points were approximated by second degree polynomials to yield the following equations. The coefficients of these equations constitute the input values used in the computer programs for the earth aerodynamic braking modes.

$$W_R = 7,000 \text{ lbs}$$

$$W_{ERM} = 37.0\ \Delta V_{AE}^2 - 201.0\ \Delta V_{AE} + 10,512$$

$$W_R = 10,000 \text{ lbs}$$

$$W_{ERM} = 46.8\ \Delta V_{AE}^2 - 324.4\ \Delta V_{AE} + 14,929$$

$$W_R = 15,000 \text{ lbs}$$

$$W_{ERM} = 56.0\ \Delta V_{AE}^2 - 380.0\ \Delta V_{AE} + 21,256$$

$$W_R = 20,000 \text{ lbs}$$

$$W_{ERM} = 56.0\ \Delta V_{AE}^2 - 308\ \Delta V_{AE} + 26,936$$

Mars Aerodynamic Braking

The weight scaling law for aerodynamic braking at Mars was based on an equation obtained from Lewis Research Center. The equation is:

$$\frac{W_S}{W_{AM}} = 0.2 + 0.0076\,(\bar{V}^2 - 1)\left[1 + \frac{1}{(L/D)^2}\right]^{1/2}$$

$$= K\,(0.001385\ V_{AP}^2 + 0.183)$$

where

$W_S$ - Heat shield weight including all jettisonable ablative material, structure, and insulation (lbs)

$W_{AM}$ - Gross vehicle weight arriving at Mars (lbs)

$\bar{V} = \dfrac{V_{AP}}{V_{mc_{167}}}$ where $V_{AP}$ is the Mars arrival velocity at an altitude of 167 km, and $V_{mc_{167}}$ is the circular orbital velocity at 167 km (km/sec)

L/D - Vehicle lift-to-drag ratio; assumed equal to 0.5

K - Arbitrary constant used to vary scaling law parametrically. A value of K = 1 was used unless specifically noted otherwise.

Graphs of this equation are shown in Fig. III-11

As in the case of earth aerodynamic braking, it was necessary to normalize the scaling law to a different Mars orbital altitude (600 km) and transform the velocity variable to a characteristic velocity. This was accomplished by substituting the following:

$$V_{AP} = (\Delta V_{AP} + V_{mc_{600}})^2 + 2(V^2_{mc_{167}} - V^2_{mc_{600}})$$

$$= \Delta V^2_{AP} + 6.60\,\Delta V_{AP} + 13.64$$

where

$\Delta V_{AP}$ - Characteristic velocity corresponding to velocity data stored in computer program; i.e., the impulsive velocity change required to brake into a 600 km circular orbit for the Mars arrive phase.

This substitution yields the following equation whose coefficients constitute the input values used in the computer program for Mars aerodynamic braking

$$\frac{W_S}{W_{AP}} = K(0.001386\ \Delta V^2_{AP} + 0.00916\ \Delta V_{AP} + 0.2019)$$

## CRYOGENIC PROPELLANT STORAGE THERMAL ANALYSIS

A cryogenic propellant storage analysis was made to permit the sizing of the required tankage insulation and calculation of the weight of propellant boiled off during the mission. This analysis determines the optimum trade-off between the thickness or weight of insulation and weight of vaporized propellant such that a minimum weight vehicle results. The equations obtained from this analysis form the basis of the insulation/boiloff optimization subroutine in the mission evaluation computer programs.

The assumption of vented tanks was made throughout this study and no attempt was made to evaluate the regime of operation of a vented tank, as compared to a non-vented tank. The insulation requirements were considered and sized only for the conditions and storage durations commencing with the point just prior to boost out of earth orbit. At this initial point, it was assumed that all tanks were full.

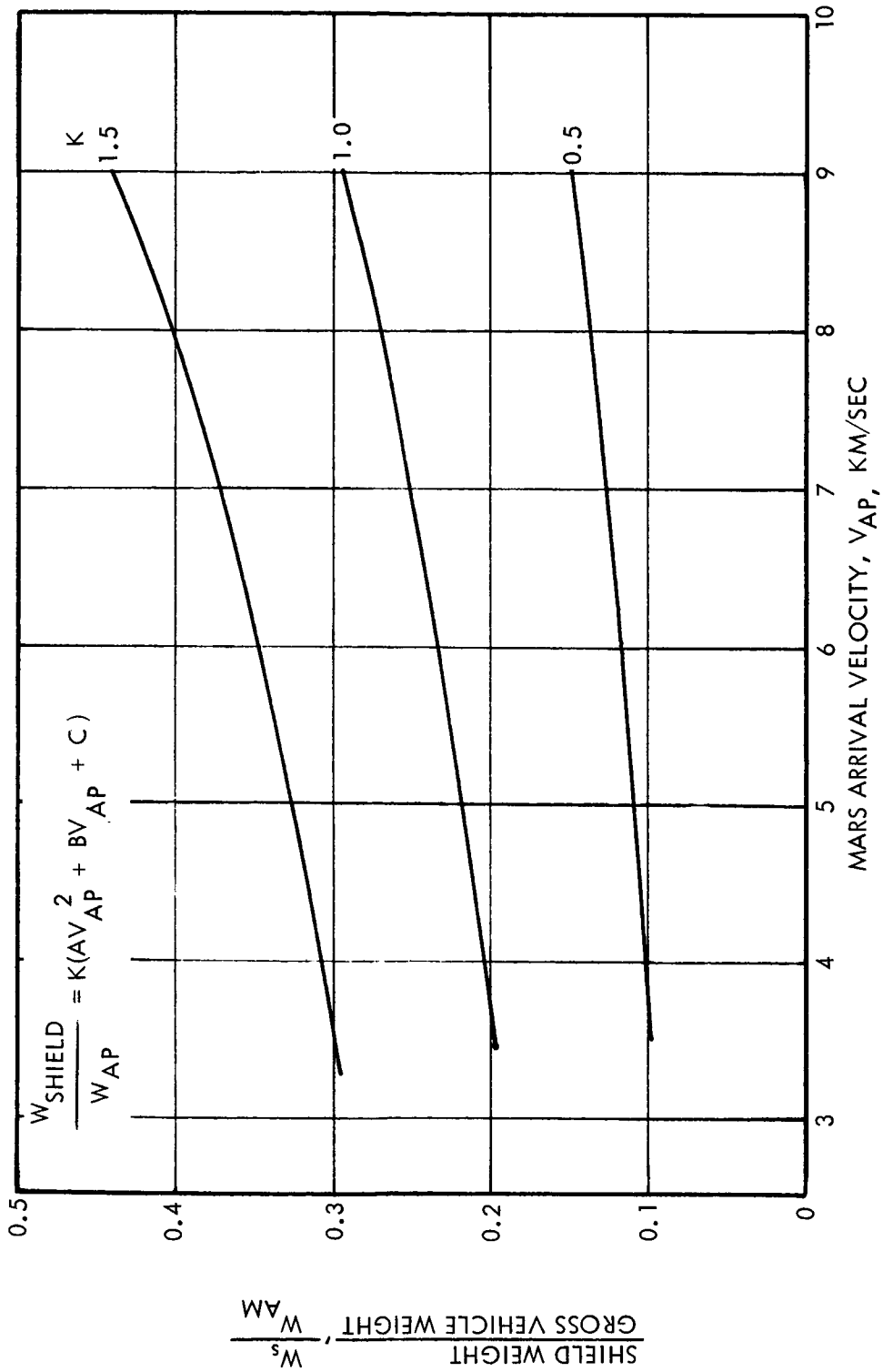


Figure III-11 Mars Aerodynamic Braking Scaling Laws

Optimization Analysis

The optimum selection of the insulation requirements for a cryogenic propellant tank is dependent not only on the insulation and thermal parameters (density, conductivity, temperatures, etc.) but also on the duration of storage and the size, number, and time of vehicle propulsive velocity changes. For a multistage vehicle, the relationships between these latter factors has a major influence in the trade-off between insulation and propellant boiloff.

The optimization equations will be developed below only for the second stage of a multistage vehicle. This stage corresponds to the arrive Mars stage of a stopover mission. From the fundamental rocket equation

$$r_{(AM)} = \frac{W_o - W_{S(DE)} - W_{I(DE)} - W_{P(DE)} - W_{V(AM)out}}{W_{PL} + W_{S(AM)} + WI_{(AM)}} \qquad (29)$$

where:

- $r$ = Mass Ratio
- $W_o$ = Initial gross vehicle weight in earth orbit
- $W_S$ - Inert stage weight (less insulation)
- $W_I$ - Insulation weight
- $W_P$ - Propellant weight (less propellant vaporized)
- $W_V$ - Propellant vaporized
- $W_{PL}$ - Payload weight

subscripts:

- (DE) - Depart earth stage
- (AM) - Arrive Mars stage
- out - Outbound leg

Equation (29) may be rewritten

$$W_o = r_{(AM)} \left( W_{PL} + W_{S(AM)} + W_{I(AM)} \right) + W_{S(DE)} + W_{I(DE)} + W_{P(DE)} + W_{V(AM)out} \qquad (29a)$$

The weight of propellant burned in the depart earth stage is

$$W_{P(DE)} = (r_{(DE)}-1)\left[W_{PL} + W_{S(DE)} + W_{I(DE)} + W_{S(AM)} + W_{I(AM)} + W_{P(AM)} + W_{V(AM)out}\right] \quad (30)$$

and similarly

$$W_{P(AM)} = (r_{(AM)}-1)\left[W_{PL} + W_{S(AM)} + WI_{(AM)}\right] \quad (31)$$

The weight of insulation and vaporized propellant is given by

$$W_I = A\,d\,t \quad \text{and} \quad (32)$$

$$W_V = \frac{k\,A\,(\Delta T)\,T}{h\,t} \quad (33)$$

where

- A - Tank surface area
- d - Insulation density
- t - Insulation thickness
- k - Insulation thermal conductivity
- $\Delta T$ - Temperature difference across insulation
- T - Time
- h - Propellant heat of vaporization

From equations (29a), (30) and (31), for minimum initial vehicle weight and assuming constant inert stage and payload weights

$$\frac{\partial W_o}{\partial t_{(AM)}} = r_{(AM)}\frac{\partial W_{I(AM)}}{\partial t_{(AM)}} + (r_{(DE)}-1)\left[\frac{\partial W_{I(AM)}}{\partial t_{(AM)}} + \frac{\partial W_{V(AM)out}}{\partial t_{(AM)}} + (r_{(AM)}-1)\frac{\partial W_{I(AM)}}{\partial t_{(AM)}}\right] + \frac{\partial W_{V(AM)out}}{\partial t_{(AM)}}$$

$$= 0$$

or

$$\frac{\partial W_{V(AM)out}}{\partial t_{(AM)}} + r_{(AM)}\frac{\partial W_{I(AM)}}{\partial t_{(AM)}} = 0 \quad (34)$$

But from equations (32) and (33)

$$\frac{\partial W_{I(AM)}}{\partial t_{(AM)}} = A_{(AM)} d \quad \text{and} \tag{35}$$

$$\frac{\partial W_{V(AM)out}}{\partial t_{(AM)}} = \frac{k A_{(AM)} (\Delta T) T_{out}}{h t^2_{(AM)}} \tag{36}$$

therefore:

$$t_{(AM)opt} = \left[ \frac{k (\Delta T) T_{out}}{h d r_{(AM)}} \right]^{1/2} \tag{37}$$

By extending this analysis to the other vehicle stages, similar expressions are obtained for the optimum insulation thicknesses. Substituting the optimum insulation thicknesses into equations (32) and (33) gives the expressions for the optimum weights of stage insulation and propellant boiloff. The following additional subscripts are used.

(DM) - Depart Mars
(AE) - Arrive earth
stov - Stopover phase
in - Inbound leg

Arrive Mars Stage

$$W_{I(AM)} = A_{(AM)} \left[ \frac{k d (\Delta T) T_{out}}{h r_{(AM)}} \right]^{1/2} \tag{38}$$

$$W_{V(AM)} = r_{(AM)} W_{I(AM)} \tag{39}$$

Depart Mars Stage

$$W_{I(DM)} = A_{(DM)} \left[ \frac{k d (\Delta T) (T_{out} + r_{(AM)} T_{stov})}{h r_{(AM)} r_{(DM)}} \right]^{1/2} \tag{40}$$

$$W_{V(DM)} = \frac{(T_{out} + T_{stov}) r_{(AM)} r_{(DM)}}{T_{out} + r_{(AM)} T_{stov}} \cdot W_{I(DM)} \tag{41}$$

Arrive Earth Stage

$$W_{I(AE)} = A_{(AE)} \left[ \frac{k\, d\, (\Delta T)\, (T_{out} + r_{(AM)}\, T_{stov} + r_{(AM)}\, r_{(DM)}\, T_{in})}{h\, r_{(AM)}\, r_{(DM)}\, r_{(AE)}} \right]^{1/2} \quad (42)$$

$$W_{V(AE)} = \frac{(T_{out} + T_{stov} + T_{in})\, r_{(AM)}\, r_{(DM)}\, r_{(AE)}}{(T_{out} + r_{(AM)}\, T_{stov} + r_{(AM)}\, r_{(DM)}\, T_{in})} \cdot W_{I(AE)} \quad (43)$$

The assumption that all tanks are full just prior to boost out of earth orbit leads to the result that the insulation thickness and vaporized propellant for the depart earth stage are zero. If a storage time with its attendant boiloff were to be considered for the earth parking orbit phase, then the optimization equations for all other stages would have to be revised with the appropriate parking orbit storage time and depart earth mass ratio terms and factors. The equations for the depart earth stage would be similar to equations (38) and (39) except that all subscripts would change.

The manner in which the equations are expanded for each additional stage is clearly evident from equations (38) through (43). Therefore, the equations for additional stages can be written by inspection.

It should be noted that although the optimization equations have been derived for a minimum initial vehicle weight in earth orbit, identical equations would be obtained for the condition of maximum payload. In that case, the payload, $W_{PL}$, is the independent parameter and the initial vehicle weight, $W_o$, is a constant.

The optimization equations apply for either cryogenic monopropellants, or bipropellants. For bipropellants, the equations are employed for the fuel and oxidizer separately, obtaining separate insulation and boiloff weights for each propellant component. The appropriate tank areas, heats of vaporization, and temperature differences must be used in each case.

In the computation of the cryogenic propellant thermal provisions, it was assumed that the tank insulating supports could be designed so that the weight requirements of and heat transfer through the supports would be negligible compared to the weight of and the heat transfer through the tank surface insulation. Nevertheless, the derived equations are also applicable (with appropriate parameter values) for determining the optimum insulation support weight and vaporized propellant due to heat leaks through the supports.

Insulation and Thermal Constants

The following assumptions and values were used for specifying the various insulation and thermal constants in the optimization equations.

The insulation was assumed to be National Research Corporation's NRC-2, which consists of layers of crinkled aluminized mylar 0.25 mil thick. The nominal values of the insulation thermal conductivity and density are $7 \times 10^{-5}$ Btu/hr. ft. $^{o}$R and 3 lb./ft.$^{3}$, respectively. In the sensitivity analysis these values were varied over a range, the thermal conductivity from $1 \times 10^{-5}$ to $7 \times 10^{-5}$ Btu/hr. ft. $^{o}$R and the density from 1 to 7 lb./ft.$^{3}$.

In determining the temperature differences across the insulation, a non-spinning tank was assumed and an average temperature difference over the entire tank surface was calculated. No planetary influence or heat sources other than the sun were assumed and an average distance to the sun of 1.2 A.U. was used. A solar absorptivity of 0.20 and an emissivity equal to 0.80 were used for the tank surface conditions. The average temperature differences across the insulation computed for liquid hydrogen tanks is 160$^{o}$R and for liquid oxygen tanks, 34 $^{o}$R. The heats of vaporization for hydrogen and oxygen are 192.7 and 91.6 Btu/lb., respectively.

PAYLOADS

The payloads or fixed weights assigned to the various missions were selected jointly by MSFC and TRW/STL. They represent reasonable values obtained from the many interplanetary mission studies performed by NASA and industry in the past three years.

The earth recovered payload used for the stopover and flyby missions lands the crew on the earth's surface after aerodynamic braking has been accomplished. It consists of the crew and the required structure, landing and recovery aids, power supply, communications, guidance, and navigation equipment, reaction jets, life support systems, and any space or planetary payloads that may be returned to earth.

The mission module used for the stopover and flyby mission contains all systems, equipment, and living quarters required during the full duration of the mission. This module is jettisoned just prior to retrobraking at earth or aerodynamic braking if a retro is not employed. It consists of

structure, crew quarters, life support systems, medical supplies and recreation equipment, communication, guidance, and navigation systems, power supplies, maintenance facilities and spare parts, air locks, and the solar flare shield. (For the stopover mission, the solar flare shield is not included in the inputted mission module weight. The shield weight is computed as a function of the assumed solar activity and trajectory perihelion distance. This weight is added to the inputted weight to determine the total mission module weight to be jettisoned.)

The planet entry module for the stopover mission and the planet probe for the flyby mission are similar payloads. That is, they are both jettisoned from the spacecraft in the vicinity of the target planet, out of circular orbit for the stopover mission and just prior to or during the flyby phase for the flyby mission. They contain the required systems and equipment for landing the module on the planet surface and subsequently performing scientific and engineering experiments. In addition, the planet entry module for the stopover mission contains the ascent or orbit return module which returns the crew and payload to the orbiting spacecraft. The specified weight for the orbit return module includes only that portion of the module which is taken onboard the orbiting spacecraft and subsequently boosted out of planetary orbit.

The payload for the lunar transfer orbit is the useful weight delivered into a 100 nm circular lunar orbit. This weight was varied parametrically.

The nominal payload weights are given below.

Stopover Mission

| | | |
|---|---|---|
| Earth recovered payload | - | 10,000 lb. |
| Mission module (8 man) | - | 68,734 lb. (plus solar flare shield) |
| Planet entry module | - | 80,000 lb. |
| Orbit return module | - | 1,500 lb. |

Flyby Mission

| | | |
|---|---|---|
| Earth recovered payload | - | 8,500 lb. |
| Mission module (3 man) | - | 65,000 lb. (including solar flare shield) |
| Planet probe | - | 10,000 lb. |

Lunar Transfer Mission

Payload in lunar orbit - 100,000 lb.
200,000 lb.
300,000 lb.
400,000 lb.

## SOLAR FLARE SHIELD WEIGHT SCALING LAWS

The crew exposure to solar flare radiation is limited by a solar flare shield. The amount of shielding, or the shield weight, depends on the solar activity, the trip time, the total dose permitted, the distance from the sun, and the volume of space to be protected by the shield. Since the shield weight depends on trajectory parameters, i.e., trip time and distance from the sun, its effect is included in the optimization equations.

The solar flare activity varies in an approximate 11 year cycle from a quiet sun to an active sun and back again. This yearly variation was accounted for by developing three solar flare shield weight scaling laws, for a quiet, intermediate, and active sun. Since the stopover trajectories used in this study all have trip times of approximately 400 to 450 days, the total trip time has a weak influence on the required solar flare shield weight. Therefore, the scaling laws were developed for this range and have no functional dependence on trip time within the program. The total dose to the crew during the trip is approximately 100 REM. The value of the closest perihelion distance of the two or three legs of the mission is used as the distance variable in the shield weight calculation. The protected space is assumed to have a 500 $ft^2$ surface. The net result of these considerations lead to the scaling laws listed below and shown in Fig. III-12. They are based in part on information supplied by Lewis Research Center.

Active Solar Flare Activity

$$W_S = 12,672 + \frac{2615}{r_p - 0.27165}$$

Intermediate Solar Flare Activity

$$W_S = 14,463 + \frac{1315}{r_p - 0.27085}$$

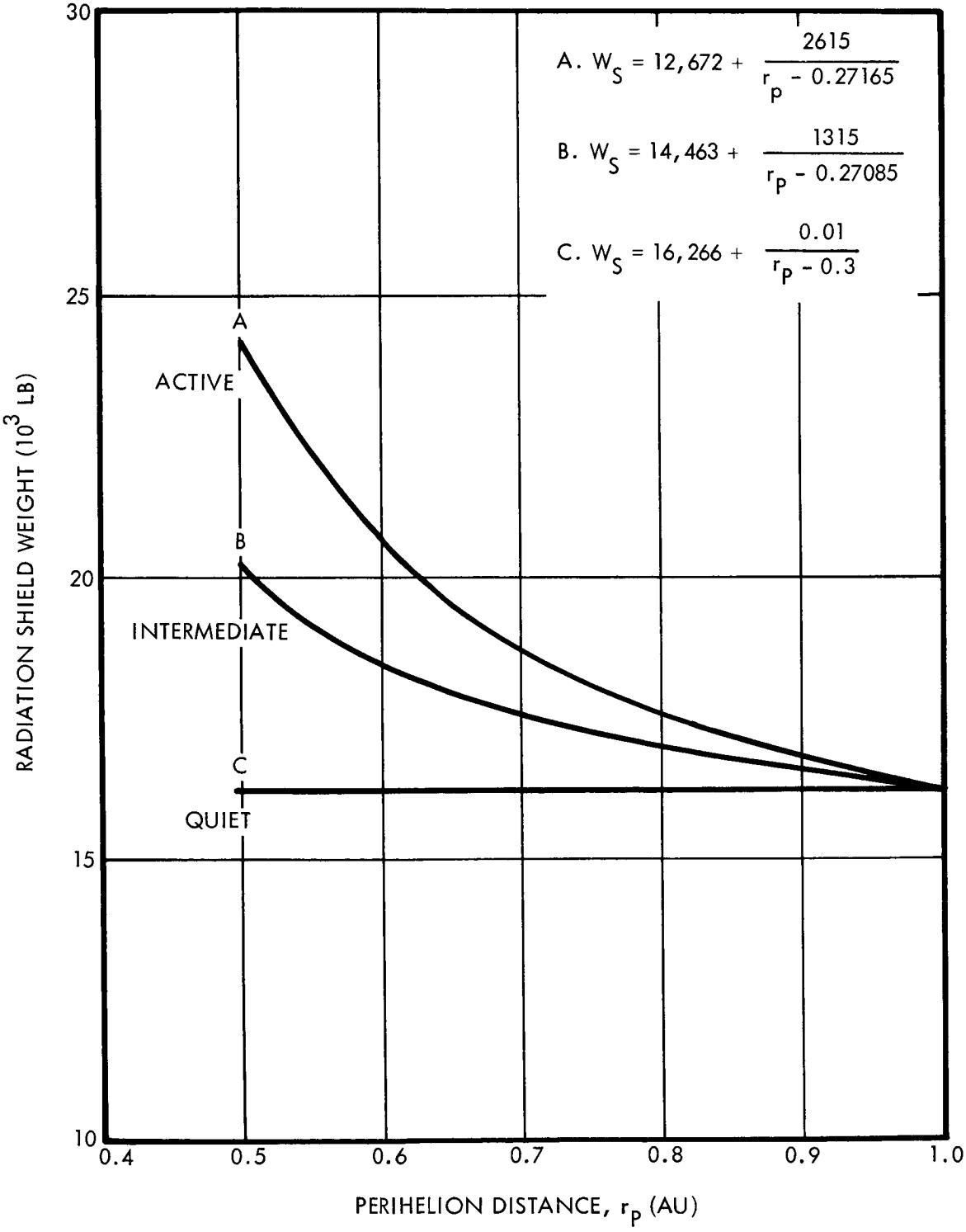


Figure III-12 Solar Flare Shield Weight

Quiet Solar Flare Activity

$$W_S = 16,266 + \frac{0.01}{r_p - 0.3}$$

The scaling law for the quiet sun was used for opposition years 1975 and 1986. The intermediate sun scaling law was used for the 1978, 1984, and 1988 opposition years. For 1980, 1982, and 1990, the active sun solar flare radiation shield weight scaling law was used. These equations were used only for the vehicle weight computations for stopover missions. The solar flare shield weight for flyby missions is assumed constant and is included as part of the mission module weight.

Since the shield weight defined by each scaling law is only dependent on perihelion distance, each stopover mission is optimized considering the additional shield weight required as the vehicle approaches closer to the sun.

## LIFE SUPPORT EXPENDABLES

The life support expendables for the manned stopover and flyby missions include all of the crew's environmental and biological requirements which are expended at an average daily rate for the duration of the mission. Although the computer program permits selection of different rates of life support expenditures for the outbound, stopover, and inbound phases of the mission, a constant rate of expenditure was used for the entire duration of each type of mission.

As in the case of the payload weights, the life support expendable weights were selected jointly by MSFC and TRW/STL. These weights represent reasonable values based on interplanetary mission studies performed by NASA and industry. A life support expendable rate of 50 lb/day was used for the stopover mission and 40 lb/day for the flyby mission.

## MIDCOURSE CORRECTION

The midcourse and terminal velocity correction requirements used in the vehicle weight calculations are based in part on results obtained from an interplanetary guidance error analysis performed by TRW/STL as part of another NASA contract, NAS2-1408 for Ames Research Center. The

details of this analysis are given in section 7 of the final study report, Ref. 8. The results of other NASA and industry interplanetary and lunar mission studies also were considered in determining the midcourse correction requirements. The values used are listed below.

| | |
|---|---|
| Stopover mission, outbound leg | 100 m/sec |
| Stopover mission, inbound leg | 100 m/sec |
| Swingby mission, third leg | 100 m/sec |
| Flyby mission, outbound leg | 200 m/sec |
| Flyby mission, inbound leg | 300 m/sec |
| Lunar transfer mission | 30 m/sec |

It was assumed in all mission calculations, that the midcourse corrections were performed with a liquid storable propellant system having a specific impulse of 330 sec. Separate jettisonable stages were used for the outbound and inbound leg velocity corrections.

ATTITUDE CONTROL

The weight provisions allocated for attitude control of the spacecraft was selected somewhat arbitrarily due to the lack of onboard system definitions and requirements. The attitude control functions are assumed to include orientation for midcourse corrections, spinning of the spacecraft or mission module for artificial gravity or thermal control, orientation of communication antennas, sensors, radiators, or solar panels or collectors, and orientation for planetary rendezvous and aerodynamic braking or propulsive maneuvers.

One percent of the vehicle weight was used for attitude control during each leg of the planetary missions and during the lunar transfer mission. The attitude control provisions during the planetary stopover period were computed on the basis of 0.2 percent of the vehicle weight in planetary orbit.

ORBIT ADJUSTMENT

A separate propulsion system is included in the spacecraft for circularizing and adjusting the orbit after braking at Mars for all modes employing aerodynamic braking at Mars. This jettisonable propulsion stage utilizes liquid storable propellants at a specific impulse of 330 sec and is sized for a characteristic velocity of 130 m/sec.

## REPRESENTATIVE VEHICLE DESIGN

The overall objective of this study was to select the design and operating characteristics for the compromise nuclear rocket engine. The final results appear as a preliminary design of the selected optimum engine together with a representative vehicle design which could be employed for the most important classes of missions.

The details of the compromise engine performance and design requirements appear in Vol. V of this set of final reports. They also are summarized in this section for the sake of continuity and completeness. The constraints and requirements for the remaining vehicle systems have been described and delineated previously in this chapter. The evaluation of the performance capabilities of the compromise nuclear engine (as well as perturbations about the nominal engine characteristics) are presented in the succeeding chapter of this volume and also in Vol. V. The representative vehicle design is fully described in this section.

### Compromise Engine Selection

The engine selection process was complicated by the fact that there are many different missions that can profitably utilize a nuclear engine. These range from lunar transfer missions to Mars stopover missions and beyond. They involve different payloads, aerobraking capabilities, propulsion system combinations, and operating procedures. As a result, there is no one engine that is best suited for all missions. However, by clustering several nuclear engines on one stage when appropriate, it is possible to find a set of engine design parameters that permit near-optimum vehicle performance for most missions.

Early study results obtained with the mission optimization programs (SWOP and FLOP) allowed an optimum engine thrust range to be established. Within this thrust range, the details of the nuclear engine and its sensitivity to design parameter changes were determined using the nuclear engine optimization program (NOP). Then using the results obtained by the engine computer program as input values to the SWOP program, the vehicle performance as a function of the principal engine design parameters were studied to find the best combination of engine characteristics.

Thrust Range Selection - The first step in the determination of the compromise nuclear engine was the narrowing of the range of engine thrusts or power levels. This was accomplished by representing the engine by approximate scaling laws that relate the basic engine parameters of weight and thrust as shown previously in Table III-6. These engine scaling laws, along with a detailed simulation of the vehicle trajectory, were used in the mission optimization programs to find the minimum weight vehicle in earth orbit as a function of the engine thrust and the number of engines clustered on the leave earth stage. The optimum thrust range for the nuclear engine was determined for the manned Mars and Venus stopover and flyby missions, and lunar transfer missions.

The results of these evaluations, which are reported in detail in the succeeding chapter show that the selection of the optimum thrust range is relatively insensitive to the engine weight and specific impulse. The optimum thrust primarily is a function of the initial vehicle weight and the number of clustered nuclear engines for the leave earth stage. The optimum thrusts range from 50,000 to 300,000 pounds for all of the missions investigated and from 125,000 to 300,000 pounds for the manned Mars stopover missions.

The mission evaluation results show that any increase in payload or system weights or decrease in performance increases the vehicle weight, thus increasing the optimum thrust level. Furthermore, the vehicle weight is more sensitive to a decrease in thrust from the optimum value than for an increase in thrust. These two conditions tend to favor the selection of a compromise thrust that is greater than the midrange of the optimum values. An engine thrust between 200,000 and 250,000 pounds appears reasonable for the manned interplanetary missions in the 1975 to 1990 time period.

Engine Parameter Analysis - The sensitivity of nuclear engine performance to the principal engine design parameters and constraints was examined for engines of the 200,000 to 250,000-pound thrust class. This was accomplished using the NOP program. For each specified combination of engine performance parameters and constraints, the program determines the minimum weight engine, and specifies the combination of engine

variables producing the minimum weight engine. From the results of these preliminary analyses the influence of each engine design parameter on engine performance, i.e., engine weight, specific impulse, and thrust could be evaluated. An assessment of these data permitted the determination of minimum weight engines for combinations of engine parameters.

The SWOP program then was used with the engine weights, thrusts, and specific impulses associated with the minimum weight engines, to determine the influence on initial weight in earth orbit as a function of the major engine variables. The influence of the engine parameters was investigated to determine the effect on a vehicle designed for a 1982 and 1986 manned Mars stopover mission. By determining the influence of the principal engine design parameters and constraints on vehicle performance, the combination of engine design variables which produced the highest performance nuclear engine consistent with state-of-the-art was selected.

These results, which are reported in detail in Vol. V, show that the engine parameters which significantly influence the specific impulse have the greatest effect on the initial vehicle weight in Earth orbit. The most influential engine design parameters are the main nozzle expansion ratio and nozzle chamber pressure. The maximum available engine performance also is a straong function of the engine state-of-the-art design constraints such as peak fuel temperature, fuel element web thickness, fuel element web temperature rise, and maximum allowable nozzle wall temperature.

The typical sensitivity of vehicle weight and engine performance to the major engine design parameters is shown in Table III-9 for the 1982 Mars stopover mission. The vehicle weight sensitivity varies significantly depending on the mission, mission mode, and mission year.

Engine Design Characteristics - As a result of these mission, vehicle, and engine trade-offs, an integrated set of engine and vehicle characteristics were selected for operational applicability in the 1980's. The selected engine was obtained using values of peak fuel temperature, nozzle wall temperature, fuel element web temperature rise, and fuel element web thickness determined from physical and manufacturing limitations which were considered to be representative of the future "state-of-the-art". The candidate engine characteristics are shown in Table III-10.

Table III-9 Typical Engine Performance and Vehicle Weight Sensitivity*

| Engine Parameter | Sensitivity | | | |
|---|---|---|---|---|
| | Specific Impulse | Engine Thrust | Engine Weight | Vehicle Weight |
| Peak Fuel Temp. (Exit Gas Temp) | $+0.08 \frac{\text{sec. } I_{sp}}{^{o}R}$ | $-35 \frac{\text{lb. thrust}}{^{o}R}$ | Negligible Effect | $-440 \frac{\text{lb. weight}}{^{o}R}$ |
| Nozzle Expansion Ratio | $+0.40 \frac{\text{sec. } I_{sp}}{1}$ | $+110 \frac{\text{lb. thrust}}{1}$ | $+23 \frac{\text{lb. weight}}{1}$ | $-1600 \frac{\text{lb. weight}}{1}$ |
| Nozzle Chamber Pressure | $-0.06 \frac{\text{sec. } I_{sp}}{\text{psi}}$ | $+10 \frac{\text{lb. thrust}}{\text{psi}}$ | $+6.8 \frac{\text{lb. weight}}{\text{psi}}$ | $+460 \frac{\text{lb. weight}}{\text{psi}}$ |
| Core Pressure Drop | $-0.04 \frac{\text{sec. } I_{sp}}{\text{psi}}$ | Negligible Effect | $-29 \frac{\text{lb. weight}}{\text{psi}}$ | $-330 \frac{\text{lb. weight}}{\text{psi}}$ |
| Maximum Nozzle Wall Temperature | $+0.01 \frac{\text{sec. } I_{sp}}{^{o}R}$ | Negligible Effect | $-3 \frac{\text{lb. weight}}{^{o}R}$ | $-100 \frac{\text{lb. weight}}{^{o}R}$ |

*1982 Mars stopover mission

Table III-10 Engine Characteristics

| | |
|---|---|
| Engine Thrust | 226,000 lb. |
| Specific Impulse | 850 sec. |
| Engine Weight | 37,500 lb. |
| Nozzle Expansion Ratio | 120:1 |
| Reactor Power | 5100 Mw |
| Nozzle Chamber Pressure | 450 psia |
| Nozzle Chamber Temperature | 4700°R |
| Core Pressure Drop | 200 psi |
| Nozzle Wall Temperature | 1960°R |

## Vehicle Design

Vehicle Analysis - The compromise engine characteristics, i.e., the engine thrust, specific impulse, and engine weight were used as input parameters for a series of Mars stopover mission evaluations using the SWOP program. The 1982 Mars opposition year and a maximum aerodynamic earth braking capability of 15 km per sec were selected for the evaluations. From the results of these vehicle computations, the vehicle which best utilized the compromise nuclear engine was selected. The basis of this selection was the minimum vehicle weight in earth orbit. The scaling laws, payloads, and vehicle constraints which were used are those given in the previous sections of this chapter.

The vehicle configuration analysis was performed in two parts. First, a series of missions were simulated and the vehicles sized for variations in the number of engines clustered in the depart earth stage (single engine stages were used for the arrive Mars and depart Mars phases) and for configurations employing two and three clustered tanks for the depart earth stage. These initial analyses established gross estimates of the vehicle size and propellant requirements. These results were then used in a detailed structural analysis in order to determine accurately the weight of the interstage structures and the additional structure required due to tank clustering. The tank weight scaling laws were revised to

include this additional weight and the SWOP program was employed to re-optimize and resize the vehicle. Again, the number of clustered engines and tanks were parametrically varied. The results of these latter evaluations permitted the selection of the representative vehicle design.

The interstage structures and additional structure required due to tank clustering increased inert stage weights for the depart earth, arrive Mars, and depart Mars stages by 8253, 3187, and 1994 pounds, respectively. The addition of this inert weight increased the initial vehicle weight by 2.5 to 3.5 percent depending on the vehicle configuration (number of clustered engines and tanks). This increase in initial vehicle weight amounted to approximately 60,000 pounds.

In all cases, the initial vehicle weight for the two clustered engine configuration was less than either the three clustered engine or single engine configurations; 2.3 percent (50,000 pounds) less than three clustered engines and 2.7 percent (57,000 pounds) less than the single engine. The use of two clustered tanks instead of three for the depart earth stage reduced the initial vehicle weight by approximately 1.3 percent or 28,000 pounds. These results, therefore, led to the selection of a two-engine, two-tank, depart earth stage configuration for the vehicle best utilizing the compromise nuclear engine for the 1982 Mars stopover mission. The data in Table III-11 summarize the trajectory parameters for the 1982 mission and Table III-12 lists the vehicle and stage weights for this representative vehicle.

The use of two clustered tanks for the depart earth stage assumed that each tank had a total propellant capacity of approximately 370,000 pounds. This is 8.5 percent greater than the 342,540 pound limitation determined in the LMSC modular tank study (Ref. 3). The use of two tanks instead of three has definite advantages. It not only yields a minimum weight vehicle but accommodates the optimum, two-engine cluster while preserving the "one tank - one engine" modular concept. In addition, by clustering the two tanks on either side of the arrive Mars stage (as described in the next section) the nozzle expansion ratio of 120:1 can be accommodated with a minimum of interstage structure.

Table III-11 Representative Vehicle Trajectory Summary

| Mission Phase | Julian Date | Characteristic Velocity*(km/sec) | Mass Ratio | Gravity Loss Factor |
|---|---|---|---|---|
| Depart Earth | 2,444,967 | 3.810 | 1.581 | 1.051 |
| Arrive Mars | 2,445,186 | 3.215 | 1.472 | 1.024 |
| Depart Mars | 2,445,206 | 5.327 | 1.898 | 1.017 |
| Arrive Earth | 2,445,422 | 17.967 ** | 1.993 *** | 1.0 |

* including gravity losses

** arrival velocity with respect to nonrotating earth

*** characteristic velocity for cryogenic retro stage = 2.967 km/sec

Trip Times

| | |
|---|---|
| Outbound Leg - | 219 days |
| Stopover Period - | 20 |
| Inbound Leg - | 216 |
| Total - | 455 |

Minimum Perihelion Distance - 0.526 A.U. (inbound leg)

Table III-12 Representative Vehicle and Stage Weights

| Stage | Description | | Weight (lbs) |
|---|---|---|---|
| I | Leave Earth - Nuclear | | 973,308 |
| II* | Outbound Midcourse - Storable | | 47,828 |
| III | Arrive Mars - Nuclear | | 433,729 |
| IV | Leave Mars - Nuclear | | 322,296 |
| V** | Inbound Midcourse - Storable | | 8,342 |
| VI | Earth Retro - Cryogenic ($LH_2/LO_2$) | | 30,804 |
| Payload | | | 206,749 |
| | Mars Entry and Ascent Module (80,000 - 1,500) | 78,500 | |
| | Solar Radiation Shield | 22,939 | |
| | Crew Compartment | 68,734 | |
| | Life Support (50 lb x 455 days) | 22,750 | |
| | Reentry Capsule (10,000 lb earth landed payload) | 13,826 | |
| VEHICLE GROSS WEIGHT-EARTH DEPART | | | 2,023,056 |

*Includes 10,127 pounds of attitude control weight provisions.

**Includes attitude control weight provisions.

Mars Stopover - 931 lbs.

Inbound Leg - 1,485 lbs.

TOTAL 2,416 lbs.

Table III-12 Representative Vehicle and Stage Weights (continued)

| Stage I - Leave Earth - Nuclear | Weight (lbs.) |
|---|---|
| Structure | 151,616 |
| Engine | 77,957 |
| Jettison Weight | 229,573 |
| Propellant | 743,735 |
| Gross Weight | 973,308 |
| **Stage II - Outbound Midcourse - Storable** | |
| Structure, Engine | 5,676 |
| Jettison Weight | 5,676 |
| Propellant - Impulse | 32,025 |
| Propellant - Attitude Control | 10,127 |
| Gross Weight | 47,828 |
| **Stage III - Arrive Mars - Nuclear** | |
| Structure | 66,489 |
| Engine | 37,445 |
| Insulation | 7,940 |
| Jettison Weight | 111,874 |
| Propellant - Main | 310,166 |
| Propellant - Boiloff | 11,689 |
| Gross Weight | 433,729 |
| **Stage IV - Leave Mars - Nuclear** | |
| Structure | 48,904 |
| Engine | 37,445 |
| Insulation | 4,519 |
| Jettison Weight | 90,868 |
| Propellant - Main | 219,281 |
| Propellant - Boiloff | 12,147 |
| Gross Weight | 322,296 |

Table III-12 Representative Vehicle and Stage Weights (continued)

| Stage V - Inbound Midcourse - Storable | Weight (lbs) |
|---|---|
| Structure<br>Engine | 1,248 |
| Jettison Weight | 1,248 |
| Propellant - Impulse | 4,678 |
| Propellant - Attitude Control (Stopover) | 931 |
| Propellant - Attitude Control (Inbound Leg) | 1,485 |
| Gross Weight | 8,342 |

| Stage VI - Earth Retro-Cryogenic | |
|---|---|
| Structure<br>Engine | 6,672 |
| Insulation | 762 |
| Jettison Weight | 7,434 |
| Propellant - Main | 21,104 |
| Propellant - Boiloff | 2,266 |
| Gross Weight | 30,804 |

| Propellant Boiloff Rates | Propellant Wt(lbs) | Time(days) | Rate (lb/day) |
|---|---|---|---|
| Stage III | 11,689 | 219 | 53.4 |
| Stage IV | 12,147 | 239 | 50.8 |
| Stage VI | 2,266 | 455 | 4.98 |

Vehicle Description - The vehicle employs the modular concept based on the DI tank configuration as described in Ref. 3 and currently being investigated by NASA. A drawing of the vehicle is shown in Fig. III-13.

The vehicle consists of three main nuclear stages plus a payload stage which, continuing the modular concept contains the midcourse stages, Mars lander, earth reentry capsule, earth retro stage and mission module.

Stage I, the depart earth stage, consists of two tanks each having a nuclear engine. A portion of the engine nozzle is retracted during launch to orbit and nests over the engine body to allow the engine and tank to fit within the maximum envelope of the launch vehicle. This launching procedure is typical for all of the nuclear stages. The nozzles for the depart earth and arrive Mars stages are extended in earth orbit during assembly. The depart Mars stage nozzle is extended after braking into Martian orbit.

The Stage I tanks overlap the second stage tank and attach to the aft portion of Stage II at diametrically opposed points. This arrangement still provides radiation shadow shielding from the Stage I engines. Three points of pickup are provided for the tank attachment. A single point on the forward skirt of each Stage I tank picks up a point in the body of the Stage II tank and two points in the body of each Stage I tank pick up a cradle mounted to the aft ring on Stage II.

Stage II, the arrive Mars stage, is similar to the Stage I module. Attached to the aft skirt of this tank is a cylindrical interstage that supports the two cradles that pick up the body points of the Stage I tanks. These cradles hinge toward the center when stowed at launch. The launch fairing attaches to the end of this interstage.

The aft skirt of Stage III, the depart Mars stage, is a cylindrical interstage structure that tapers from the 396-inch tank diameter to the diameter of the docking mechanism envelope shown in Ref. 3. Mounted to the aft end of this interstage is the mating portion of the above docking mechanism. The tie between Stage II and Stage III is by means of this docking mechanism. Separation between Stage II and Stage III is accomplished by cutting the interstage circumferentially just forward of the tapered section to allow a $15^{o}$ flyout angle for the Stage III engine.

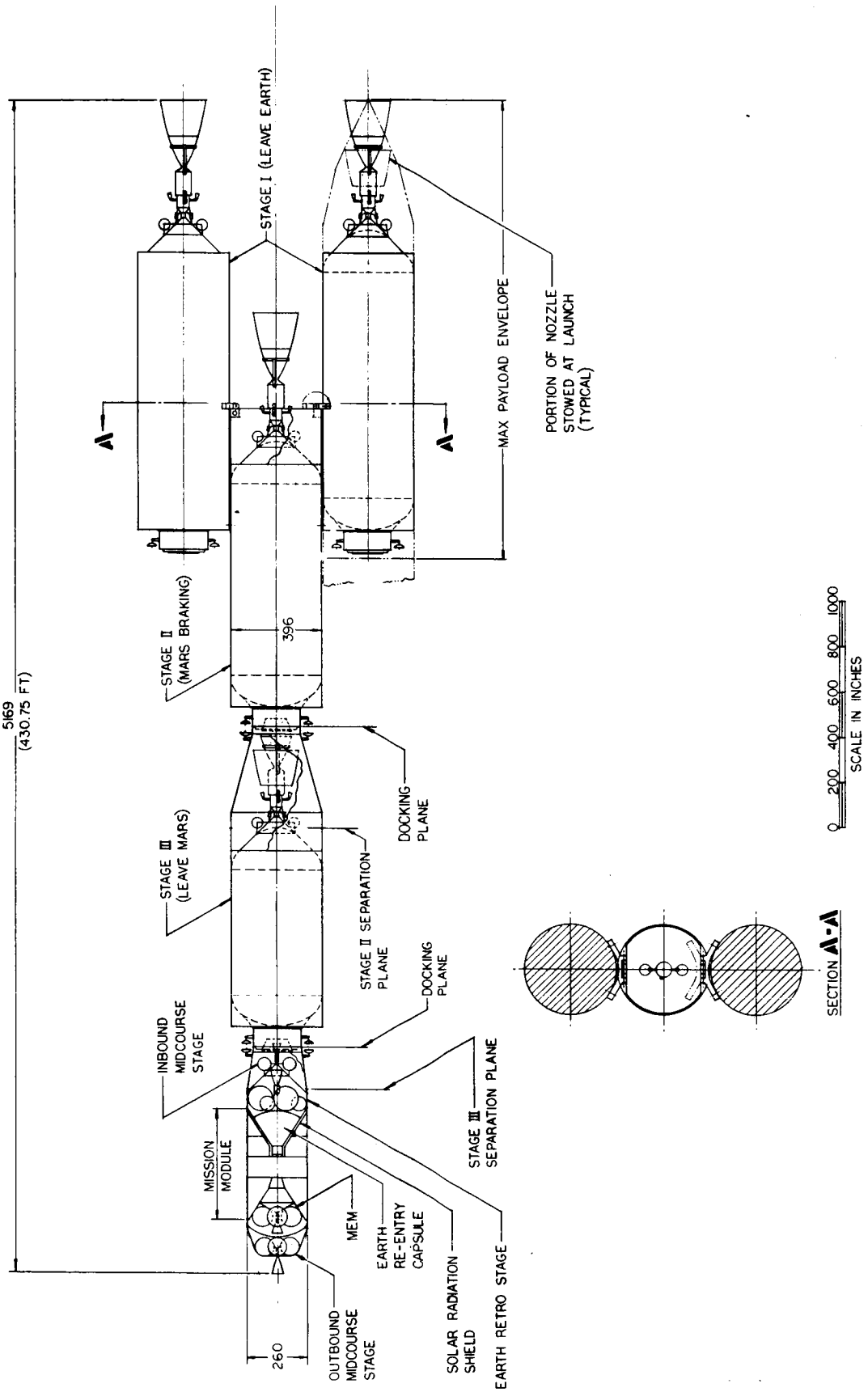


Figure III-13 Representative Vehicle Design

The payload stage or the fourth module consists of a cylindrical structure 260 inches in diameter. A tapered section at the aft end contains the portion of the docking mechanism that mates with the forward end of Stage III. The tie between these stages is by means of this docking mechanism. The inbound midcourse correction stage consists of two spherical tanks and engine that are supported within the aft tapered section by a conical structure that ties to the ring at the taper transition point. Stage III is separated by cutting the tapered section circumferentially just aft of this joint thus providing a $15^{o}$ flyout angle.

Within the conical section and just forward of it is the earth retro stage which consist of three large spherical fuel tanks, three smaller spherical oxidizer tanks, and engine. Forward of this stage is the earth entry capsule surrounded by the solar radiation shield. This arrangement allows the use of the capsule as a "storm cellar" during unusual solar radiation periods.

Surrounding the capsule and including the area forward is the mission module which includes crew living and working space, equipment and supply storage, and the Mars entry module docking mechanisms and air locks. Forward of the mission module is the Mars entry and ascent module. Attached to the forward end is a tapering interstage that supports the four spherical tanks and engine of the outbound midcourse correction stage.

The buildup of the vehicle would be accomplished as follows. Each stage would be placed in orbit partially loaded but not exceeding the payload capability of the launch vehicle. Tankers would then rendezvous, dock with and transfer fuel to each stage. The manned payload module would then rendezvous and dock first with Stage III and then with Stage II. Docking a Stage I tank would be accomplished by moving it horizontally to engage the single point on the forward skirt of the tank. The Stage I tank then would be rotated about this point until the tank centerline was parallel to the centerline of the vehicle. At that time, the cradle on the aft end of Stage II would be rotated outboard and the two points in the body of the Stage I tank engaged. This procedure would be repeated for the second tank. Extending the depart earth and arrive Mars nozzles would complete the vehicle assembly.

An artist's conception of the vehicle in its initial propulsive phase is shown in Fig. III-14.

Interstage Structure Design

The scaling laws used to size the propellant tanks for the various stages in the computer program omit the interstage structures and additional structure required due to tank clustering. This omitted weight is a function of the final vehicle configuration. Therefore, a preliminary structural analysis was made of this additional structure for the representative vehicle design. Then as previously discussed, the resulting structure weight was added to the scaling laws and a design iteration was carried out. The results are reflected in the final weight statement, Table III-12.

The structural design analysis was based on no detremental yielding at limit load, the maximum load expected in service, and no failure at ultimate load, defined as 1.4 x limit load. This ultimate factor of safety of 1.4 is consistent with the MSFC criteria for manned missions.

Depart Earth - Arrive Mars - Each of the depart earth tanks is attached to the arrive Mars stage at three points. The single forward attach point loads the ring structures in the tanks by radial loads only. The aft attachment transfers the thrust load, as well as a radial load component, through two attachment points.

Two basic designs were considered, designated configuration 1 and 2. Both have the identical structure for thrust transfer but the ring structure in the tanks and interstages in configuration 1 were conventional ring frames whereas braced rings were used in the configuration 2. That is, the forward rings used in configuration 2 have a strut attaching the diametrically opposite attachment points. For configuration 1, the critical case design condition occurs at leave earth stage burnout. For configuration 2, this same design condition is critical for all structural components except the ring frames in the arrive Mars stage which due to the bracing would not be loaded. The critical condition for these rings is obtained when one of the two depart earth stages burns out before the other, which then loads these rings.

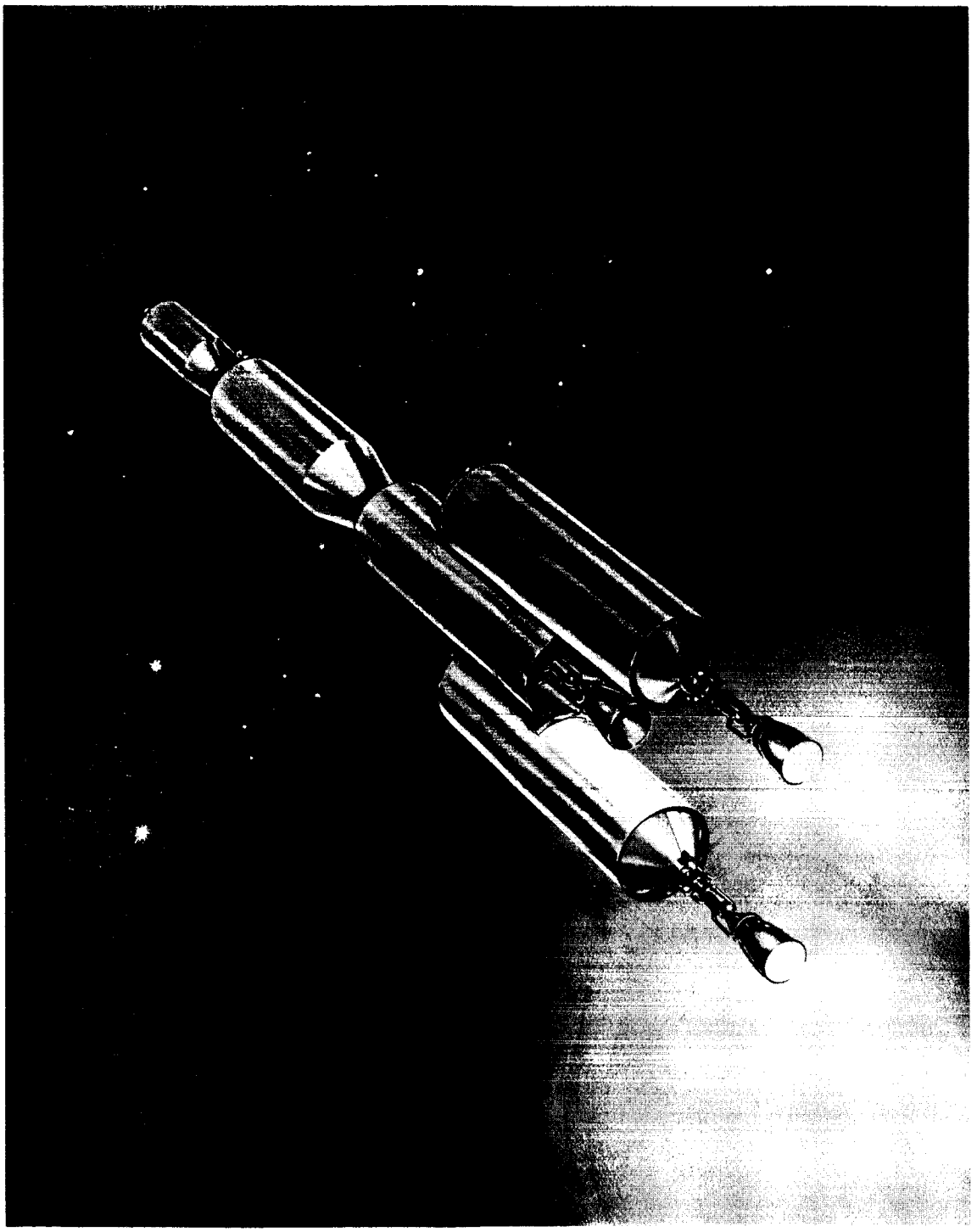

Figure III-14 Nuclear Propelled Vehicle

Each ring was optimized by computing the ring weight versus depth of the ring cross section, thereby obtaining the minimum ring weight. The ring sizing was based on conventional fabrication techniques using high strength aluminum alloys. As the ring depth increases, the cross sectional area of the cap elements and, hence, the cap weight decreases for a specific bending moment. However, increasing the ring depth increases the web thickness as well as its depth giving increasing web weight for a constant shear load. In computing the cap weights, stress levels of 40,000 and 56,000 psi at limit and ultimate loads, respectively, were assumed. Two design criteria were used in the web design, (1) no buckling at limit load, (2) and no failure but allowing tension field effects to take place at the ultimate load condition. Radial web stiffeners were used to obtain an efficient web design, and to develop tension field capability. The results of tension field designs of Ref. 10 were plotted to give the web thickness,t, and the stiffener spacing, d, versus the maximum ultimate shear flow in the web. The stiffener cross sectional area, $A_u$, was computed from $A_u = 0.7\ td$. With this resulting stiffener spacing and the ring depth, the web thickness to ensure no buckling at limit load was determined. The resulting web weight was based on the greater of the two values of web thickness obtained plus the web stiffeners. The ring weights are conservative as is the weight based on a constant ring cross section since in the actual design, the caps can be tapered and the web thickness varied to match the load intensity at any position around the ring.

The compression struts used for bracing the forward rings on each stage in configuration 2 were optimized by the procedure of Ref. 11 based on the use of 7075-T6 aluminum alloy tubular struts. The optimization equations assume that the two modes of failure, local crippling and the primary strut failure mode, occur simultaneously. The tension struts in the aft rings in the stages were sized for a tensile stress of 60,000 psi at ultimate load. The bracing structure at the aft attachment point on the arrive Mars stage has to accommodate the engine and consists of two tension ties and a 16-foot ring around the engine.

The thrust transfer between the stages requires a longeron on the aft skirt of the arrive Mars stage and a longeron and additional tank skin thickness on the leave earth stages at the aft attachments. The skirt on the arrive Mars stage is aluminum truss core construction, 246 inches long and has a maximum effective skin thickness of 0.131 inches. (The design of the skirt was based on equations from Ref. 12.) This thickness assumes the skirt is located below the hydrogen tank module when launched by a C-5 vehicle. If it were located above the tank at launch, a thickness of 0.057 inches would be applicable. Either of these thicknesses would provide adequate capacity for transferring the load from the longeron into the arrive Mars stage. A weight for the four longerons in the aft skirt was estimated assuming an allowable compressive stress level of 50,000 psi at ultimate load.

The structure of the leave earth tankage was assumed identical to that of configuration D1 of Ref. 3. The estimated structural modification to the tank would be an increase in tank wall thickness from 0.1 to 0.151 inches over the four panels adjacent to the attachment point to provide adequate shear capacity to transfer the load from the longeron which runs 38 inches fore and aft of each of the two aft attachment points. The longerons on the arrive Mars stage were assumed capable of carrying an ultimate stress level of 50,000 psi at ultimate load in order to compute the longeron weight.

The total weight of the depart earth and arrive Mars stage attachment and interstage structure is 9162 pounds. Of this weight, 8253 pounds are chargeable to the depart earth stage and 909 pounds to the arrive Mars stage.

Arrive Mars - Depart Mars - The arrive Mars-depart Mars interstage structure consists of a cylindrical and a conical section. The cylindrical section is 396 inches diameter and 170 inches long and is attached to the aft skirt of the depart Mars stage. The conical section is 348 inches long and tapers down to the 216 inch-diameter docking structure on the forward dome of the arrive Mars stage.

It was assumed that the cylindrical section was formed as part of the launch vehicle external structure and, therefore, critical design condition would occur during the launch to orbit. Based on data in Ref. 3, the effective thickness of the aluminum alloy truss core construction is

dependent on the launch vehicle configuration. However, the effective thickness will be in the range 0.057 to 0.131 inches. The 0.057 inches is representative of structure located above the tank module at launch whereas the 0.131-inch thickness is compatible with a launch interstage located below the tank module. Conservatively, the 0.131-inch effective thickness was assumed applicable which resulted in a weight of 2270 lb for the cylindrical section. The separation plane is positioned such that 1630 lb of this structure remains with the depart Mars stage.

It was assumed that the conical section was not a part of the launch vehicle external structure, and therefore, the critical design condition occurs at leave earth stage burnout. This results in a 285,000 lb ultimate axial compressive load on this section of the interstage. The first analysis of this conical section assumed the same type aluminum alloy truss core construction used in Ref. 3, for the interstage structures and tank skirts. The resulting weight for the conical section was 872 lb, based on an effective skin thickness of 0.0252 inches. However, the sheet material thicknesses of 0.0085 inches for the facing sheets and 0.0046 for the core material were considered impractical. Furthermore, the fabrication of the truss core conical sections may not be possible geometrically. Consequently, a conventional aluminum honeycomb conical section was investigated. The required facing thickness, core thickness, and core density were determined at four stations along the conical section using the procedure in Ref. 13. The resulting variations in the required core thickness, 0.45 to 0.4 inches, and the facing thickness, 0.007 to 0.006 inches, was considered negligible and the weight was based on constant thicknesses taken at the maximum values. The core density is 1.6 lb per cubic foot (designation 1/4 in. - 5052 - 0.0007 in.) and a conservative bond weight of 0.2 lb per square ft. for both surfaces was used. The resulting weight for the honeycomb conical section is 1093 lb. The rings at each end of the section weigh 45 lb for a total of 1138 lb charged to the arrive Mars stage.

The total weight of this interstage structure is 3908 lb, 1630 lb charged to the depart Mars stage and 2278 lb to the arrive Mars stage. These results indicate that the use of the launch vehicle external shell structure as interstages for earth orbit assembled vehicles leads to weight penalties. The cylindrical section of the interstage was based on an effective thickness

of aluminum of 0.131 inches. Had a section of structure located above a tank module at launch been used, an effective thickness of 0.057 inches would have been applicable. However, both of these values are greater than 0.0315 inches, the effective thickness of the honeycomb construction of the conical section which, therefore, is a more efficient interstage structure.

Depart Mars - Payload - The payload - depart Mars stage interstage structure is a conical section 188 inches long, tapering in diameter from 260 inches at the payload end to 216 inches at the forward dome of the depart Mars stage. An aluminum honeycomb construction was considered for this section as for the similar section on the interstage between the arrive Mars and depart Mars stages. The analysis resulted in 0.006 inch facings on a 1.0 lb per cubic foot core (designation 3/8 inc. - 5052 - 0.00007 in.) and a core thickness of 0.22 inches. The weight of this conical section, allowing 0.2 lb per square ft. for the bonding of both surfaces is 355 lb. The rings at each end of this section have a total weight of 9 lbs as computed from the ring loading. Therefore, 364 lbs of interstage structure is chargeable to the depart Mars stage.

Summary - A tabulation of the total interstage weight chargeable to each stage is given below.

| | | |
|---|---|---|
| Depart Earth Stage | - | 8253 lbs |
| Arrive Mars Stage | - | 3187 lbs |
| Depart Mars Stage | - | 1994 lbs |

# IV MISSION EVALUATION RESULTS

The mission optimization programs (SWOP and FLOP) were employed, together with the derived vehicle scaling laws and constraints, to evaluate a number of different mission and operational modes. These mission evaluation results were used to determine the compromise engine and representative vehicle designs (as described in the preceding chapter), establish the sensitivity of the vehicle weight to variations in engine, vehicle, and mission parameters, compare the advanced nuclear engine with chemical propulsive systems, and explore the utility of the advanced nuclear engine for various missions and vehicle types.

Over 20,000 individual lunar transfer, planetary flyby, and planetary stopover mission simulations were made and the minimum vehicle weight requirements computed. The resulting data from these mission runs have been reduced, graphed, and cross plotted in order to present sets of parametric data comprehensive enough to be useful but at the same time concise enough to be manageable and capable of interpretation. A vast amount of the computed data obtained, other than the initial vehicle weights, have not been reduced or graphed. But all of the computer printouts have been retained and catalogued for possible future use. All of the reduced parametric data is presented in Vol III of this series of reports. The evaluation and interpretation of these data are presented in this chapter.

Wherever feasible, the conclusions and interpretations made in this section are substantiated by accompanying data. For a complete data background to the sections in this chapter, the reader is referred to Vol III.

## COMPROMISE THRUST SELECTION

The first step in the determination of an optimum nuclear engine design was the selection of the compromise thrust level in order to narrow down the range of thrusts within which a more detailed analysis could be performed to directly relate the engine parameters to the mission performance.

The engine was represented by approximate scaling laws (Table III-6) that relate the basic engine parameters of weight and thrust, for constant specific impulse, as previously shown. These scaling laws assigned appropriate weight penalties to clustered engines. The assumption was made that the selection of the optimum thrust range was relatively insensitive to the engine weight and specific impulse, and therefore, the nuclear engine specific impulse was held constant.

## Mission Matrices

Several combinations of propulsive system types, operational modes, and earth aerodynamic braking capabilities were analyzed for planetary stopover and flyby missions and lunar transfer missions. Three mission years and two trajectory types were investigated for the stopover mission. The matrices of cases used for the various missions are shown in Tables IV-1, IV-2, and IV-3. In addition, a set of Mars stopover missions were analyzed in which the thrust of the nuclear engines used in the upper stages, i.e., the arrive and depart Mars stages, were held at a constant value, either 50,000 lbs or 100,000 lbs, while the depart earth nuclear engine thrust was varied. The complete matrix of cases is shown in Table IV-4 for this latter set of missions.

## Mission Criteria

The mission criteria used for the missions are discussed and set forth in detail in Chapter III. The major payload and performance criteria are summarized in Table IV-5 for ease of reference.

## Mission Analysis

Figure IV-1 is typical of the graphs obtained for all of the missions contained in the matrices. The initial vehicle weight in earth orbit and the maximum firing time of any single nuclear engine is plotted as a function of the nuclear engine thrust and the number of engines in the leave earth stage. From this and many other similar figures, the optimum thrust (minimum vehicle weight) could be determined for the many vehicle configurations, aerodynamic braking capabilities, and mission years investigated.

Table IV-1 Stopover Mission Matrix

| MISSION | YEAR | TYPE | NUCLEAR THRUST/ ENGINE | MODE AND NUMBER OF ENGINES: DEPART EARTH STAGE | ARRIVE MARS STAGE | DEPART MARS STAGE | ARRIVE EARTH STAGE |
|---|---|---|---|---|---|---|---|
| MARS STOPOVER | 1978 - INTERMEDIATE SUN | I B | 50,000 LB | 1-NUCLEAR | 1-NUCLEAR | 1-NUCLEAR | AERO |
| | | II B | 100,000 | 2-NUCLEAR | | 1-AFTERCOOL AM ENGINE | RETRO 18-$LO_2/LH_2$ |
| | 1982 - ACTIVE SUN | | 200,000 | 3-NUCLEAR | | $LO_2/LH_2$ | RETRO 15-$LO_2/LH_2$ |
| | 1986 - QUIET SUN | | 300,000 | 4-NUCLEAR | | | RETRO-PARABOLIC-$LO_2/LH_2$ |
| | | | 400,000 | 7-NUCLEAR | | | RETRO-18-STORABLE |
| | | | 500,000 | | | | RETRO-15-STORABLE |
| | | | | | | | RETRO-PARABOLIC-STORABLE |

Table IV-2 Flyby Mission Matrix

| MISSION | PLANET/YEAR | TYPE | NUCLEAR THRUST/ENGINE | NO. OF ENGINES DEPART EARTH STAGE | ARRIVE EARTH STAGE |
|---|---|---|---|---|---|
| FLYBY | MARS/1978 | LOW ENERGY | 50,000 LB | 1-NUCLEAR | AERO |
| | MARS/1980 | LOW ENERGY | 100,000 | 2-NUCLEAR | RETRO-18-$LO_2/LH_2$ |
| | VENUS/1980 | HIGH ENERGY | 200,000 | 3-NUCLEAR | RETRO 15-$LO_2/LH_2$ |
| | | | 300,000 | | RETRO-PARABOLIC-$LO_2/LH_2$ |
| | | | 400,000 | | RETRO 18-STORABLE |
| | | | 500,000 | | RETRO 15-STORABLE |
| | | | | | RETRO-PARABOLIC-STORABLE |

Table IV-3 Lunar Transfer Mission Matrix

| MISSION | TYPE (70 HR) | PAYLOAD | NUCLEAR THRUST/ ENGINE | NO. OF ENGINES DEPART EARTH STAGE | RETRO TO 100 N MI LUNAR ORBIT |
|---|---|---|---|---|---|
| LUNAR TRANSFER FROM 485 KM EARTH ORBIT | APOGEE TRANSFER | 100,000 LB | 50,000 LB | 1-NUCLEAR | STORABLE |
| | PERIGEE TRANSFER | 200,000 | 100,000 | 2-NUCLEAR | $LO_2/LH_2$ |
| | MEAN TRANSFER | 300,000 | 200,000 | 3-NUCLEAR | |
| | | 400,000 | 300,000 | | |
| | | | 400,000 | | |
| | | | 500,000 | | |

## Table IV-4 Stopover Mission Matrix (Constant Thrust Upper Stages)

| MISSION | YEAR | TYPE | NUCLEAR THRUST/ENGINE: DEPART EARTH | NUCLEAR THRUST/ENGINE: ARRIVE AND DEPART MARS | MODE AND NUMBER OF ENGINES: DEPART EARTH STAGE | MODE AND NUMBER OF ENGINES: ARRIVE MARS STAGE | MODE AND NUMBER OF ENGINES: DEPART MARS STAGE | MODE AND NUMBER OF ENGINES: ARRIVE EARTH STAGE |
|---|---|---|---|---|---|---|---|---|
| MARS STOPOVER | 1978 - INTERMEDIATE SUN | IIB | 50,000 LB | 50,000 LB | 1-NUCLEAR | 1-NUCLEAR | 1-NUCLEAR | AERO |
| | | | 100,000 | 100,000 | 2-NUCLEAR | | | RETRO-18-$LO_2/LH_2$ |
| | 1982 - ACTIVE SUN | | 200,000 | | 3-NUCLEAR | | | RETRO-15-$LO_2/LH_2$ |
| | | | 300,000 | | 4-NUCLEAR | | | RETRO-PARABOLIC-$LO_2/LH_2$ |
| | 1986- QUIET SUN | | 400,000 | | | | | RETRO-18-STORABLE |
| | | | 500,000 | | | | | RETRO-15-STORABLE |
| | | | | | | | | RETRO-PARABOLIC-STORABLE |

Table IV-5 Nominal Mission Criteria

GENERAL

Specific Impulse

Nuclear - 800 sec

Cryogenic Chemical ($LO_2/LH_2$) - 440 sec

Storable Chemical - 330 sec

Attitude Control

1 percent each leg

Micrometeoroid Protection

Optimum Cryogenic Insulation/Boiloff

MARS STOPOVER MISSION CRITERIA

| | | |
|---|---|---|
| Earth Recovered Payload | - | 10,000 lb |
| Mission Module (8 Man) | - | 68,734 lb plus solar flare shield |
| Mars Lander (MEM) | - | 80,000 lb |
| Weight Recovered from MEM | - | 1,500 lb |
| Life Support Expendables | - | 50 lb/day |
| Stopover Time | - | 20 days |
| Midcourse Correction | - | 100 m/sec each leg storable propellant |

FLYBY MISSION CRITERIA

| | | |
|---|---|---|
| Earth Landed Payload | - | 8,500 lb |
| Mission Module (3 Man) | - | 65,000 lb including solar flare shield |
| Planet Probe | - | 10,000 lb |
| Life Support Expendables | - | 40 lb/day |
| Planet Passage Altitude | - | Mars - 1,000 km ($R_d$ = 1.3)<br>Venus - 1,000 km ($R_d$ = 1.16) |
| Midcourse Correction | - | 200 m/sec outbound leg<br>300 m/sec inbound leg<br>storable propellant |

LUNAR TRANSFER MISSION CRITERIA

Payload in 100 nmi Lunar Orbit - 100,000 to 400,000 lb

Midcourse Correction - 30 m/sec storable propellant

Transfer Time - 70 hr

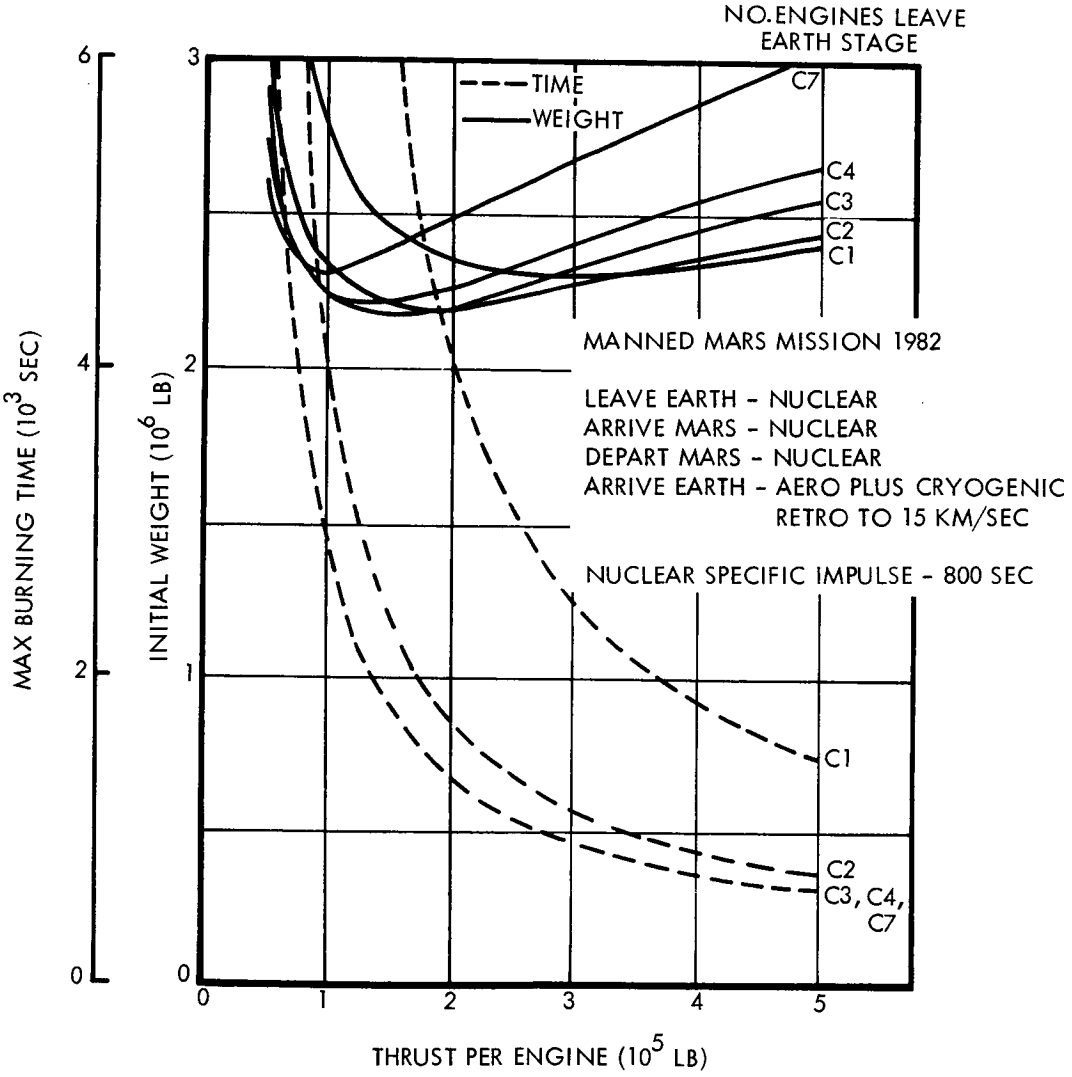


Figure IV-1 Typical Mission Evaluation Result

With the exception of the set of missions employing constant thrust engines for the upper stages (50,000 and 100,000 lbs) noted earlier, all of the nuclear engines used for a given mission case have the same thrust level which is indicated by the abscissa value. Wherever clustered engines are employed for the depart earth stage, the total thrust for that stage is the product of the thrust given by the abscissa value and the number of engines in the cluster. The vehicle weight corresponding to this optimum thrust point was recorded from all of the data graphs and plotted against various parameters in order to determine the optimum thrust ranges and to analyze the influence of various parameters on the optimum thrust.

The thrust point was selected in all cases consistent with a maximum nuclear engine firing time of 1800 sec for any single engine in the vehicle. This 1800-second firing time limitation is somewhat arbitrary, but represented a near optimum value from a mission performance standpoint. When the limitation on maximum firing time is removed, the reduction in initial vehicle weight is negligible, and the firing time corresponding to the optimum thrust level does not exceed 2800 seconds except where after-cooling the arrive Mars stage is used in which case the maximum total burn time for that engine approaches 4000 sec. Although the optimum thrust level can be reduced from 16 to 35 percent depending on the mission year by longer firing times, one or two additional engines are required for the depart earth stage. The primary disadvantage of these lower thrust, longer firing time engines is that any marked payload or system weight increases will require the clustering of engines for the arrive Mars stage to maintain maximum firing times below one hour.

A review of all of the computer printouts showed that for all mission cases, the optimum thrust point corresponded to a vehicle in which the number of clustered propellant tanks was either equal to or less than the number of engines clustered for that stage. Thus on a parametric basis, the mission simulations indicated compatibility with a modular stage and tank concept.

Stopover Mission - Before the influence of thrust level on initial vehicle weight was examined, the initial vehicle weight requirements were compared and evaluated for the various engine modes, mission years, and earth aerodynamic braking capabilities for the Mars stopover mission. The bar graphs in Fig IV-2 represent the minimum initial weight required in earth orbit for the three opposition years representing the least favorable, 1978, to the most favorable, 1986. (The opposition years 1990 and 1992 have very similar mission characteristics to 1978.) The three basic combinations of arrive Mars and leave Mars propulsive modes are compared for all aerodynamic braking at earth. Figure IV-3 is a similar bar graph for a vehicle that utilizes a propulsive retro to decelerate the vehicle to 15 km per sec after which aerodynamic braking is employed for the remainder of the reentry phase. This arrive earth mode permits the additional performance comparison between a cryogenic propellant ($LO_2/LH_2$) retro and a liquid storable retro.

All of the stopover mission data presented here are for trajectory type IIB. A comparison of the data from the curves similar to Fig IV-1 showed that for the years 1978 and 1986, the initial vehicle weight was less for the Type IIB trajectory than for the IB. For the missions performed in 1982, the initial vehicle weight for the IIB trajectory was either equal to or only slightly greater than for the IB trajectory. At best, a savings of weight of less than 5 percent was possible with the 1982 IB trajectory but an additional 50 days was added to the total trip time. Therefore, the IIB was selected as the preferred trajectory.

Figures IV-2 and IV-3 indicate that the use of an aftercooled nuclear engine for the Martian velocity changes requires approximately ten percent more initial vehicle weight than for the nonaftercooled mode. This decided weight disadvantage of the aftercooled mode favors the use of the nonaftercooled mode in all cases.

The use of a cryogenic propulsion stage for departing Mars increases the required vehicle weight by 20 to 30 percent over the all nuclear mode. Therefore, there appears to be no weight or operational factors that could justify the use of a chemical stage for departing earth when nuclear engines are available and utilized for the other propulsive phases.

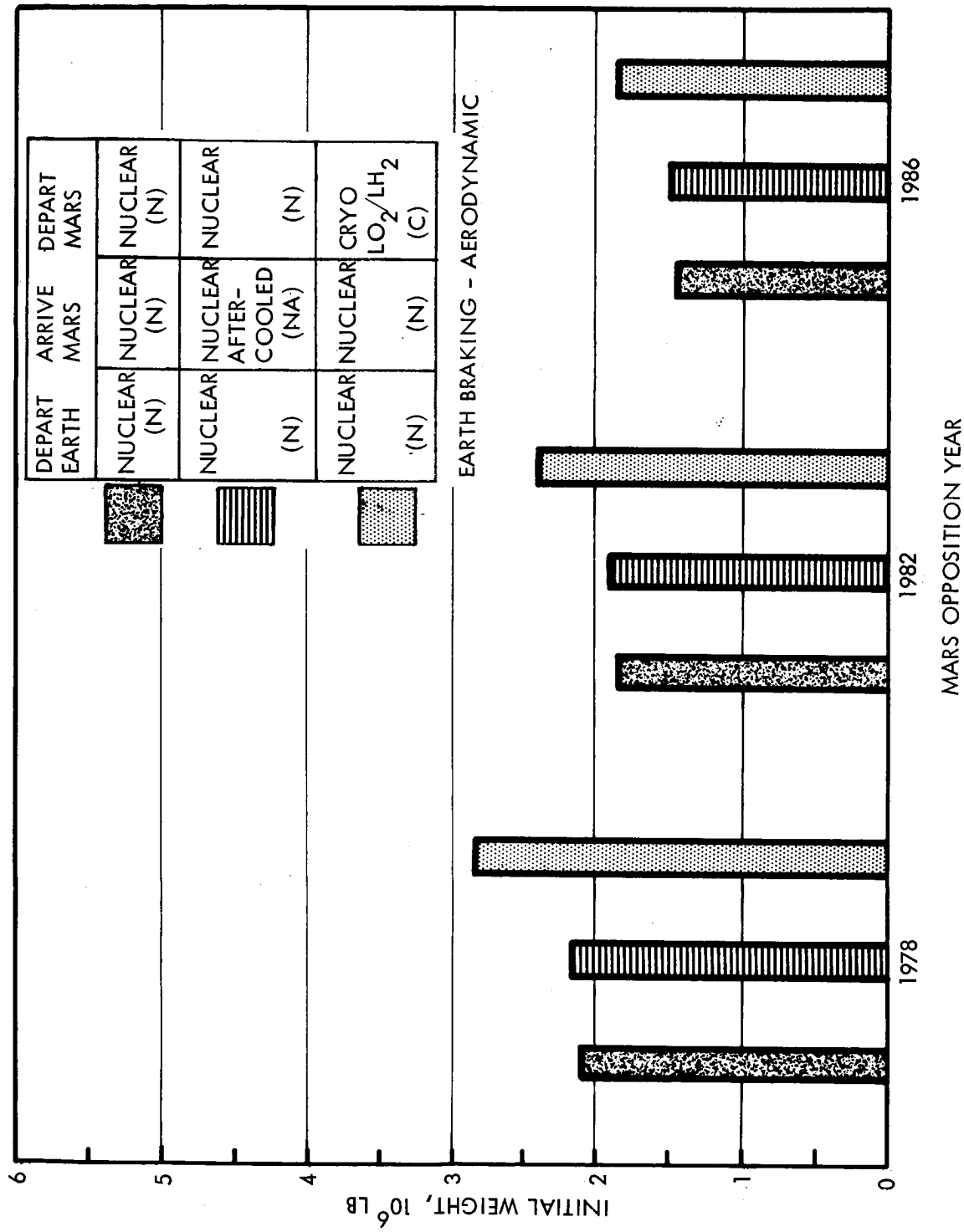


Figure IV-2 Mars Stopover Mission - Aerodynamic Earth Braking

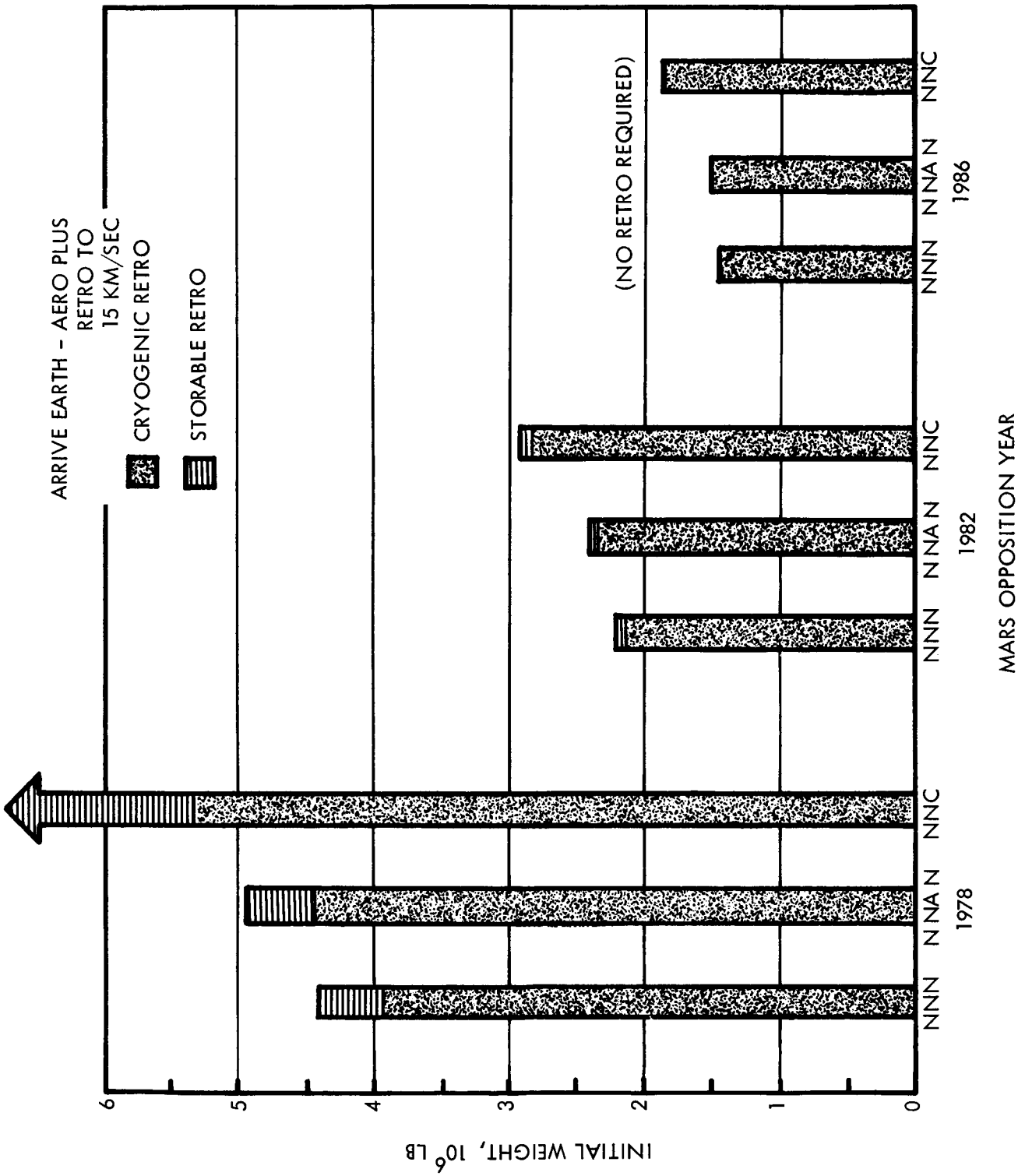


Figure IV-3 Mars Stopover Mission - Earth Retro to 15 km per sec

Figure IV-3 shows that the storable arrive earth retro stage leads to a lower performance vehicle than can be obtained with a cryogenic retro stage. In other words, the trade-off between the additional vehicle weight required by the cryogenic stage for insulation and propellant boiloff with the lower specific impulse for the storable stage favors the cryogenic retro stage. The increased weight requirements for the storable propellant vary from 5 to 20 percent and are a direct function of the required retro velocity as well as the required velocity changes for the preceding mission phases.

Figure IV-4 is similar to the preceding bar graphs with the difference that the earth retro stage is employed to decelerate the vehicle to parabolic velocity. Due to the high velocities for the year 1978, the initial vehicle weight requirements exceed six million pounds for this year. The comparisons and conclusions made for the preceding two graphs are also applicable for this aerodynamic braking capability.

In summary, these conclusions indicate that no weight advantage is gained by using the aftercooling mode, the cryogenic ($LO_2/LH_2$) depart Mars mode, or a storable propellant for the arrive earth retro stage.

Figure IV-5 summarizes the comparisons from the three previous graphs for the all nuclear nonaftercooled mode. Three capabilities of earth braking are shown, all aerodynamic, and two modes in which a cryogenic retro is employed to decelerate the vehicle to 15 km per sec and parabolic velocities after which the vehicle enters the earth's atmosphere aerodynamically.

This figure shows the sensitivity of the initial vehicle weight to the mission year and the earth aerodynamic braking capability. For earth retro braking to 15 km per sec, the vehicle weight for 1978 is over twice that required for 1986. In addition, the vehicle weight more than doubles for the extreme possibilities of earth aerodynamic braking capability for both the years 1978 and 1982. These results indicate the sensitivity effect that is seen throughout all of these and the subsequent mission results. That is, the more difficult the mission or the less the vehicle performance capability, the greater the sensitivity of the vehicle weight to variations in any given parameter.

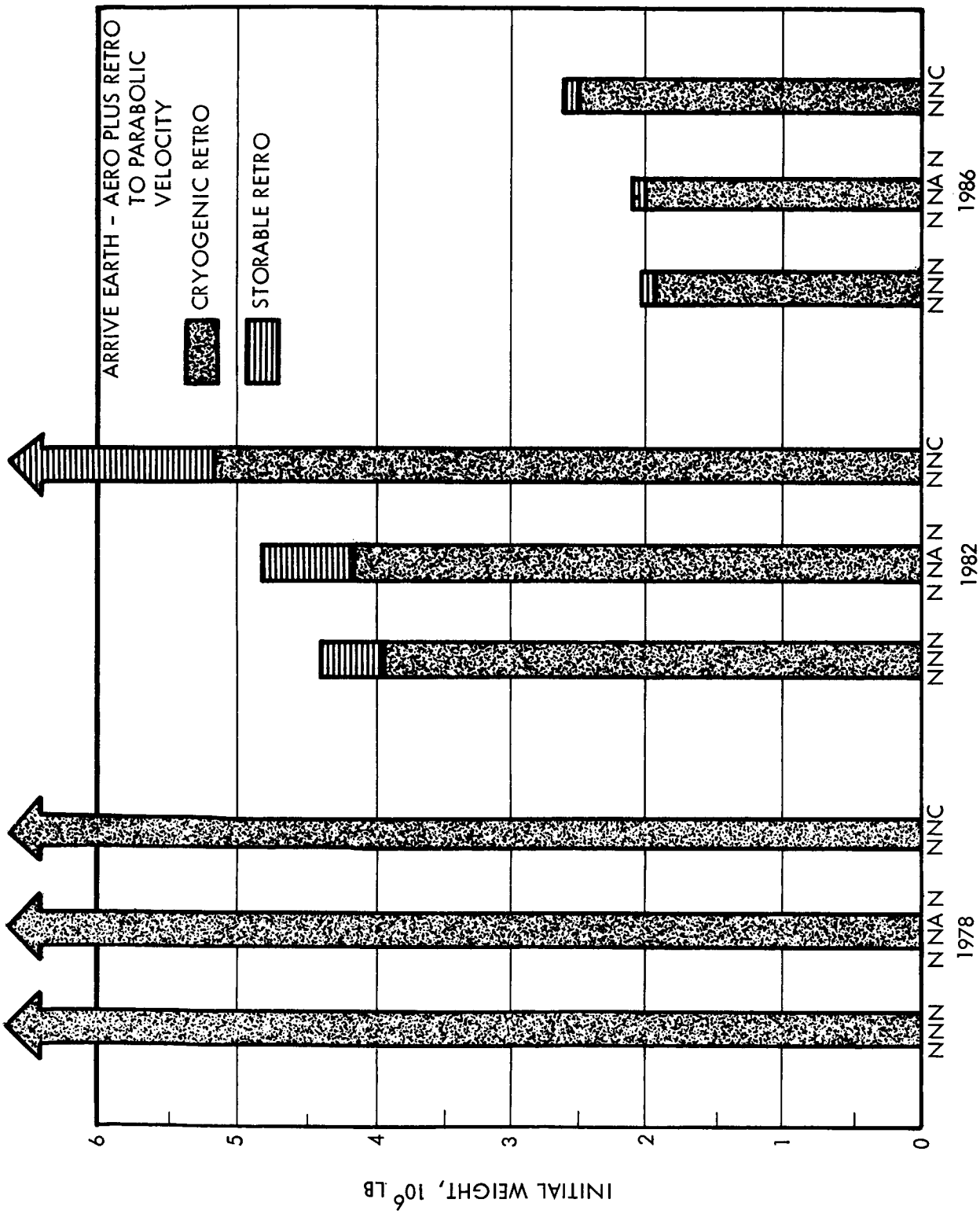


Figure IV-4 Mars Stopover Mission - Earth Retro to Parabolic Velocity

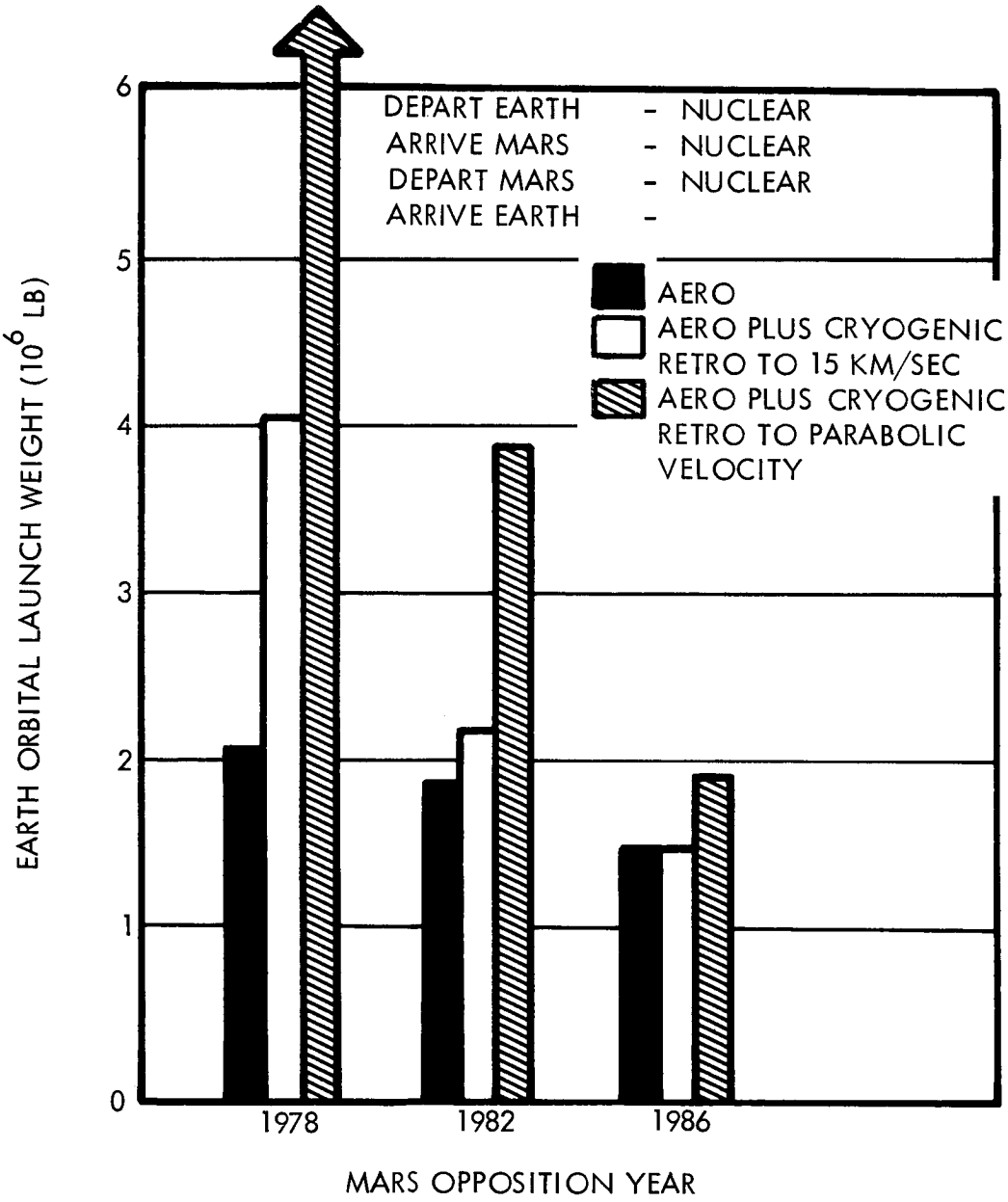


Figure IV-5 Mars Stopover Mission - All Nuclear Propulsion

The optimum thrust levels for the manned Mars vehicles are primarily a function of the vehicle weight. Therefore, it is to be expected that the optimum thrust requirements will vary widely throughout the range of mission years. This variation is seen in Fig IV-6 which is a composite of the many curves similar to Fig IV-1. This figure shows the relationships that exist among the initial vehicle weight requirements, the thrust per engine, and the mission year. The discontinuities in the curves occur when an engine firing time of 1800 seconds is attained, at which point an additional nuclear engine is employed in a clustered arrangement to reduce the firing time for the leave earth stage. As the engine thrust is further and further diminished, the firing time for the arrive Mars stage increases until the 1800-second limitation is exceeded. The curves are then drawn in dashed lines.

For these typical Mars stopover missions, the optimum thrusts range from approximately 125,000 to 300,000 pounds. Although in 1986, an 80,000-pound thrust engine yields a lower weight vehicle, a 2,000-sec burn time is required as well as an extra engine. Therefore, the negligible savings in weight probably do not warrant the use of an engine of this low thrust with its limited utility for other missions.

System weight increases from the assumed nominal values can easily occur due to the uncertainty of environmental factors and future technological developments, such as cryogenic propellant storage, micrometeoroid protection, mission and crew requirements, system redundancy, etc. Any increase in payload or system weights or decrease in performance will increase the vehicle weight, thus increasing the optimum thrust level. Furthermore, the vehicle weight is more sensitive to a decrease in thrust from the optimum value than for an increase in thrust. These two conditions tend to favor the selection of a compromise thrust that is greater than the midrange of the optimum values. An engine thrust between 200,000 and 250,000 pounds appears reasonable for the manned Mars stopover missions. It should be remembered that the three years, 1978, 1982, and 1986, include the entire range of vehicle weight requirements for the years 1975 and 1992 and, therefore, these results are representative for this time period.

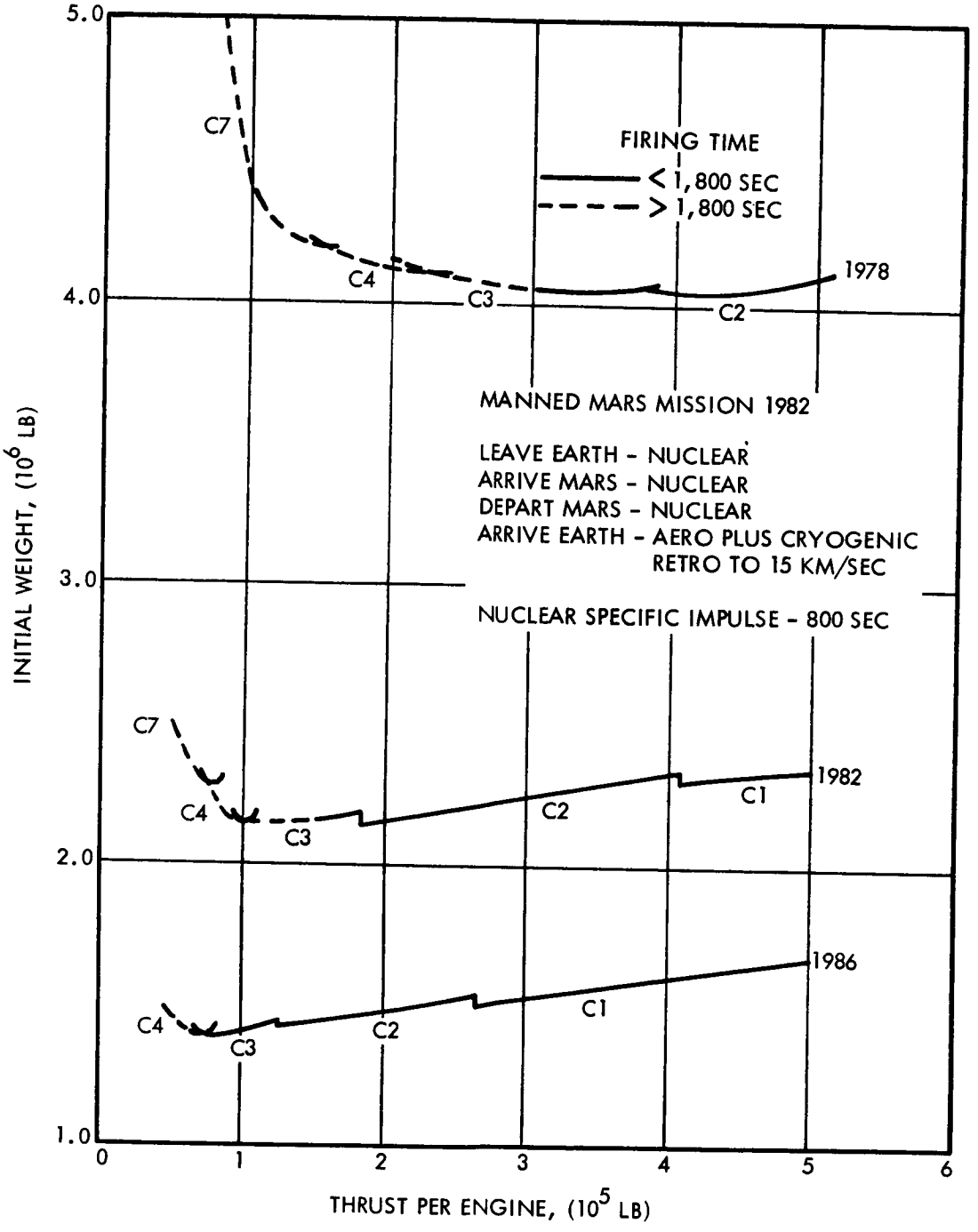


Figure IV-6 Mars Stopover Mission - Nuclear Engine Thrust Requirements

Constant Thrust Upper Stages - The optimum thrust ranged from approximately 300,000 to 500,000 pounds for the series of missions in which the thrust level of the arrive and depart Mars stages was held constant at either 50,000 pounds or 100,000 pounds. This increased optimum thrust range was to be expected since a trade-off between the higher thrust depart earth requirements and the lower thrust Mars propulsive phase requirements was not required. For the same reason, a single engine or at most a cluster of two engines was optimum for depart earth stage.

A comparison with the preceding optimum results for a vehicle using a single thrust level engine was made. The use of the 50,000 - pound thrust upper stage engine increased the initial vehicle weight requirements by almost 30 percent for 1978, by 8 percent for 1982, and by 2 percent for 1986. The firing times for the arrive Mars stage for these three years were 19,700 sec, 7,000 sec, and 3,300 sec, respectively. Clearly, the use of this engine thrust level would be acceptable only for 1986.

The use of the 100,000-pound engine for the arrive and depart Mars stages increased the vehicle weight by 5 percent for 1978 and decreased the weight by 2.5 percent for 1982 and by 3 percent for 1986. The maximum firing times were 7,600 sec, 3,000 sec, and 1,500 sec for the three years, respectively. The use of this engine appears advantageous from a vehicle weight standpoint for both the years 1982 and 1986 although the maximum firing time for 1982 is exceeding 45 minutes.

It should be noted that the above comparisons are based on a vehicle that assumes an earth aerodynamic braking capability of 15 km per sec arrival velocity. If this capability is decreased, i.e., a larger retro required, the use of these constant upper stage thrust engines would result in comparatively higher weight vehicles. Conversely, an increase in aerodynamic braking capability or any other system change which decreases the vehicle weight would tend to increase the comparative gains for this mode of engine utilization.

It appears that the mission attractiveness of these constant thrust upper stage engines (especially the 100,000-pound thrust engine) can be enhanced by resorting to clustered arrive Mars engines. The increased thrust thus available will both decrease the vehicle weight (lower gravity losses) and decrease the maximum engine firing time. Additional effort is required to fully explore these possibilities.

Lunar and Flyby Missions - As mentioned earlier, the compromise nuclear engine should also be capable of reasonable performance for departing earth for planetary flyby and lunar logistic missions. The relationship between the optimum initial vehicle weight and engine thrust is presented in Fig IV-7 for these missions. For the range of payloads shown, the vehicle performance for lunar missions is relatively insensitive to changes in engine thrusts from 50,000 to 400,000 pounds, if engine clustering is utilized. The 200,000 to 250,000-pound thrust range is nearly optimum for the larger lunar payloads, while the required vehicle weight is increased from the optimum by only four percent for the 200,000 pound payload.

The vehicle weight is slightly more sensitive to the engine thrust for flyby missions than for the lunar missions. Fig IV-7 shows a maximum increase of eight percent in vehicle weight from the optimum when 200,000 to 250,000-pound thrust engines are used. A cryogenic retro stage which decelerates the vehicle to parabolic velocity before aerodynamic earth entry is used for the flyby missions. An all aerodynamic earth braking mode reduces the initial vehicle weight by approximately 16 percent for both the Mars and Venus missions although the character of the curve or the point at which the minimum weight occurs is not significantly altered. The trajectories used for the Mars flyby missions are of the low energy type, characterized by trip times of 600 to 700 days. Therefore, there is very little variation in vehicle weight requirements between 1978 and 1980. For the high energy or shorter trip time trajectories, the initial vehicle weight will approach one million pounds. For these missions, a 200,000 to 250,000-pound thrust engine would be near the optimum.

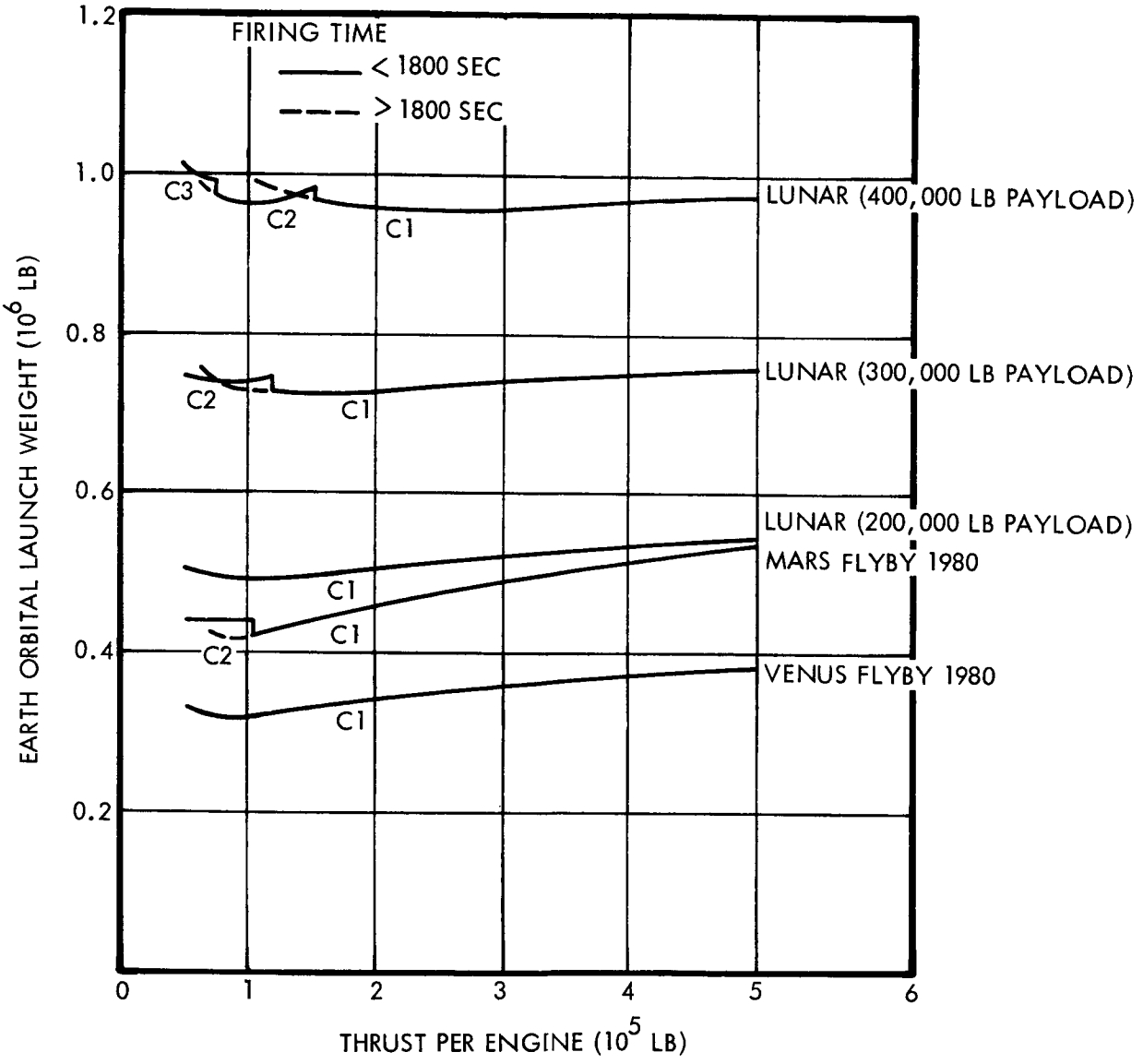


Figure IV-7 Planetary Flyby and Lunar Missions
Nuclear Engine Thrust Requirements

Compromise Thrust Summary

Since a thrust range between 200,000 and 250,000 pounds is desirable for the advanced nuclear engine, a nuclear engine with an approximate thrust of 230,000 pounds was selected for further mission and engine analyses. This selection was made by NASA and reflects the results obtained in this study as well as the results of current technical effort on advanced nuclear engines being performed elsewhere.

This thrust is well situated within the range of optimum thrusts, and appears to be a reasonable selection as a tentative compromise thrust for the nuclear engine. For the specified payload assumptions, use of this thrust level produces an increase in initial vehicle weight of seven percent for the 1986 mission, but for 1982, the vehicle weight is within two percent of the optimum. Since the 1982 Mars stopover mission requires a two million pound vehicle in earth orbit, it is likely that the subsequent 1986 Mars mission will utilize this developed launch and rendezvous capability rather than the 1.5 million pound optimum vehicle. Such increases in initial vehicle weight will reduce the penalty incurred with the 230,000-pound thrust engine.

## SENSITIVITY ANALYSIS

The ultimate performance capability of the nuclear engine for any stated mission will be largely a function of the finally developed engine thrust, specific impulse, and weight. The performance will also depend on the final mission payload and system weight requirements. This performance capability is measured by the initial vehicle weight requirement.

The effect that changes in the mission, vehicle, and engine performance parameters produce on the initial vehicle weight are of interest in order to determine a range of orbital vehicle weights that could be required for the various missions as well as to establish the relative importance of discrete changes in performance or system weights.

For these investigations, a nuclear engine thrust of 230,000 pounds was assumed as nominal. This thrust level was selected as a nominal value on the basis of evaluations and interpretations made in the previous section. Perturbations about this nominal value were made as well as about the nominal values of the other engine characteristics, payloads, and system weights.

Both Mars stopover and lunar transfer missions were analyzed for various time periods, clusters of nuclear engines, and Mars and earth braking systems and capabilities. Parameters that were varied include thrust, specific impulse, payloads, tank weights, stopover time, engine weight, and cryogenic storage insulation parameters.

The data obtained from the computer runs were used to generate over 240 sensitivity graphs. These graphs present the initial vehicle weight as a function of the variable parameter. In some cases the maximum engine firing time is also shown. All of these graphs are reproduced in Vol III.

Primarily, the value of these data is for the information available directly from the graphs. Since the graphs "speak for themselves", so to speak, no attempt will be made here to reproduce the major part of the data.

A listing of the mission matrices and parameter criteria and several summary cross plots are presented in this section. These summary graphs permit a comparison of the vehicle sensitivity to changes in some of the major parameters.

Mission and Parameter Matrix

The primary matrix of variations of mission destination, time period, and propulsive modes established for the sensitivity analysis is shown in Table IV-6.

For each combination within this matrix of missions, years, and modes, specific mission, vehicle, and engine performance parameters were varied over a range of values. Most of these parameter variations were performed successively, i.e., all other parameters were held constant at their nominal values as each parameter was varied singly. Two exceptions to this were for the combination of thrust and specific impulse, and thrust and mission module weight; analyses were made over square matrices composed of these two sets of parameters.

Table IV-6 Sensitivity Analysis Mission Matrix

Mars Stopover Mission

Opposition years - 1978, 1982, and 1986
Trajectory type - IIB
Depart earth stage - Nuclear (1 to 5 engines)
Arrive Mars stage - Nuclear
Depart Mars stage - Nuclear
Arrive earth stage - Aero
Cryogenic retro to 18 km per sec ($LO_2/LH_2$)
Cryogenic retro to 15 km per sec ($LO_2/LH_2$)
Cryogenic retro to parabolic velocity ($LO_2/LH_2$)

Lunar Transfer Mission

Trajectory type - Mean transfer (70 hr)
Depart earth stage - Nuclear (single engine)
Arrive moon - Cryogenic retro ($LO_2/LH_2$)
Storable retro
Payload - 100,000 to 400,000 lbs

The parameters varied in the sensitivity analysis are given in Table IV-7 together with their range and nominal value.

Table IV-7 Sensitivity Analysis Parameter Variations

| Parameter | Range | Nominal Value |
|---|---|---|
| Thrust | 150,000 to 400,000 lbs | 230,000 lbs |
| Specific impulse | 700 to 900 sec | 800 sec |
| Mars entry module | 60,000 to 100,000 lbs | 80,000 lbs |
| Mars mission module | 60,000 to 110,000 lbs | 85,000 lbs |
| Earth recovered payload | 7,000 to 20,000 lbs | 10,000 lbs |
| Engine weight | -30 to + 30% | 34,200 lbs (0%) |

Table IV-7 Sensitivity Analysis Parameter Variations (cont'd)

| Parameter | Range | Nominal Value |
|---|---|---|
| Engine clustering penalty | -10 to + 30% | |
| Tank weight | -15,000 to + 15,000 lb per tank | Basic scaling laws |
| Stopover time | 10 to 40 days | 20 days |
| Cryogenic insulation density | 1 to 7 $lb/ft^3$ | 3 $lb/ft^3$ |
| Cryogenic insulation thermal conductivity | $1 \times 10^{-5}$ to $7 \times 10^{-5}$ Btu/hr $ft^oR$ | $7 \times 10^{-5}$ Btu/hr $ft^oR$ |

The propellant tank weight was varied over the range specified in three different ways. First, only the depart earth tank weights were varied; second, the arrive Mars and depart Mars tank weights were varied while the depart earth tank weights were maintained at their nominal values; and third, all tank weights were varied, i.e., the depart earth, arrive Mars, and depart Mars tanks.

In addition to the above analysis, the sensitivity of the initial vehicle weight and the required heat shield weight to variations in Mars aerodynamic braking capability and the number of clustered nuclear engines in the depart earth stage was investigated. The aerodynamic braking capability was varied by varying the "K" constant in the shield weight equation

$$\frac{W_S}{W_{AM}} = K\,(0.001385\ V_{AM}^2 + 0.183)$$

The matrix of modes considered is given in Table IV-8.

Table IV-8 Mars Aerodynamic Braking Sensitivity Analysis

Mars Stopover Mission

*Opposition years - 1978, 1982, and 1986
Trajectory type - IIB
Depart earth stage - Nuclear (1 to 4 engines)
Cryogenic ($LO_2/LH_2$)
Arrive Mars stage - Aerodynamic

Table IV-8 Mars Aerodynamic Braking Sensitivity Analysis (cont'd)

| | |
|---|---|
| Depart Mars stage - | **Nuclear (single engine) |
| | Cryogenic ($LO_2/LH_2$) |
| | Storable |
| Arrive earth stage - | Aero |
| | Cryogenic retro to 15 km per sec ($LO_2/LH_2$) |
| | Cryogenic retro to parabolic velocity ($LO_2/LH_2$) |
| | Storable retro to 15 km sec |
| | Storable retro to parabolic velocity |

*For the years 1978 and 1986, only modes NANA and NANC (15) were analyzed.
**A nuclear engine for the depart Mars stage is used only when a nuclear engine is used for the depart earth stage.

Stopover Mission

The effect on initial vehicle weight of changes in specific impulse, engine thrust, engine weight, Mars entry module weight, mission module weight, and earth recovered weight is shown in Figs. IV-8, IV-9, and IV-10 for the Mars opposition years of 1978, 1982, and 1986, respectively. An all nuclear vehicle is assumed in these figures with an aerodynamic braking capability at earth of 15 km per sec.

All of these figures indicate the greater vehicle weight sensitivity to a decrease in thrust than an increase in thrust. Also indicated is the relative insensitivity of the vehicle to engine weight variation; a 12 percent change in engine weight from nominal affects the vehicle weight by less than 3 percent.

The specific impulse, on the other hand exerts a large influence on the vehicle; a 12 percent increase in specific impulse can reduce the vehicle weight by 20 to 30 percent while a similar decrease in specific impulse can cause a 30 to 50 percent increase in weight. The more difficult the mission in terms of velocity requirements, the greater the effect on the vehicle for any given change in specific impulse.

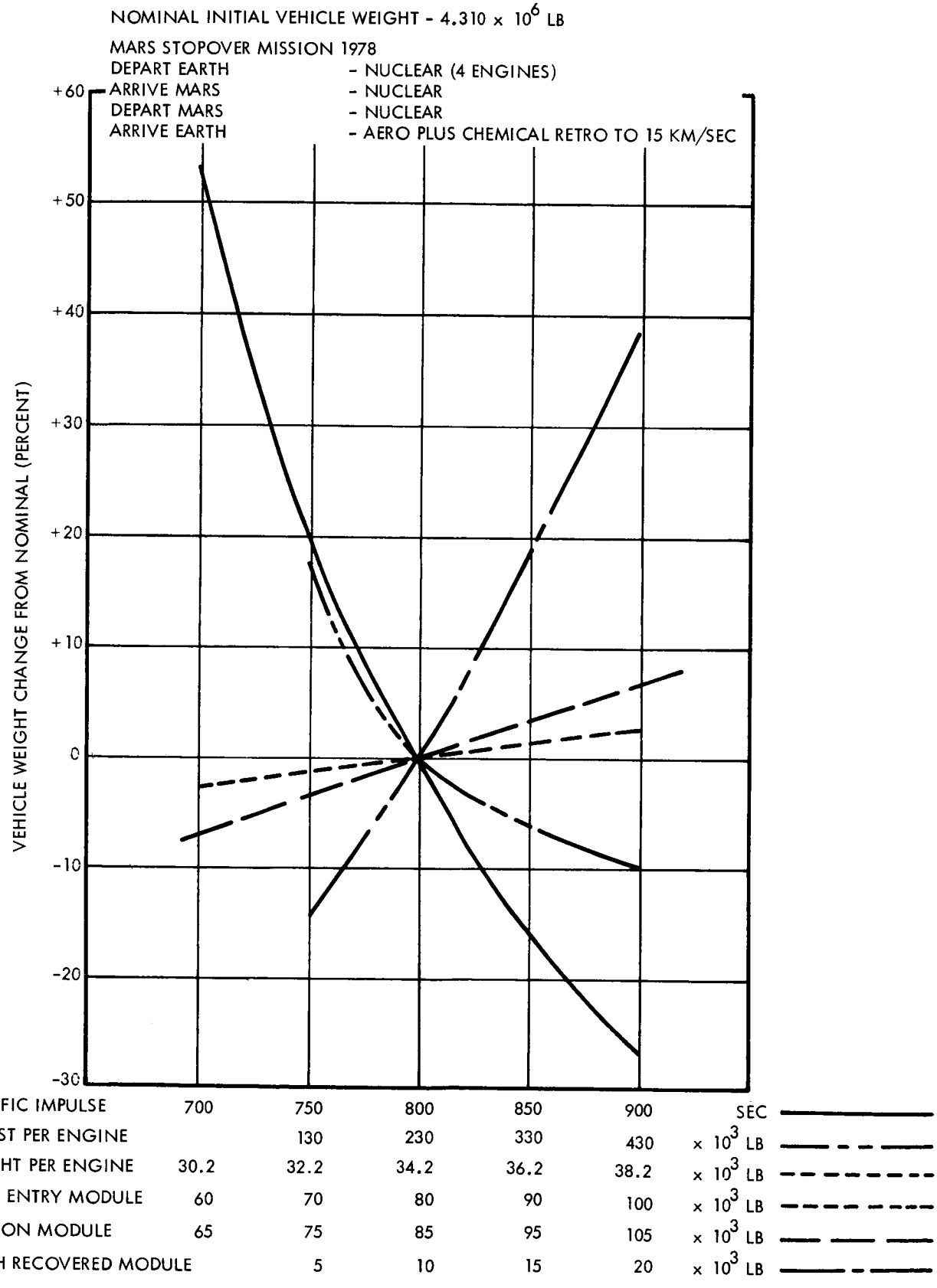


Figure IV-8 1978 Vehicle Weight Sensitivity

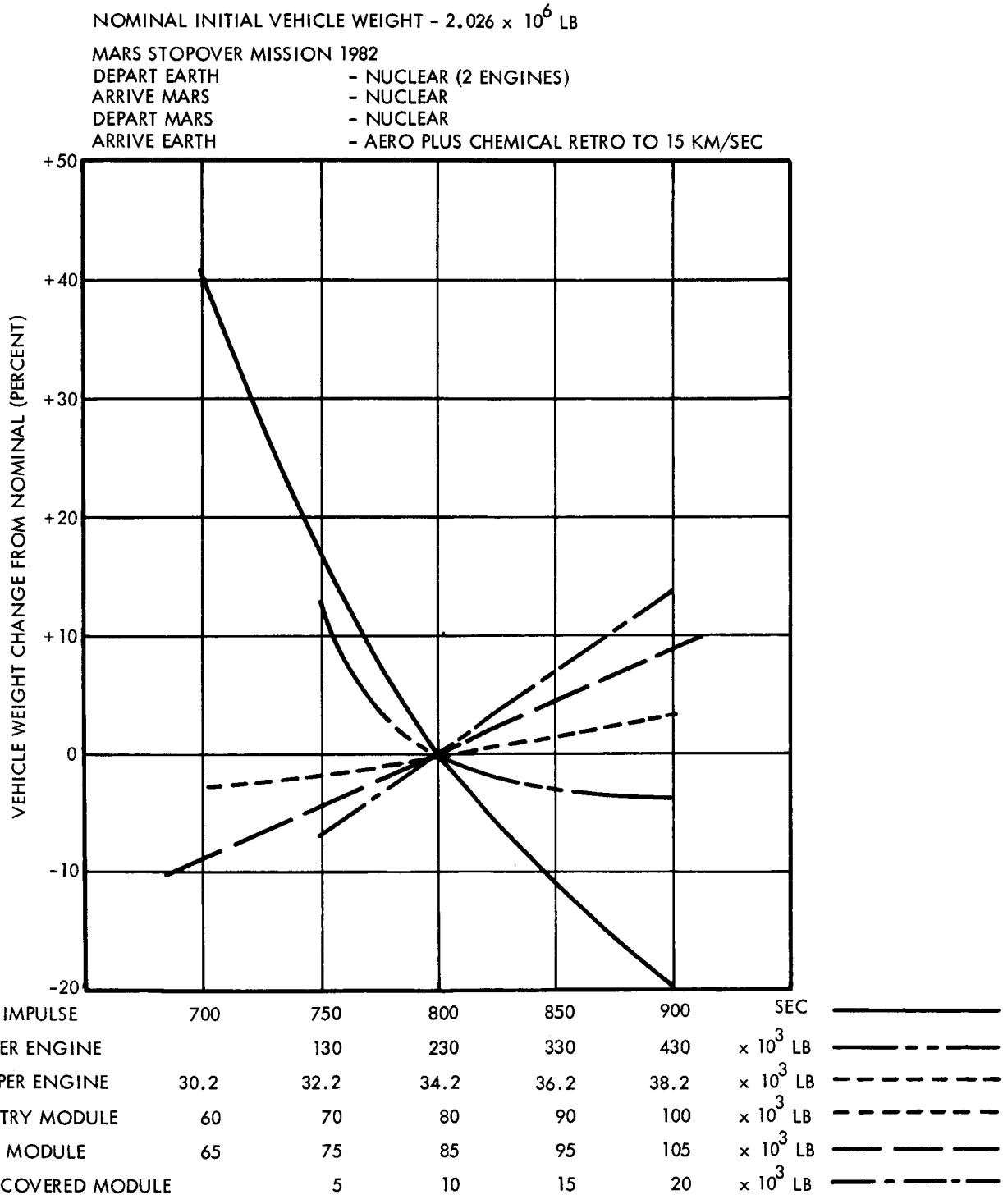


Figure IV-9 1982 Vehicle Weight Sensitivity

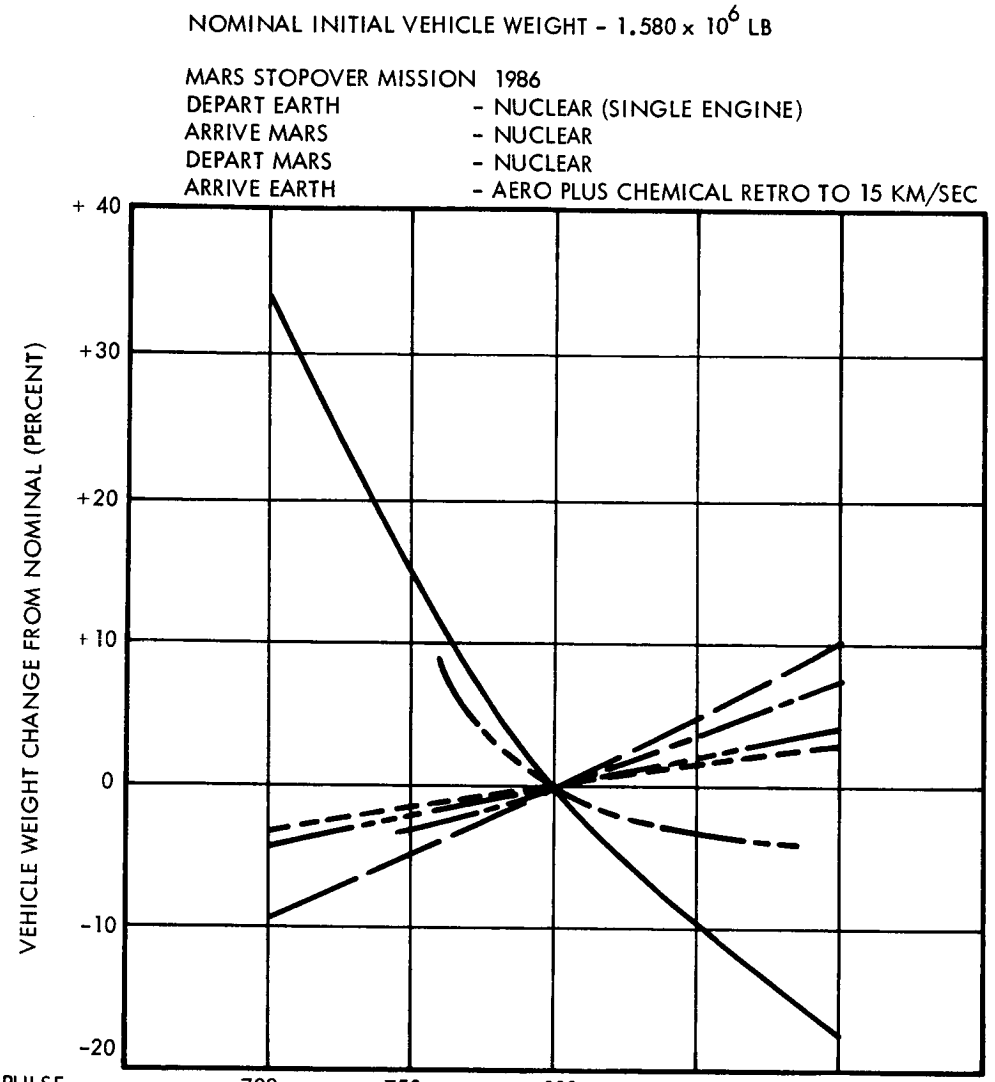


| | | | | | | |
|---|---|---|---|---|---|---|
| SPECIFIC IMPULSE | 700 | 750 | 800 | 850 | 900 | SEC |
| THRUST PER ENGINE | | 130 | 230 | 330 | 430 | x $10^3$ LB |
| WEIGHT PER ENGINE | 30.2 | 32.2 | 34.2 | 36.2 | 38.2 | x $10^3$ LB |
| MARS ENTRY MODULE | 60 | 70 | 80 | 90 | 100 | x $10^3$ LB |
| MISSION MODULE | 65 | 75 | 85 | 95 | 105 | x $10^3$ LB |
| EARTH RECOVERED MODULE | | 5 | 10 | 15 | 20 | x $10^3$ LB |

Figure IV-10 1986 Vehicle Weight Sensitivity

A given change in weight of the earth recovered module in the year 1978 produces a 200 percent greater change in the vehicle weight than in 1982 and almost 300 percent greater than in 1986. This is primarily due to the greater characteristic velocity required for the arrive earth retro in 1978. The 1978 retro velocity is 5.89 km per sec (mass ratio = 3.9); for 1982, 2.98 km per sec (mass ratio = 2.00); and for 1986, 0.47 km per sec (mass ratio = 1.12).

The trade-offs between the compromise engine performance parameters and payload weights as they vary from their nominal values is typically shown in these figures. For example, for 1982 (Fig. IV-9) an increase of 2500 pounds in earth-landed payload increases the initial vehicle weight by 3.5 percent; an increase of 15 seconds in specific impulse or 150,000 pounds in thrust is required to offset this increase. Alternatively, the vehicle weight increase can be offset by reducing the Mars entry module by 20,000 pounds. Similar trade-offs are available for the years 1978 and 1986 from Figs. IV-8 and IV-10.

Mars Aerodynamic Braking

The sensitivity of the vehicle weight to Mars aerodynamic braking capability is of extreme interest due to the potential savings in vehicle weight that use of this mode can produce. In order to vary the Mars aerodynamic braking capability, the "K" factor in the scaling law was varied between 0.1 and 1.5. The graphs of the resulting data, i.e., initial vehicle weight and heat shield weight vs K, are given in Vol. III for the various years and earth braking modes.

In order to establish a reasonable range of K over which to perform the evaluations, K was first varied from 0.01 to 3.0. The results are shown in Fig. IV-11 for a 1982 mission utilizing all aerodynamic braking at earth.

It appears that a K factor of 0.3 to 1.0 would be acceptable in terms of vehicle weight requirements. As K is increased above this range, the vehicle weight increases rapidly. At a K of 1.8, the vehicle weight requirement is identical to a vehicle that employs a nuclear engine for braking at Mars. Below a value of K = 0.3, the initial vehicle weight savings become negligible and the technical difficulty of developing such an efficient aerodynamic braking system would increase rapidly.

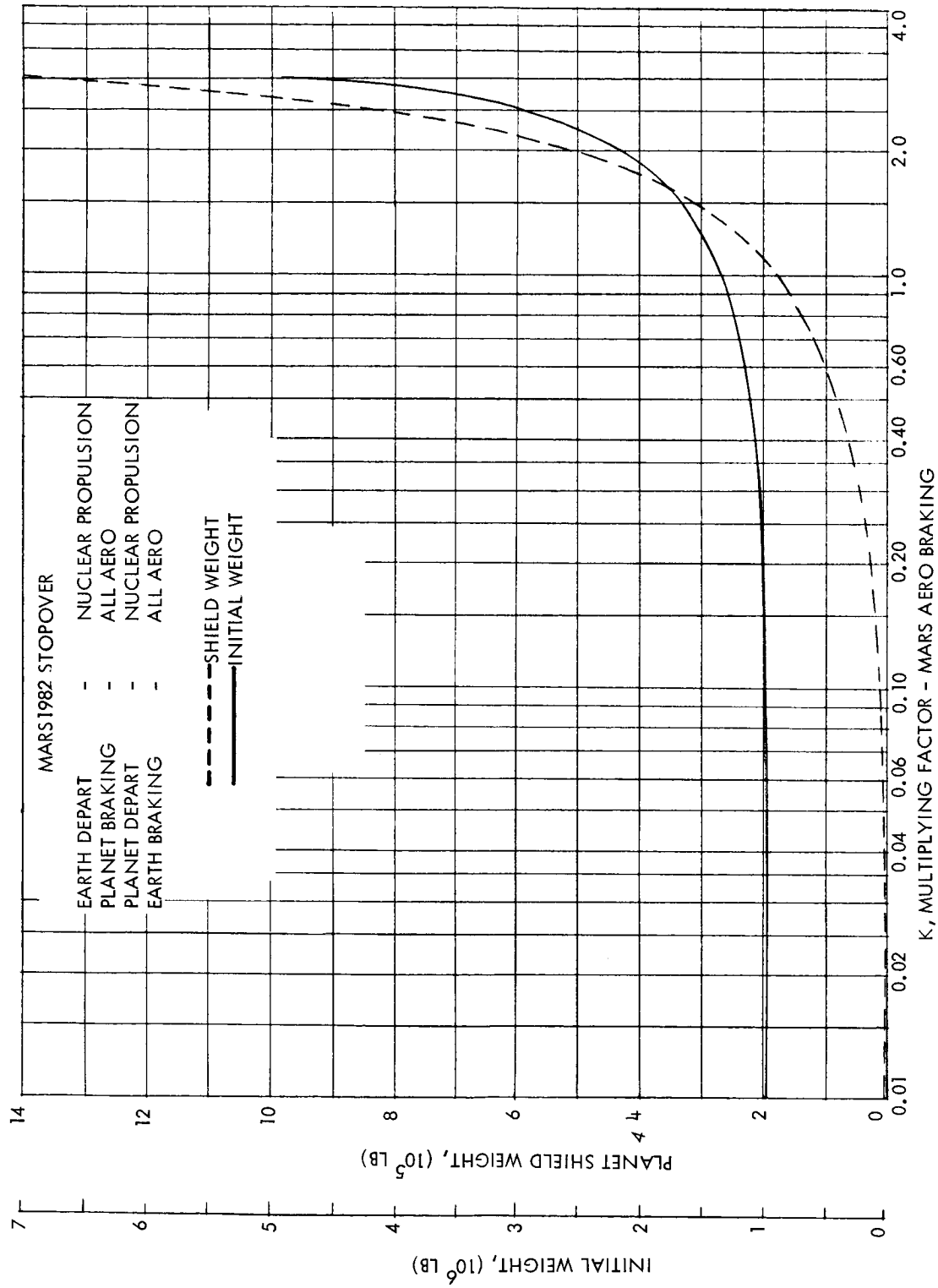


Figure IV-11 Mars Aerodynamic Braking Variation

## SUPPLEMENTARY MISSION MATRIX

A supplementary matrix of missions was established in order to permit a comparison of nuclear and chemical propulsions systems and to extend the breath of the investigations to additional operational mode combinations and parameter variations. The data obtained from these investigations further relate the initial vehicle weight requirements for stopover missions to variations in planet destination, mission year, propulsive system types, and aerodynamic braking modes at Mars and earth. Also varied parametrically throughout the matrix of cases are the scaling laws used for computing the propellant tank jettison weights. Other system and performance variations include the storable propellant specific impulse and Venus swingby trajectories.

### Mission Matrix

The basic supplementary mission matrix is shown in Table IV-9. The matrix consists of three separate types of missions; a Mars stopover, a Mars stopover with an unpowered Venus swingby during the inbound leg, and a Venus stopover. Each of these missions have been analyzed for the earth and Mars, depart and arrive modes as shown. For the Mars stopover missions, 1982 opposition, both type IB and IIB trajectories were investigated. Also for the Mars stopover and Venus swingby missions, a nuclear depart Earth and arrive Mars with a cryogenic depart Mars mode was analyzed for the year 1978 and 1984. In addition to this basic matrix, additional selected operational modes or parameter perturbations were analyzed in order to answer specific questions that were posed during the study.

Four additional classes or "levels" of scaling laws were used for this segment of the study to define the various propellant tank jettison weights or mass fractions (ratio of total useable propellant-to-total gross stage weight ). These are designated as mass fraction case numbers 1 through 4, and are defined by the scaling laws given in Chapter III. The average mass fractions given by the scaling laws decrease in an approximate linear fashion with increasing case number. The average mass fraction given by these four sets of scaling laws are listed in Table IV-10 for the various propulsive modes and mission phases. It must be remembered that the equations and average mass fractions for the nuclear stages do not include the weight of the nuclear engine.

## Table IV-9 Supplementary Mission Matrix

| MISSION | YEAR | DEPART EARTH STAGE | ARRIVE PLANET STAGE | DEPART PLANET STAGE | ARRIVE EARTH STAGE |
|---|---|---|---|---|---|
| MARS STOPOVER | 1975 TO 1990 TYPE IIB | NUCLEAR* | AERO NUCLEAR | NUCLEAR | AERO<br>RETRO-15-$LO_2/LH_2$<br>RETRO-PARABOLIC-$LO_2/LH_2$<br>RETRO-15-STORABLE<br>RETRO-PARABOLIC-STORABLE |
| | | NUCLEAR $LO_2/LH_2$ | AERO $LO_2/LH_2$ | $LO_2/LH_2$ | |
| | | NUCLEAR $LO_2/LH_2$ | AERO | STORABLE | AERO<br>RETRO-15-STORABLE<br>RETRO-PARABOLIC-STORABLE |
| MARS STOPOVER-VENUS SWINGBY | 1978 & 1984 INBOUND SWINGBY | NUCLEAR | AERO NUCLEAR | NUCLEAR $LO_2/LH_2$ | AERO<br>RETRO-PARABOLIC-$LO_2/LH_2$<br>RETRO-PARABOLIC-STORABLE |
| | | NUCLEAR $LO_2/LH_2$ | AERO $LO_2/LH_2$ | $LO_2/LH_2$ | |
| | | NUCLEAR $LO_2/LH_2$ | AERO | STORABLE | AERO<br>RETRO-PARABOLIC-STORABLE |
| VENUS STOPOVER | 1980 TYPE IIB | NUCLEAR | NUCLEAR | NUCLEAR | AERO<br>RETRO-PARABOLIC-$LO_2/LH_2$<br>RETRO-PARABOLIC-STORABLE |
| | | NUCLEAR $LO_2/LH_2$ | $LO_2/LH_2$ | $LO_2/LH_2$ | |

*ALL NUCLEAR DEPART EARTH STAGES ANALYZED FOR 1, 2, 3, AND 4 CLUSTERED ENGINES

Table IV-10 Propellant Tank Mass Fractions

| | AVERAGE MASS FRACTION | | | |
|---|---|---|---|---|
| | NO. 1 | NO. 2 | NO. 3 | NO. 4 |
| NUCLEAR ($H_2$) LEAVE EARTH | .88 | .84 | .80 | .76 |
| NUCLEAR ($H_2$) 200 DAY STORAGE | .87 | .83 | .79 | .75 |
| CRYOGENIC ($H_2$-$O_2$) LEAVE EARTH | .94 | .90 | .86 | .82 |
| CRYOGENIC ($H_2$-$O_2$) 200 DAY STORAGE | .92 | .87 | .82 | .77 |
| STORABLE 200 DAY STORAGE | .95 | .91 | .87 | .83 |
| CRYOGENIC ($H_2$-$O_2$) EARTH RETRO | .79 | .74 | .69 | .64 |
| STORABLE EARTH RETRO | .91 | .87 | .83 | .79 |

The payload criteria and additional system weight scaling laws are based on the data given in Chapter III. In all cases, a nominal engine of 230,000 pounds thrust was used.

Mission Evaluations

The mission matrix represents over 6,000 individual mission simulations or cases. The resulting data for all of these missions were listed in tabular form, plotted, and in some cases, cross plotted to reveal the influence of mission year, propulsive mode, and scaling law variations on vehicle weight. These tables and graphs are fully presented in Vol. III. A few of the graphs will be repeated here in order to indicate the more significant or typical vehicle-parameter relationships.

Figure IV-12 compares the orbital launch weight requirements for four different propulsive and Mars aerodynamic braking mode combinations for Mars and Venus stopover missions. All Martian opposition years from 1975 to 1990 are given. The requirements for the 1980 Venus mission are typical for all conjunction years. The propellant tank weights are based on mass fraction case number 2 and a cryogenic retro is employed at earth arrival to brake the vehicle to 15 km per sec.

This figure shows that the weight of the all cryogenic propellant vehicle is over two times that of the all nuclear vehicle for the favorable opposition of 1986. In the unfavorable year of 1978, the ratio of weights increases to four. The weight differences between the $LO_2/LH_2$ and the nuclear vehicles are reduced if aerodynamic braking is used for capture into Mars orbit. In that case, the cryogenic propellant vehicle requires approximately 50 percent more weight in 1986 and 100 percent in 1978.

Figure IV-12 also shows that the weight requirement for the Venus mission is approximately equal to the 1986 Mars mission for the nuclear vehicle and to the 1984 Mars mission for the cryogenic vehicle. In all cases, the earth arrival velocity for the Venus mission is less than 15 km per sec and therefore, no retro stage is required for the assumed aerodynamic braking capability used in this figure.

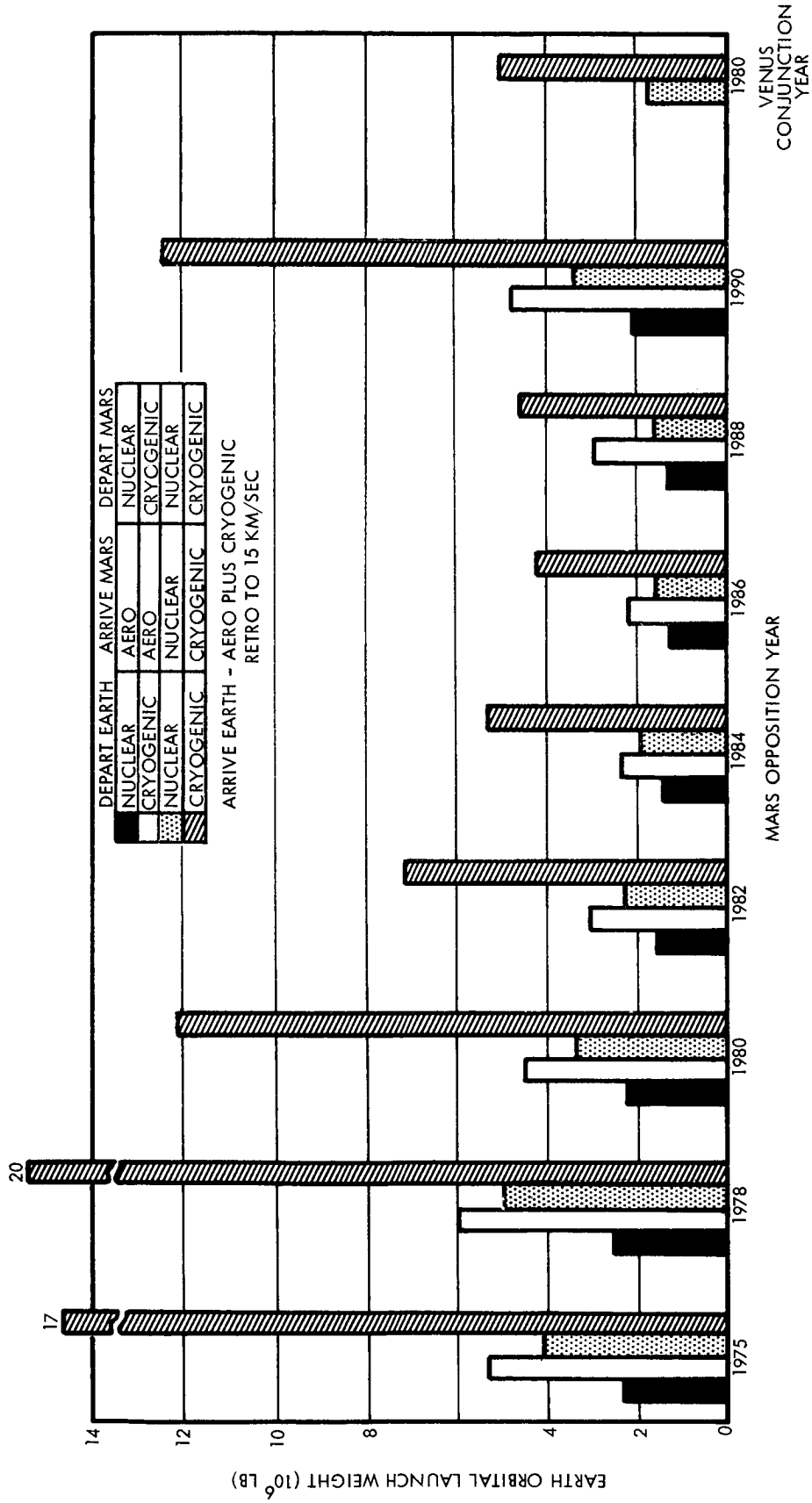


Figure IV-12 Orbital Launch Weight Comparison

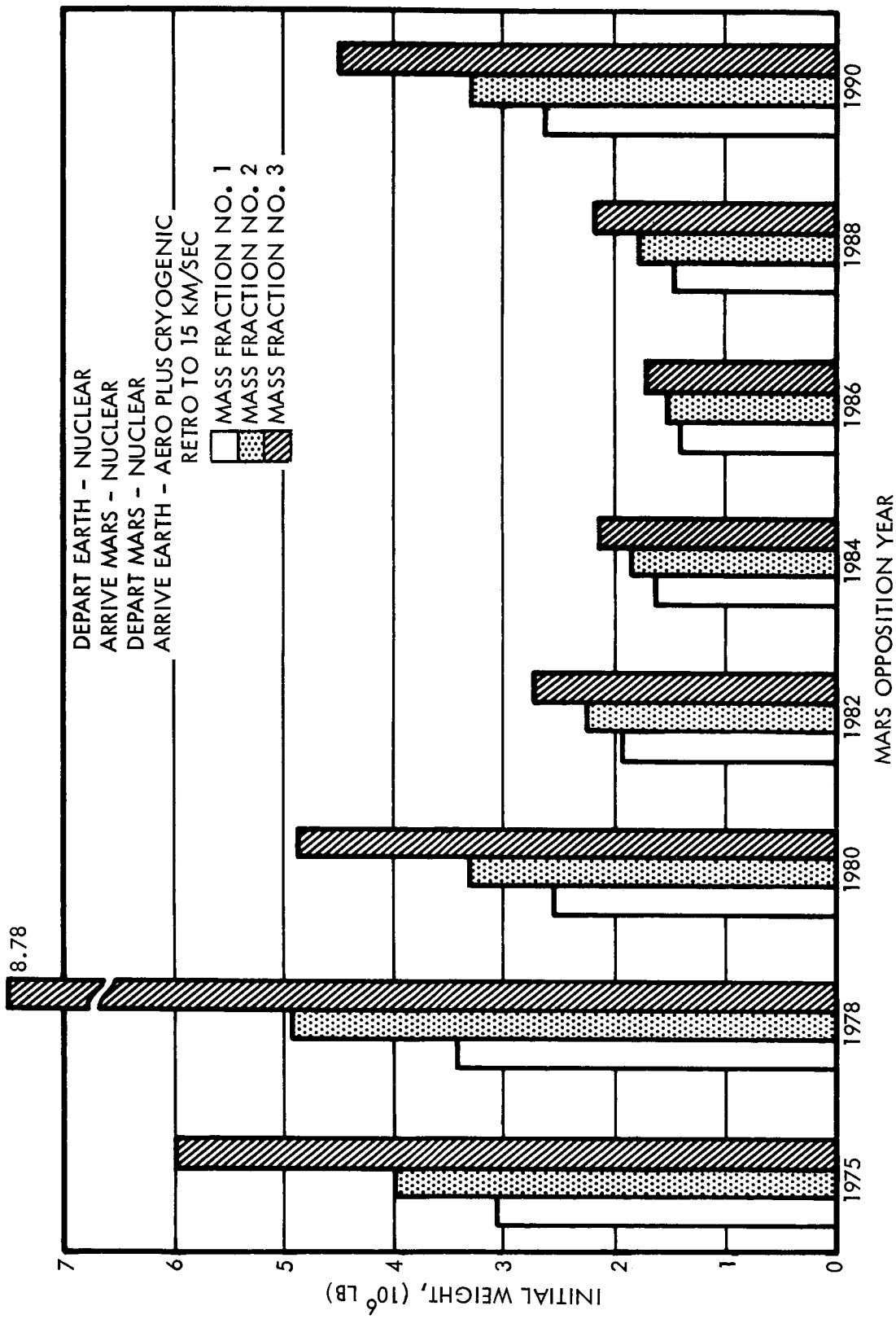


Figure IV-13 Vehicle Weight vs Mass Fraction and Mission Year

This figure indicates the large reduction in vehicle weight that can be obtained with aerodynamic braking at Mars. Use of this braking mode reduces the vehicle weight for the cryogenic propellant vehicle by one-half in 1986 and by over two-thirds in 1978. In contrast, the nuclear vehicle weight is reduced by one-fifth in 1986 and by one-half in 1978. These results are based on a K = 1 in the aerodynamic braking scaling law. If a more "efficient" braking system would be developed, further weight savings would result.

This latter comparison further exemplifies the sensitivity effect mentioned previously. That is, the more difficult the mission or the less the vehicle performance capability, the greater the sensitivity of the vehicle weight to variations in any given parameter or operational mode.

Figure IV-13 shows this same effect on vehicle weight for variations in the tank jettison weight as functions of mission year. Approximately 20 percent more vehicle weight is required for the 1986 mission for a vehicle whose propellant tank mass fractions are decreased by about 10 percent (mass fraction case no. 1 to case no. 3). This same decrease in propellant tank mass fractions increases the vehicle weight by over 150 percent for the most unfavorable mission year, 1978.

Figure IV-14 shows the effect on initial vehicle weight of variations in the tank jettison weight as a function of several combinations of vehicle propulsive and Mars aerodynamic braking modes. The mission is for the 1982 opposition and an earth braking capability of 15 km per sec is assumed. The vehicle weight for highest performing vehicle, curve D, increases by 45 percent for an increase in propellant tank weights from mass fraction case no. 1 to case no. 4. If cryogenic propellant propulsion systems are used in lieu of the nuclear engines (curve B), the vehicle weight increases by almost 150 percent for the extremes of tank weight scaling laws. An all cryogenic vehicle (curve A) increases in weight by 400 percent.

Case no. 4 represents mass fractions for tanks of extremely inefficient design, even in terms of present state-of-the-art. Nevertheless, there can occur sizable tank weight increases due to the final determination of micrometeoroid protection and cryogenic propellant storage requirements. These weight increases could conceivably decrease the tank mass fractions into the region of case no. 3.

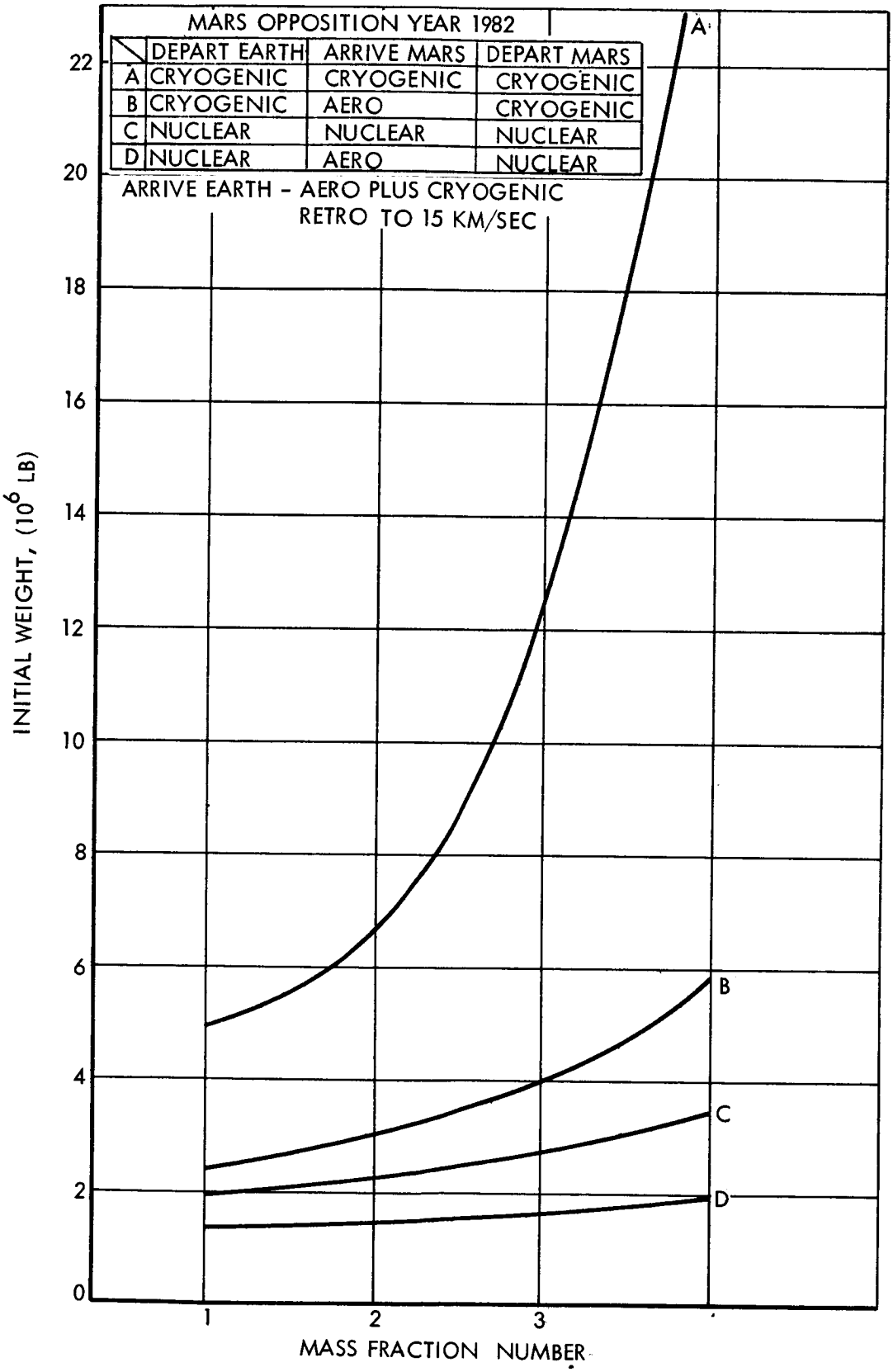


Figure IV-14 Vehicle Weight vs Mass Fraction & Vehicle Mode

Figure IV-15 shows the effect on vehicle weight of variations in the storable propellant specific impulse for six different combinations of propulsive and Mars aerodynamic braking modes. In all mode combinations, storable propellants are used for the midcourse correction stages and for braking the vehicle upon earth arrival to 15 km per sec. Modes B and E also utilize a storable propellant stage for departing Mars. As might be expected, the vehicle weights for these latter two modes show the greatest effect to changes in the storable propellant specific impulse. An increase in specific impulse of 18 percent (330 sec to 390 sec) decreases the initial vehicle weight for these two modes by approximately 25 percent. The vehicle weights for all of the other modes are reduced by only about 5 percent for the same increase in specific impulse.

Due to a lack of available trajectory data, the results obtained for the Venus swingby missions are not necessarily optimum, i. e., minimum initial vehicle weight. The 1978 Venus swingby was computed for a fixed set of trajectory parameters. This trajectory was selected on the basis of previous analysis which indicated it to be a desirable trajectory for certain modes and performance constraints. Therefore, for some of the modes, the vehicle weight could be substantially reduced if the trajectory parameters that were optimum for those modes were used.

For the 1984 Venus swingby computations, sets of trajectory data for the swingby leg were available at ten-day increments for the inbound (or swingby) leg. For each incremental set of inbound trajectory data, the optimum outbound trajectory was determined. Then the set of inbound trajectory data (with its optimum outbound trajectory data) that produced the minimum initial vehicle weight in earth orbit was selected as the quasi-optimum trajectory. These trajectories are probably within an average of five days of the optimum arrive Mars date. Due to the fact that for swingby trajectories, the depart Mars and arrive earth velocities can vary drastically with only a few days change in launch date or trip times, some of the computed vehicle weights could be considerably greater than the true minimum.

This brief and incomplete analysis of Venus swingby missions indicated that some of the extremes in vehicle weight variations due to the unfavorable years or high earth arrival velocities could be eliminated and the overall vehicle

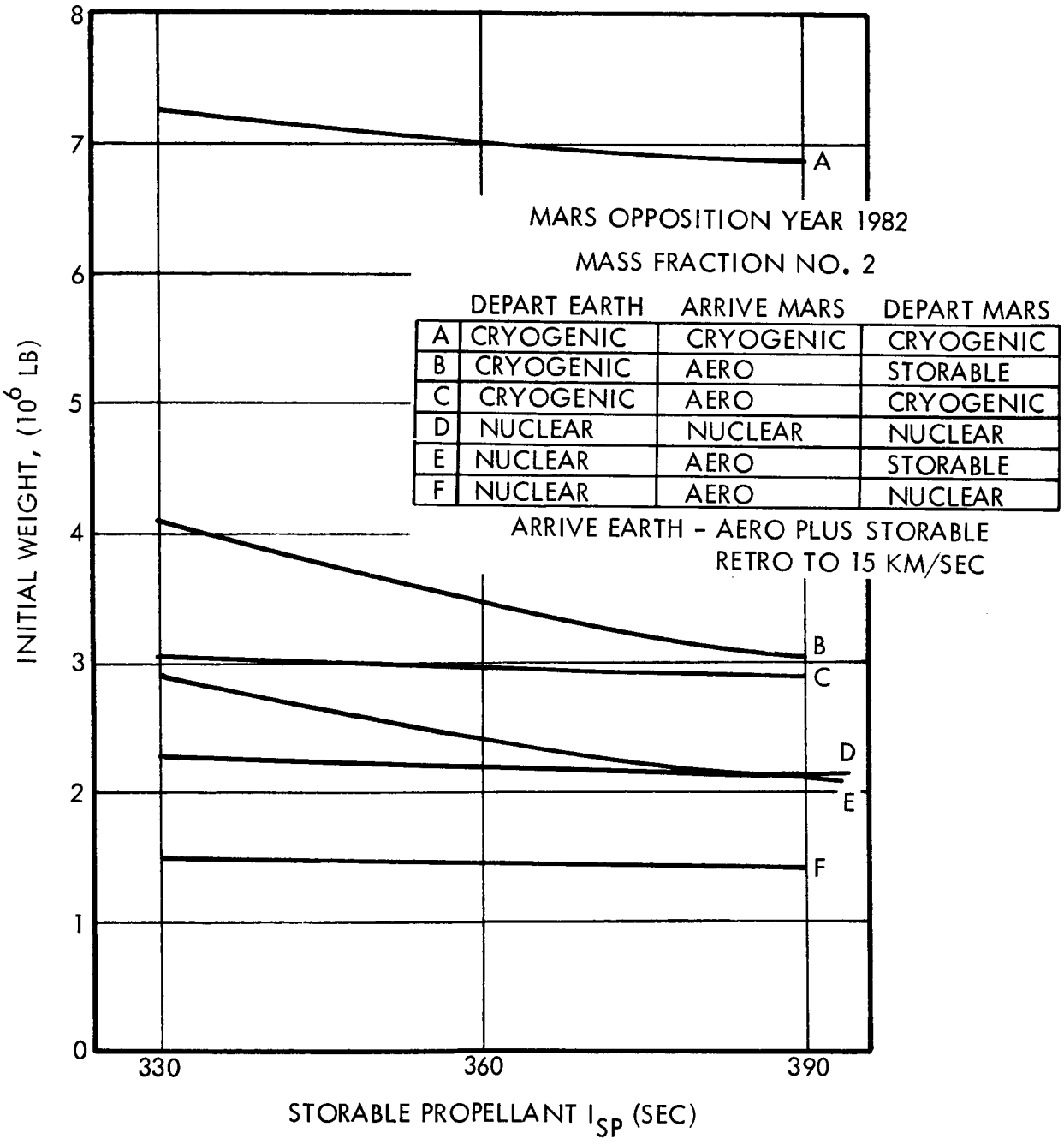


| | DEPART EARTH | ARRIVE MARS | DEPART MARS |
|---|---|---|---|
| A | CRYOGENIC | CRYOGENIC | CRYOGENIC |
| B | CRYOGENIC | AERO | STORABLE |
| C | CRYOGENIC | AERO | CRYOGENIC |
| D | NUCLEAR | NUCLEAR | NUCLEAR |
| E | NUCLEAR | AERO | STORABLE |
| F | NUCLEAR | AERO | NUCLEAR |

Figure IV-15 Vehicle Weight vs Storable Propellant Specific Impulse

weight requirements reduced by resorting to a trajectory in which the vehicle swings by Venus either during the inbound or outbound leg of the mission. For example, the use of the Venus swingby mode in 1978 reduces the vehicle weight of the all nuclear vehicle by 22 percent, (from 4.9 to 3.8 million pounds) for a mission in which earth retro braking to 15 km per sec is employed. In 1984, the weight of a similar nuclear vehicle but which employs earth retro braking to parabolic velocity is reduced by 10 percent (from 2.50 to 2.34 million pounds).

The investigations made during the study were by no means exhaustive and future effort in this area is certainly desirable in order to determine the ultimate potential of the Venus swingby mode.

# V SUMMARY AND CONCLUSIONS

A summary of the major study results and conclusions is given in this chapter.

## INITIAL VEHICLE WEIGHT REQUIREMENTS

The initial vehicle weights required in earth orbit in order to perform a wide variety of interplanetary missions for various operational and vehicle modes were established.

For the Mars stopover mission and an earth aerodynamic braking capability from 15 km per sec, the all nuclear propelled vehicle requires an orbital launch weight of 1.5 million pounds in 1986 and 4.3 to 5.0 million pounds in 1978. By contrast, the all cryogenic propellant ($LO_2/LH_2$) vehicle requires 4.0 million pounds in 1986 and upwards of 20 million pounds in 1978. If aerodynamic braking is employed for capture into Martian orbit, the nuclear vehicle weight is reduced to 1.2 million pounds in 1986 and 2.4 million pounds in 1978. The cryogenic vehicle weight reduces to 2.2 million pounds in 1986 and 5.0 to 6.0 million pounds in 1978.

The other Mars mission opportunities will require vehicle weights between the extremes given above.

The Venus stopover mission requires approximately 2.0 million pounds for the nuclear vehicle and 5.0 and 6.0 million pounds for the cryogenic propellant vehicle. These values only vary slightly among conjunction dates.

The low energy, manned Mars flyby mission requires a nuclear vehicle weighing between 340,000 and 430,000 pounds depending on the nuclear engine thrust and earth aerodynamic braking capability. The vehicle weight for a high energy Venus flyby mission will vary between 270,000 and 350,000 pounds again depending on thrust and aerodynamic braking capability.

A lunar transfer mission delivering a payload into lunar orbit requires vehicles weighing approximately 500,000 pounds for a 200,000-pound payload; 750,000 pounds for a 300,000-pound payload; and 950,000 pounds for a 400,000-pound payload.

## NUCLEAR ENGINE THRUST REQUIREMENTS

For the Mars stopover missions, the optimum thrusts ranged from approximately 125,000 to 300,000 pounds. For the flyby missions, the optimum thrusts were approximately 100,000 pounds and for the lunar missions, the vehicle performance was relatively insensitive to engine thrusts ranging from 50,000 to 400,000 pounds.

Any increase in payload or system weights or decrease in performance will increase in vehicle weight, thus increasing the optimum thrust level. Furthermore, the vehicle weight is more sensitive to a decrease in thrust from the optimum value than for an increase in thrust. Consideration of these two factors as well as the relative importance of the various missions and the maximum firing time of the nuclear engines prompted the selection of 200,000 to 250,000 pounds as the desirable thrust range for the advanced nuclear engine.

An approximate thrust of 230,000 pounds was selected by NASA as a nominal value for further mission and engine analysis. This selection reflects the results obtained in this study as well as the results of current technical effort on advanced nuclear engines being performed elsewhere.

## INFLUENCE OF ENGINE PARAMETERS ON VEHICLE PERFORMANCE

By determining the influence of the principal engine design parameters and constraints on vehicle performance, the combination of engine design variables which produced the highest performance nuclear engine consistent with the state-of-the-art could be selected.

The effect of the variation in engine weight and performance on the initial vehicle weight in earth orbit for the 1982 manned Mars mission was determined as a function of chamber pressure. For a fixed chamber temperature, the higher specific impulses obtainable at the lower chamber pressures result in lower vehicle weights. For specific impulses less than 800 sec, the effect of chamber pressure is relatively small. For higher values of specific impulse, the chamber pressure becomes increasingly important. For this class of engine, nozzle chamber pressures in the vicinity of 350 to 450 psi lead to minimum vehicle weight. For a nozzle chamber temperatures of 4700°F, a reduction in nozzle chamber pressure from 700 to 450 psia resulted

in an increase of 12 sec in specific impulse and a 110,000 lb or a 5.0 percent reduction in vehicle weight. Due to the sensitivity of vehicle weight to specific impulse, the selection of the peak fuel element temperature constraint is extremely important because it determines the attainable exit gas temperature. Each $100^{o}R$ increase in peak fuel temperature increases the specific impulse by 8 sec and results in vehicle weight savings of from 30,000 to 50,000 lbs.

A significant reduction in initial vehicle weight in earth orbit is obtained by increasing the nozzle expansion ratio. It is possible to achieve an 8 percent vehicle weight saving by increasing the nozzle expansion ratio from 40:1 to 140:1. The results demonstrated that increasing the nozzle expansion ratio, for a fixed nozzle chamber temperature, has a diminishing effect on decreasing vehicle weight. At nozzle expansion ratios greater than 140:1 very little vehicle weight savings can be realized. It was also shown that the effect of nozzle expansion ratio becomes more significant at lower values of exit gas temperature.

The sensitivity of initial vehicle weight in earth orbit to core pressure drop was determined. Increasing the core pressure drop from 125 psi to 200 psi results in a vehicle weight decrease of 40,000 lb. The effect of core pressure drop is relatively insensitive to the value of specific impulse. For the range of core pressure drops investigated, higher pressure drops reduced the vehicle weight in earth orbit.

These results show that the engine parameters which significantly influence the specific impulse have the greatest effect on the initial vehicle weight in earth orbit. The most influential engine design parameters which affect vehicle performance are the main nozzle expansion ratio and nozzle chamber pressure. Improper selection of these parameters can result in vehicle weight penalties as high as 5 to 10 percent of the total vehicle weight. Other engine parameters such as coolant channel diameter and core pressure drop primarily affect engine weight, and thus, have a relatively small effect on vehicle weight. Typical variations in core pressure drop or coolant channel diameter produce changes amounting to 1 or 2 percent of the gross vehicle weight in earth orbit.

The maximum available engine performance is a strong function of the engine state-of-the-art design constraints such as peak fuel temperature, fuel element web thickness, fuel element web temperature rise, and maximum allowable nozzle wall temperature. The design constraints which significantly influence specific impulse are extremely critical and require judicious selection. Selection of peak fuel temperature, fuel element internal and external web thickness, and the maximum allowable nozzle wall temperature are particulary crucial because their influence on vehicle performance is great. The fuel element web temperature rise primarily affects the engine weight and, therefore, has a smaller influence on the vehicle performance than the other design constraints.

## COMPROMISE ENGINE DESIGN CHARACTERISTICS

As a result of the mission, vehicle, and engine trade-offs, an integrated set of engine characteristics could be proposed for operational applicability in the 1980's.

The selected engine was obtained using values of peak fuel temperature, nozzle wall temperature, fuel element web temperature rise, and fuel element web thickness determined from physical and manufacturing limitations which were considered to be representative of the future "state-of-the-art". The candidate engine characteristics are shown below.

| | |
|---|---|
| Engine Thrust | 226,000 lb |
| Specific Impulse | 850 sec |
| Engine Weight | 37,500 lb |
| Nozzle Expansion Ratio | 120:1 |
| Reactor Power | 5100 Mw |
| Nozzle Chamber Pressure | 450 psia |
| Nozzle Chamber Temperature | 4700$^{o}$R |
| Core Pressure Drop | 200 psi |
| Nozzle Wall Temperature | 1960$^{o}$R |

## REPRESENTATIVE VEHICLE DESIGN

A representative vehicle design using the compromise engine for the 1982 manned Mars stopover mission was established. This vehicle utilizes the modular tank approach currently being investigated by NASA. It consists of the three main nuclear stages plus a payload stage which, continuing the modular

concept, contains the midcourse stages, Mars lander, earth reentry capsule, earth retro braking stage, and mission module. The earth retro stage decelerates the vehicle to 15 km per sec after which the payload module is landed aero-dynamically.

The data below lists the vehicle and stage weights for this representative vehicle.

| Stage | Description | | Weight (lbs) |
|---|---|---|---|
| I | Leave earth - Nuclear | | 973,308 |
| II | Outbound Midcourse and Attitude Control - Storable | | 47,828 |
| III | Arrive Mars - Nuclear | | 433,729 |
| IV | Leave Mars - Nuclear | | 322,296 |
| V | Inbound Midcourse and Attitude Control - Storable | | 8,342 |
| VI | Earth Retro - Cryogenic | | 30,804 |
| Payload | | | 206,749 |
| | Mars Entry and Ascent Module | 78,500 | |
| | Solar Radiation Shield | 22,939 | |
| | Crew Compartment | 68,734 | |
| | Life Support | 22,750 | |
| | Reentry Capsule and Earth Landed Payload | 13,826 | |
| INITIAL VEHICLE WEIGHT | | | 2,023,056 |

## VEHICLE SENSITIVITY

A comprehensive vehicle sensitivity analysis was performed. This analysis determined the effects on initial vehicle weight that are produced for variations in mission, vehicle, and performance parameters. The analysis was made for various mission years, vehicle configurations, and operational modes. The parameters that were varied included thrust, specific impulse, payloads, engine weight and clustering penalty, tank weight, stopover time, cryogenic storage thermal constants, and Mars aerodynamic capability. In general, the results indicated that the more difficult the mission or the less the performance capability, the greater the sensitivity of the vehicle weight to variations in any given parameter or mode.

The vehicle weight can increase by factors of two or three from a mission performed in the most favorable year (1986) to the least favorable (1978). Similar extreme variations in vehicle weight requirements can also result for any given year for the extreme possibilities of earth aerodynamic braking capabilities.

Of the three engine performance parameters, specific impulse, thrust, and engine weight, changes in the specific impulse produces the largest effect on vehicle weight. Typically, a 2 percent increase in specific impulse decreases the initial vehicle weight by 3.5 percent. In order to decrease the vehicle weight by this same amount the thrust would have to be increased by 65 percent or the engine weight reduced by 12 percent.

The use of aerodynamic braking at Mars can result in comparatively large vehicle weight reductions. Use of this mode can reduce the weight of a nuclear propelled vehicle by 20 percent in 1986 and 50 percent in 1978. A more "efficient" braking system from that assumed (K = 1) would further reduce the vehicle weights.

The vehicle weight can be significantly increased due to discrete system weight increases. Particularly important are the weight provisions required for micrometeoroid protection and cryogenic propellant storage. Both the operational environment and the required technology concerning these two areas are currently not available. Therefore, the weight estimates assumed for these systems in this and other studies could be considerably in error.

A 20 percent increase in the arrive and depart Mars hydrogen tank weights due to increased micrometeoroid protection requirements would increase the initial vehicle weight requirements by 5.5 and 10.5 percent for the years 1986 and 1978, respectively.

## VENUS SWINGBY MISSIONS

An incomplete analysis indicated that some of the extremes in vehicle weight variations due to the unfavorable years or high earth arrival velocities could be eliminated and the overall vehicle weight requirements reduced by resorting to the Venus swingby trajectories. Reductions in vehicle weight of over 20 percent were found to be possible for some of the cases investigated.

distance, are obtained as a function of the third leg time for the fixed planet date and inbound leg time. If PP < PPMIN, the VI corresponding to PPMIN is obtained.

The inbound leg time is then changed by a uniform interval, and the process repeated for another range of third leg times. This is continued over the desired inbound leg time range. The leave planet date is then incremented, and the entire process repeated for another inbound leg time range, and more third leg time ranges. These ranges may change every time so that only those trajectories giving minimum and near minimum velocities need be stored in the program.

Since no consistent set of powered swingby trajectory data was available, it was not possible to analyze any powered swingby missions during the study. Nevertheless, the powered swingby option of the SWOP program is fully developed and has been checked out as far as is feasible without actual trajectory data being available.

Derivation of Optimization Equations

There are several sets of optimization equations for the different combinations of stopover missions and powered and unpowered, inbound and outbound, swingby missions. In addition, different forms of the equations result when certain constraints are imposed, such as a specified or constrained total trip time. For the purposes of reporting, it is only necessary to derive the optimization equations for one of these sets. Therefore, only the optimization equations for the inbound powered swingby mission are derived in detail. However, the equations for all missions are listed at the end of this section.

The optimization of the trajectory to obtain minimum initial vehicle weight uses the calculus of maxima and minima theorem that states that a function, f, is at a maxima or minima point when the total differential is equal to zero. This occurs when each partial derivative of f is equal to zero. That is,

$$df = \frac{\partial f}{\partial X_1} dX_1 + \frac{\partial f}{\partial X_2} dX_2 + \text{-----}$$

$$= 0$$

if

$$\frac{\partial f}{\partial X_i} = 0, \; i = 1, 2, \text{----}$$

## COMPUTER PROGRAMS

The mission and engine optimization and analysis techniques and computer programs (NOP, FLOP, and SWOP) which were developed during this study provide a significant major advancement over previously available methods for performing vehicle and engine systems analysis. These techniques allowed a comprehensive investigation of the influence of the engine and vehicle characteristics on the vehicle performance for a wide range of missions. During the study, the programs were modified several times to broaden their scope by including additional engine types and flow schemes, a greater number of mission types and vehicle configuration options, and additional independent parameters in the mission optimization process. The programs as they now exist, as well as with further anticipated modifications, will serve as valuable tools for future analysis and investigation of interplanetary missions, space vehicle designs, and solid core nuclear engine designs.

## PARAMETRIC DATA BOOKS

Finally, an important product developed during the course of the study is the compilation of all of the mission, vehicle, and engine parametric data which were generated into two selfconsistent data books, Vols III and V of this series of final reports.

# REFERENCES


1. Space Flight Handbooks, Planetary Flight Handbook, Vol. 3, NASA SP-35, prepared for George C. Marshall Space Flight Center, Huntsville, Alabama under Contract NAS 8-5031.
2. Frank W. Gobetz, Optimum Transfers Between Hyperbolic Asymptotes, AIAA Journal, Vol. 1, September 1963, p. 2034.
3. Module Designs for Assembly into Nuclear Orbital Vehicle, Lockheed Missiles and Space Company, LMSC/A650541, 11 June 1964, NAS 8-9500.
4. Estimating Minimum Propellant Tankage Weight from Pressure Considerations, Leon Willoughby, STL Design Manual, Section 4.4.1.
5. Weight Status Report for the Saturn V Operational Launch Vehicle, MSFC Memo No. R-P and VE-VAW-177-63, 1 October 1963.
6. Meteoroid Hazard to Space Vehicles, L. Becker, STL 9862.1-53, 22 August 1962.
7. Advanced Lunar Transportation Study Final Report, Vol. 1, Lockheed Missiles and Space Company, LMSC-B007322, 28 January 1963.
8. Manned Mars Landing and Return Mission Study, TRW/STL, 8572-6011-RU000, 28 March 1964.
9. Heat Conduction in a Semi-Infinite Slab with Sublimation at Surface, D. Baer, and A. Ambrosio, Ballistic Missile and Space Technology, Vol. II, 1961 p. 436 - 446.
10. Structural Design Manual, Northrop Aircraft.
11. Weight Strength Analysis of Aircraft Structures, F. Shanley, Section 23.
12. Strength, Efficiency, and Design Data for Beryllium Structures, R. F. Crawford and A. B. Burns, ASD Technical Report 61-692, Feb. 1962.
13. Design and Testing of Honeycomb Sandwich Cylinder Under Axial Compression, by J. H. Cunningham and M. J. Jacobson of Douglas Aircraft MSD, NASA TN 510, p 341.